

**Microbial population composition of ochrous biofilms
and water samples obtained from technical
groundwater-fed systems**

vorgelegt von
Diplom-Biologin
Josephin Schröder
geb. in Schwedt/Oder

von der Fakultät III - Prozesswissenschaften
der Technischen Universität Berlin
zur Erlangung des akademischen Grades

Doktorin der Naturwissenschaften
- Dr. rer. nat.-

genehmigte Dissertation

Promotionsausschuss:

Vorsitzender: Prof. Dr.-Ing. Sven-Uwe Geißen

Gutachter: Prof. Dr. rer. nat. Ulrich Szewzyk

Gutachter: Prof. Dr. Flynn Picardal

Tag der wissenschaftlichen Aussprache: 05. Februar 2018

Berlin 2018

Danksagung

An erster Stelle danke ich Prof. Dr. Ulrich Szewzyk für die Möglichkeit an dem spannenden und anwendungsbezogenen Thema zu arbeiten sowie für die wissenschaftliche Betreuung.

Flynn Picardal danke ich für Bereitschaft, trotz der langen Anreise, meine Arbeit zu begutachten.

Ebenfalls ein besonderer Dank gilt Dr. Burga Braun für die wissenschaftliche Betreuung während der gesamten Zeit am Fachgebiet, ihre ständige Unterstützung und für das Lesen des Manuskripts sowie die vielen wertvollen Vorschläge.

Des Weiteren möchte ich den Projektpartnern des Antiocker-Projektes danken, die mir bei der Probenahme, Organisation und fachlichen Auseinandersetzung mit dem Thema geholfen haben.

Ein besonderer Dank gilt Henrik, der zum einem als Projektpartner hervorragende Arbeit geleistet hat, mich bei der Auswertung der vielen Daten unterstützt hat, aber auch immer als guter Freund beiseite stand.

Des Weiteren möchte ich den Mitarbeiterinnen und Mitarbeitern der UMB danken. An dieser Stelle seien namentlich Anna, Micha, Heinz, Anja, Gaby, Bertram, Stefie, Bärbel und Marcella genannt sowie Stef für ihre kompetente Hilfe und freundschaftliche Arbeitsweise im Labor. Vielen Dank für eure Unterstützung, die fruchtbaren Gespräche und die netten Stunden. Allen nicht namentlich erwähnten alten und neuen Kollegen des Fachgebietes Umweltmikrobiologie danke ich für das angenehme Arbeitsklima und die vielfältige Unterstützung. Außerdem möchte ich allen Studenten danken, die ihre Bachelorarbeit im Rahmen des Dissertationsthemas angefertigt haben und somit einen wichtigen Teil zu meiner Arbeit beigetragen haben.

Nicht zuletzt gilt mein besonderer Dank meinen lieben Eltern, Geschwistern, Freunden Annika, Luise, Josi, Ulli und Johanna sowie meinem Freund André für die andauernde Unterstützung, Geduld und den notwendigen Rückhalt während der letzten Jahre.

Veröffentlichungen

Auszüge der im Folgenden dargestellten Daten wurden bereits im Vorfeld in Fachpublikationen veröffentlicht.

Fachpublikationen mit ordentlichen Begutachtungsverfahren

Braun, B.¹, Schröder, J.¹, Knecht, H., & Szewzyk, U. (2016). Unravelling the microbial community of a cold groundwater catchment system. *Water Research*, 107, 113-126.

¹These authors contributed equally to this work.

Schröder, J., Braun, B., Liere, K., & Szewzyk, U. (2016). Draft genome sequence of *Rheinheimera* sp. strain SA_1 isolated from iron backwash sludge in Germany. *Genome Announcements*, 4(4), e00853-16.

Braun, B.; Künzel, S.; Schroeder, J.; & Szewzyk, U. (2017). Draft Genome Sequence of strain R_RK_3, an iron-depositing isolate of the genus *Rhodomicrobium* isolated from a dewatering well of an opencast mine. *Genome Announcements* 5, A.00864-17.

Andere Veröffentlichungen

Schwarzmüller, H., Menz, C., Grützmacher, G., Gnierss, G., Jordan, V., Schröder, J., Braun, B., Szewzyk, U., Macheleidt, W. & Grischeck, T.

Mikrobielle Verockerung in technischen Systemen (Teil 1):

Probenahme aus dem Filterbereich eines Trinkwasserbrunnens mit neuartigem Unterwasserkamera- und Probenahme-System

wwt Wasserwirtschaft-Wassertechnik, 31–33. 2014

Schröder, J., Braun, B., Schwarzmüller, H., Menz, C., Grützmacher, G., Gnier, G., Jordan, V., Macheleidt, W., Grischek, T. & Szewzyk, U.

Mikrobielle Verockerung in technischen Systemen (Teil 2):

Molekularbiologische und mikrobiologische Untersuchungen von Ockerproben aus dem Filterbereich eines Trinkwasserbrunnens der Berliner Wasserbetriebe und von verschiedenen Proben der Betriebspumpe im Rahmen einer Instandhaltungsmaßnahme

wwt Wasserwirtschaft-Wassertechnik, 33–36. 2014

Mikrobielle Verockerung in technischen Systemen 2015. Teilprojekt 1a: Mikrobiologie der Verockerung bei neutralem pH-Wert und deren Verhinderung. BMBF Projekt Förderkennzeichen: 02WT1185.

Braun, B., Knecht, H., Neulinger, S., Schröder, J., & Szewzyk, U. (2017). Bakterienprofile in natürlichen und technischen Ökosystemen. *BIOspektrum*, 23(1), 46-48.

Bachelorarbeiten im Rahmen des Dissertationsthemas

Jan Phillip Samson (2013); Vergleichende Populationsanalysen der mikrobiellen Gemeinschaften einer russischen Wasserfassung

Jens Blume (2013); Charakterisierung von Bakterien aus einer russischen Wasserfassung

Anja Höhne (2014); Etablierung einer quantitativen Real-Time PCR zum spezifischen Nachweis von *Crenothrix* spp., *Geothrix* spp. und *Gallionella* spp. in einer russischen Wasserfassung

Annelie Höhne (2014); Quantitativer Nachweis von *Rhodospirillum rubrum* spp. in einer Wasserfassung mittels Real-Time PCR

Regina Heick (2015); Untersuchungen zur kleinräumigen Heterogenität von Biofilmpopulationen auf verockerten Unterwassermotorpumpen

Abstract

This study assessed the abundance, composition, diversity and functional organisation of bacterial communities correlated to chemical water parameters in four technical groundwater-fed systems. Each sampling site was vulnerable to iron-clogging and was characterised by its own specific technical and hydrochemical conditions. Biofilm and groundwater samples were obtained and compared for drinking water wells in Berlin, a groundwater catchment area with a subsurface iron and manganese removal system in Russia, dewatering wells in the Rhenish lignite mining area and a lab-scale reactor with a natural ochrous formation due to groundwater abstraction.

Each sampling site's bacterial composition was analysed by 16S rRNA gene clone library construction or 454-pyrosequencing to determine the dominant bacterial groups and to compare the bacterial compositions across all of the sampling sites. Samples from all sites featured highly comparable distributions of phyla, and these mainly consisted of *Proteobacteria*. However, there were differences between the sites regarding the bacterial class. Sequences with a high homology to the class of *Deltaproteobacteria* were predominantly abundant in those samples obtained from the lab-scale reactor and the Berlin drinking water wells. In addition, sequences from those samples derived from the wells located at the Russian water catchment site were associated with *Betaproteobacteria*, while sequences from the dewatering wells at the opencast mining sites belonged to *Gammaproteobacteria*.

A bacterial population analysis of the 16S rRNA gene did not reveal any shared core operational taxonomic units (OTUs) across all of the sampling sites; however, several OTUs, such as *Geobacter*, *Rhodoferrax*, *Gallionella* and *Geothrix*, were found repeatedly often at most of the sampling sites, indicating that they had an influence on the iron-clogging processes. Those groups are all involved in iron oxidation and reduction reactions, and their biofilm formation potential became apparent.

In addition, site-dependent characteristics, such as methane availability in groundwater, caused high abundances of methano- and methylotrophic bacterial

genera, such as *Crenothrix* and *Methylobacter*. Such microorganisms are common sources of water supply problems. In addition to methane's influence on the microbial community composition, the groundwater dissolved organic carbon (DOC) concentration and the redox potential, which is affected by the availability of oxygen, indicated to play a major role.

Additionally, total bacterial and species-specific quantitative real-time PCR (qPCR) enabled to calculate the relative abundance of major taxonomic groups within the samples. The gene copy numbers detected by qPCR for all biofilm samples obtained from water well equipment revealed high amounts of *Gallionella*-, *Crenothrix*-, *Geothrix*- and *Rhodoferax*-related genes (up to 10^{11} copies g⁻¹). In addition, the richness values calculated by denaturing gradient gel electrophoresis (DGGE) indicated a high degree of diversity in almost all samples.

The identification of parameters with an effect on the bacterial community structure will potentially help to prevent and remediate the clogging process in technical groundwater-fed systems.

Zusammenfassung

In dieser Arbeit wurden die Abundanz, Zusammensetzung, Diversität und funktionale Organisation (engl. functional organisation) der bakteriellen Gemeinschaften in vier technischen, mit Grundwasser gespeisten Systemen, untersucht. Zusätzlich wurden diese Daten mit den wasserchemischen Parametern korreliert. Alle untersuchten technischen Systeme zeigten Verockerungsablagerungen und waren durch standortspezifische, technische und hydrochemische Bedingungen charakterisiert. Die Biofilm- und Wasserproben stammten aus Trinkwasserbrunnen in Berlin, einer Trinkwasserfassung mit unterirdischer Enteisung und Entmanganung in Russland, Sumpfungsbrunnen aus dem rheinischen Braunkohletagebaurevier und einem Brunnenreaktor im Labormaßstab.

Die bakteriellen Gemeinschaften aller Standorte wurden auf der Ebene der 16S rDNA durch Erstellung einer Klonbibliothek und mittels 454-Pyrosequenzierungsanalyse untersucht, um die dominanten bakteriellen Gruppen zu detektieren und untereinander zu vergleichen. Das Phylum der *Proteobacteria* war die dominierende Gruppe in allen Standorten, allerdings zeigten sich Unterschiede auf der Ebene der bakteriellen Klasse. Die Sequenzen, welche eine hohe Homologie zur Klasse der *Deltaproteobacteria* aufwiesen, waren überwiegend in den Proben aus dem Bioreaktor und den Berliner Trinkwasserbrunnen zu finden. Des Weiteren zeigten die Sequenzen aus der russischen Trinkwasserfassung eine mehrheitliche Übereinstimmung zur Klasse der *Betaproteobacteria*; dagegen gehörte ein Großteil der 16S rDNA Sequenzen aus den Sumpfungsbrunnen zu den *Gammaproteobacteria*.

Die 16S rDNA Amplikonanalyse ergab keine gemeinsamen OTUs (engl. operational taxonomic units) für die verschiedenen Standorte, allerdings wurden vier OTUs (*Geobacter*, *Rhodoferax*, *Gallionella* und *Geothrix*) vermehrt in annähernd allen Proben nachgewiesen. Das erhöhte Vorkommen deutet darauf hin, dass sie einen Einfluss auf die Verockerung haben können. Des Weiteren beinhalten alle vier Gruppen Arten, die an der Eisenoxidation und -reduktion beteiligt sind.

Ferner ergaben standortspezifische Charakteristika, wie die Verfügbarkeit von Methan, hohe Abundanzen an methylo- und methanotrophen Gruppen wie den Gattungen *Crenothrix* und *Methylobacter*, welche häufig zu Problemen in Grundwasserförderanlagen führen. Neben dem Einfluss von Methan zeigten der Gehalt an gelöstem organischen Kohlenstoff (engl. DOC) und das Redoxpotential einen Einfluss auf die Zusammensetzung und Abundanz der bakteriellen Gemeinschaften.

Mit der quantitativen PCR (qPCR) Analyse der Biofilmprouben wurden Genkopien mit bis zu 10^{11} Genkopien g^{-1} der Gattungen *Gallionella*, *Crenothrix*, *Geothrix* und *Rhodoferrax* detektiert. Zusätzlich wurde eine hohe bakterielle Diversität für alle Standorte anhand der berechneten Bandenzahl der denaturierenden Gradienten-Gelelektrophorese (DGGE) bestimmt.

Die Identifizierung von Parametern, welche einen Einfluss auf die bakterielle Zusammensetzung haben, kann möglicherweise dazu beitragen, den Verockerungsprozess in technischen Grundwassersystemen zu verlangsamen und zu verhindern.

Table of contents

Abstract	V
Zusammenfassung	VII
Abbreviations.....	XII
List of tables	XIV
List of figures	XVI
1 Introduction.....	19
Aim of the study.....	24
2 Materials and methods.....	25
2.1 Chemicals and instruments	25
2.2 Software	29
2.3 Consumables	29
2.4 Oligonucleotides.....	30
2.5 Bacterial strains.....	32
2.6 Media and solutions	32
2.7 Sampling sites, sampling and chemical water analysis	35
2.7.1 Drinking water well pumps in Berlin	35
2.7.2 Water catchment system in Russia	36
2.7.3 Dewatering wells at two opencast mining areas	39
2.7.4 Lab-scale reactor with natural ochrous formation	41
2.8 Isolation of iron-depositing bacteria.....	44
2.9 DNA extraction	44
2.10 Amplification of the 16S rRNA gene and clone library construction	45
2.11 Sequence analysis performed by BioNumerics software	46
2.12 Amplification of the V3 fragment from the 16S rRNA gene	46
2.13 Denaturing gradient gel electrophoresis (DGGE) of V3 region of the 16S rRNA gene	48
2.14 Preparation of standards and quantification of 16S rRNA gene copies (qPCR).....	49
2.15 454-pyrosequencing.....	52
2.16 Elemental composition of ochrous samples	53
2.16.1 Loss-on-ignition	53
2.16.2 X-ray fluorescence analysis.....	53
3 Results.....	54
3.1 Chemical and biomolecular investigations of ochrous biofilms originating from pumps of drinking water wells.....	54

3.1.1	Hydrochemistry of the drinking water wells.....	55
3.1.2	Denaturing gradient gel electrophoresis profiling of the bacterial communities of drinking water wells.....	55
3.1.3	Bacterial population analysis of drinking water well samples by 16S rRNA gene clone libraries.....	58
3.1.4	Quantification of 16S rRNA gene copies from ochrous biofilms taken from clogged and non-clogged drinking water wells.....	60
3.1.5	Loss-on-ignition and x-ray fluorescence analysis of ochrous samples from drinking water wells	63
3.2	Chemical and biomolecular investigations of water and biofilm samples from the water catchment area in Russia.....	65
3.2.1	Hydrochemistry of the water catchment area according to sampling campaigns	65
3.2.2	Denaturing gradient gel electrophoresis profiling of the bacterial communities of the water catchment area.....	67
3.2.3	Bacterial community analysis by 16S rRNA gene 454-pyrosequencing	74
3.2.4	Quantification of 16S rRNA gene copies from ochrous and water samples taken from the water catchment area	85
3.3	Chemical and biomolecular investigations of groundwater and biofilm samples taken from dewatering wells at two different opencast mines	90
3.3.1	Hydrochemistry of two opencast mines	90
3.3.2	Denaturing gradient gel electrophoresis profiling of the bacterial communities of opencast mining wells	91
3.3.3	Bacterial population analysis of dewatering well samples by 16S rRNA gene clone libraries	98
3.3.4	Bacterial community analysis of the 16S rRNA gene by 454-pyrosequencing of the opencast mines samples ...	100
3.3.5	Quantification of 16S rRNA gene copies from ochrous and water samples taken from the opencast mines.....	103
3.4	Regeneration effects on the bacterial population of a lab-scale reactor with natural ochrous formation	107
3.4.1	Hydrochemistry of groundwater from Dresden	107
3.4.2	Denaturing gradient gel electrophoresis profiling of the bacterial communities of biofilm samples within a lab-scale reactor	107
3.4.3	Bacterial population analysis within a lab-scale reactor by 16S rRNA gene clone libraries	111
3.4.4	Quantification of 16S rRNA gene copies from biofilm samples taken from columns of a lab scale reactor	113

3.5	Isolation of iron-depositing bacteria from the biofilm samples of technical groundwater systems	119
4	Discussion	124
4.1	Comparison of the bacterial population compositions of ochrous biofilms and groundwater samples obtained from technical groundwater-fed systems	124
4.1.1	Comparison of the bacterial population composition of ochrous biofilms from clogged and non-clogged drinking water wells	124
4.1.2	Bacterial population compositions of a groundwater catchment system in Russia with a decreased specific well yield	128
4.1.3	Comparison of the bacterial population between wells equipped with aerated and non-aerated filter screens in opencast mining areas	135
4.1.4	Regeneration influence on the bacterial population of an iron clogged lab-scale reactor	139
4.1.5	Comparison of the bacterial populations of the investigated technical systems	141
4.2	Limitations of biomolecular techniques and sampling	146
5	Conclusions and Outlook	151
	Appendix	154
	References	164

Abbreviations

Abbreviation	Explanation
AF	Beginning of the abstraction phase
AG	Outgroup, wells marked which were not in operation
BWB	Berliner Wasserbetriebe
DGGE	Denaturing gradient gel electrophoresis
DNA	Deoxyribonucleic acid
DOC	Dissolved organic carbon
<i>Dy</i>	Dynamics
EDTA	Ethylenediaminetetraacetic acid
engl.	Englisch
EF	End of the abstraction phase
EPS	Extracellular polymeric substances
FAAS	Flame atomic absorption spectrometry
<i>Fo</i>	Functional organisation
H ₂ O	Environmental water media
HPLC	High-performance liquid chromatography
LOI	Loss-on-ignition
LSM2	<i>Leptothrix</i> strain media 2
MWA	Mowing window analysis
OTU	Operational taxonomic unit
PBS	Phosphate buffered saline
PCA	Principal component analysis
PCR	Polymerase chain reaction
qPCR	quantitative Polymerase chain reaction
RDA	Redundancy analysis
<i>Rr</i>	Range-weighted richness
rRNA	Ribosomal ribonucleic acid
SC I	Sampling campaign one
SL9	Trace element solution
TAE	Tris-acetate-EDTA buffer
TM7	Candidate-phylum with only one cultivated species habituating the human mouth
Tris	Tris(hydroxymethyl)aminomethane
TS I	Test series I
UPGMA	Unweighted Pair Group Method with Arithmetic mean
V3	Variable region of the 16S rRNA gene
WPS2	Candidate-division only known from 16S rRNA gene

Abbreviations

Abbreviation	Explanation
WS3	<i>Latescibacteria</i> from super-phylum <i>Fibrobacteres–Chlorobi–Bacteroidetes</i>
XRF	X-ray fluorescence
ZB2	Candidate-phylum only known from 16S rRNA gene

List of tables

Table 1. Chemicals used.....	25
Table 2. Instruments used.....	27
Table 3. Computer programs.....	29
Table 4. Consumables used.....	29
Table 5. Primer pairs used for PCR.....	31
Table 6. Primer pairs used for qPCR.....	31
Table 7. <i>Leptothrix</i> strain media 2 (LSM2 media).....	32
Table 8. H ₂ O-media.....	32
Table 9. Vitamin solution	33
Table 10. Trace element solution SL9	33
Table 11. Iron ammonium sulphate solution.....	33
Table 12. 1x phosphate-buffered saline (PBS) solution.	34
Table 13. Orange G solution.	34
Table 14. Ethidium bromide solution.	34
Table 15. SYBR Green I solution.	34
Table 16. Methods of different hydrochemical parameters.....	36
Table 17. Methods of different hydrochemical parameters.....	40
Table 18. PCR Master Mix composition for primer pair 63f and 1387r.	45
Table 19. PCR program for primer pair 63f and 1387r.	46
Table 20. Master Mix composition for primer pair p2 and p3.....	47
Table 21. PCR program for primer pair p2 and p3.	47
Table 22. Composition of DGGE stock solutions.....	48
Table 23. Master Mix composition of qPCR assay.	51
Table 24. qPCR for universal primer pair	51
Table 25. qPCR for <i>Rhodoferrax ferrireducens</i> primer pair	51
Table 26. qPCR for <i>Gallionella</i> -like group primer pair	51
Table 27. qPCR for <i>Crenothrix polyspora</i> primer pair.....	52
Table 28. qPCR for <i>Geothrix fermentans</i> primer pair	52
Table 29. Indicator species analysis.....	80
Table 30. Phylogenetic affiliation of bacterial cultures.....	120

Table A 1. Ochrous samples from pump intakes of BWB water wells and chemical analysis of associated water samples.....	154
Table A 2. Overview of well characteristics from water wells with subsurface iron and manganese removal.	155
Table A 3. Ochrous and water samples from water wells with subsurface iron and manganese removal system and chemical analysis of associated water samples.	157
Table A 4. Ochrous and water samples from two opencast mines and chemical analysis of associated water samples.....	159
Table A 5. Ochrous and water samples from different columns with ochrous formation and chemical analysis of associated water samples.	161
Table A 6. Chemical parameters of groundwater from Dresden (HTW Dresden; 2012).....	163

List of figures

Figure 1. Map of water galleries in Berlin	35
Figure 2. Location of the water catchment system area	37
Figure 3. Map of the Rhenish lignite-mining area	39
Figure 4. Different types of dewatering well filter screens.	40
Figure 5. A) Picture of the lab-scale reactor with three columns. B) Column with ochrous biofilm.....	42
Figure 6. Scheme of lab-scale reactor test series I and II.	43
Figure 7. The pump inlets of drinking water wells in Berlin.....	54
Figure 8. Dendrogram constructed with bacterial community fingerprints of biofilm samples obtained from drinking water wells in Berlin.....	56
Figure 9. Comparison of the P-L distribution curves based on the DGGE profiles of the bacterial communities of clogged and non-clogged drinking water well pumps in Berlin.	57
Figure 10. Boxplot of <i>Rr</i> -values based on DGGE profiles of samples taken from clogged and non-clogged drinking water well pumps in Berlin.....	58
Figure 11. Plots of 16S rRNA clone libraries at (A) the phylum level and (B) the top 10 OTUs (at the genus level) of the microbial communities of the biofilm samples obtained from clogged and non-clogged drinking water well pumps in Berlin.	60
Figure 12. Plot of 16S rRNA gene copies of ochrous biofilms taken from clogged and non-clogged pumps	62
Figure 13. Graphical representations of A) PCA and B) RDA.	63
Figure 14. XRF analysis and LOI	64
Figure 15. Dendrogram constructed with the bacterial community fingerprints of the water samples.....	68
Figure 16. Dendrogram constructed with the bacterial community fingerprints of samples from the aeration tank.....	69
Figure 17. Dendrogram constructed with the bacterial community fingerprints of samples from well 1101 taken during different abstraction phases.....	69
Figure 18. Dendrogram constructed with the bacterial community fingerprints of samples from well 1105 before and after regeneration.	70
Figure 19. Comparison of the P-L distribution curves based on the DGGE profiles of the various sampling campaigns.....	71
Figure 20. Plots of <i>Rr</i> -values based on the DGGE profiles from various sampling designs.	73
Figure 21. The DGGE profiles, moving window analysis (MWA) and rate of change values.....	74

Figure 22. Relative abundance of different phyla present in the water catchment system as estimated by pyrosequencing.	75
Figure 23. Relative abundance of top the 10 OTUs present in the water catchment system as estimated by pyrosequencing.	76
Figure 24. Relative abundance of the bacteria present in the water and biofilm samples taken from the aeration tank, estimated by 454-pyrosequencing.	77
Figure 25. Boxplot of alpha diversity and coverage of samples from the beginning of the abstraction phase (AF), the end of the abstraction phase (EF), outgroup samples (AG) and samples from the aeration tank.	78
Figure 26. Relative abundance of the bacteria present in water well 1101 during different abstraction phases estimated by pyrosequencing.	82
Figure 27. Plot of alpha diversity and coverage based on the OTUs.....	83
Figure 28. Relative abundance of the bacteria present in the water and biofilm samples taken from well 1105 before and after regeneration estimated by pyrosequencing.....	84
Figure 29. Plot of alpha diversity and coverage based on the OTUs.....	85
Figure 30. (A) Plot of 16S rRNA gene copies.....	87
Figure 31. Plot of 16S rRNA gene copies from the water samples obtained from well 1101 during the abstraction process.....	88
Figure 32. Plot of 16S rRNA gene copies from the samples obtained from well 1105.....	89
Figure 33. Example of the pumps used at the opencast mines; removal of riser with a pump and deposits on a pump.	90
Figure 34. Dendrogram constructed with the bacterial community fingerprints of groundwater samples taken from wells at the Hambach site (indicated by H and HR);	92
Figure 35. Dendrogram constructed with the bacterial community fingerprints of biofilm samples taken from wells at the Hambach site.....	93
Figure 36. Dendrogram constructed with the bacterial community fingerprints of groundwater samples from wells of the site Garzweiler (indicated by W and WR).....	94
Figure 37. Dendrogram constructed with the bacterial community fingerprints of biofilm samples taken from wells at the Garzweiler site.....	94
Figure 38. Comparison of the P-L distribution curves based on the DGGE profiles of the water samples derived from wells equipped with aerated and non-aerated filters at Hambach (A) and Garzweiler (B) opencast mines.	95
Figure 39. Comparison of the P-L distribution curves based on the DGGE profiles of biofilm samples taken from two opencast mines:.....	96
Figure 40. Boxplots of <i>Rr</i> -values based on the DGGE profiles of the bacterial community from (A) Hambach and (B) Garzweiler opencast mining wells.	97

Figure 41. Plot of <i>Rr</i> -values based on the DGGE profiles of the biofilm samples derived from the two opencast mines.	98
Figure 42. Phylum plots of several ochrous samples taken from water wells at the opencast mines generated by clone library construction.	99
Figure 43. The top 10 OTU plots of the 16S rRNA gene clone libraries of two opencast mines:.....	100
Figure 44. Relative abundance of the bacterial phyla present in the biofilm samples taken from the opencast mining areas, estimated by pyrosequencing: (A) Garzweiler, (B) Hambach.....	101
Figure 45. Relative abundance of the top 10 OTUs present in the biofilm samples taken in the opencast mining areas, estimated by 454-pyrosequencing: (A) Garzweiler, (B) Hambach.....	102
Figure 46. Plot of 16S rRNA gene copies from water samples taken from several water wells at the opencast mines: (A) Hambach and (B) Garzweiler. ..	104
Figure 47. Plot of 16S rRNA gene copies of the ochrous samples derived from various components of the opencast mines' dewatering wells.....	105
Figure 48. Graphical representation of RDA.....	106
Figure 49. Dendrogram constructed with bacterial fingerprints of the biofilm and groundwater samples derived from TS I.	108
Figure 50. Dendrogram constructed with bacterial fingerprints of biofilm and groundwater samples derived from TS II;	109
Figure 51. Comparison of the P-L distribution curves based on the DGGE profiles of the biofilm samples derived from the columns of the two test series .	110
Figure 52. Plots of <i>Rr</i> values based on the DGGE profiles of samples taken from the lab-scale reactor.	111
Figure 53. Plots of 16S rRNA clone libraries (A) at the phylum level and (B) the top 10 OTUs from the groundwater and biofilm samples.	112
Figure 54. Plots of 16S rRNA gene copies from the biofilm and water samples taken from several columns from test series I correlated to hydraulic conductivity.	115
Figure 55. Plots of 16S rRNA gene copies from the biofilm and water samples taken from several columns from test series II correlated to hydraulic conductivity.	117
Figure 56. Plots of 16S rRNA gene copies from the biofilm samples taken from several columns from test series II at various depths correlated to the Fe sand content.	118

1 Introduction

Microorganisms are ubiquitous in the environment and play an essential role in the global biogeochemical cycles that sustain all life on earth, but their distribution is limited by water availability. Groundwater ecosystems offer vast and complex habitats for diverse bacterial communities; these extreme habitats are characterised by their lack of light, low availability of organic carbon and nutrients, and comparably low temperatures. The microbial communities inhabiting groundwater are well-adapted to the oligotrophic groundwater system (Madsen and Ghiorse, 1993).

Drinking water sources include both surface water (lakes, rivers and reservoirs) and groundwater; however, groundwater is still the main supply source in many areas. Pumping wells play an essential role in supplying groundwater to agriculture, industry and the public drinking water system. Early microbiological investigations of groundwater date back to 1677, the year in which van Leeuwenhoek (1677) described the first bacteria-like particles in well water. Almost 200 years later, Cohn (1853) identified the first iron- and manganese-oxidising bacteria in groundwater wells. Nevertheless, not until the 1960s to 1970s did the extraction of oil and drinking water from the subsurface and the corrosion and clogging of pipes and wells result in deeper microbiological investigations of drinking water supplies on the part of several scientists, including Mulder (1964), Campbell and Gray (1975), Hutchinson and Ridgway (1977) and Cullimore and McCann (1977). When biofouling situations arise in wells, the accumulation of iron or manganese precipitates, sorbed ions and organic matter, in the form of cells and debris, leads to the development of complex microbial biofilm communities (Tuhela et al., 1997).

Bacterial biofilms are a universal phenomenon that affects almost all ecosystems. A general characteristic of a biofilm structure is that microorganisms, together with extracellular enzymes and detritus, are enclosed within a polymeric matrix (Golladay and Sinsabaugh, 1991). These extracellular polymeric substances (EPSs) provide mechanical stability to biofilms, thereby offering protection from predation, toxic substances and physical perturbations (Wingender and Flemming, 2011). Biofilms develop on a wide variety of artificial surfaces, such

as industrial or portable water system piping, where biofouling occurs due to deposition and the growth of bacterial cells or flocs. Moreover, various factors influence biofilm formation, such as the solid surface material, the characteristics of the surrounding water, and operational conditions (e.g., temperature, the level of dissolved oxygen and flow velocity; Le-Clech et al., 2006). In industrial equipment, the development of biofilms on surfaces or interfaces causes several malfunctions in water production as clogging of filter screens and pipes (Videla and Herrera, 2005). Biofilm deposition can also occur in the aquifer near the well, and it can build up quickly in comparison to mineral incrustation. In addition, the development of biofilms in water wells poses a problem when it comes to eliminating coliform bacteria, because biofilms protect such bacteria from chlorine disinfectant (Dericks, 2015).

Furthermore, in combination with biofilm formation, the abstraction of anaerobic groundwater with high amounts of reduced iron and manganese leads to incrustations in, or even around, the well, while the pump and rising pipe are also locations where such incrustations can form. A short time after their introduction, wells become clogged, and their production efficiency drops significantly as a total obstruction is neared, making clean-up and rehabilitation an economic burden (Gino et al., 2010). Oxides of iron(III) represent the most common incrustation type, and they are characterised by their large surface area and high sorption capacity (Houben, 2003b). Those precipitates result from the oxidation of the reduced forms of the metals due to the mixing of different geochemical zones that occurs because of groundwater exploitation.

The redox reactions can take place abiotically, and they can also be mediated by microorganisms (iron-oxidising or -depositing bacteria). In fully oxygenated water, at circum-neutral pH, the abiotic oxidation of iron(II) occurs very rapidly, with a half-life of <1 min; whereas the half-life of iron(II) under microaerobic conditions can be up to 300 times longer (Emerson et al., 2010). In contrast, abiotic reaction of iron(II) and nitrate is marginal in natural soil (Weber et al., 2001). In natural environments, the purely chemical oxidation process is relatively slow, and microbial activity causes an enormous increase in the reaction speed (Mendonça et al., 2003). Therefore, iron-oxidising bacteria can profit during pumping from the low oxygen concentration, as during this stage, they can successfully compete with abiotic iron oxidation (Neubauer et al., 2002; Rentz et al., 2007; Sobolev and

Roden, 2002). They are of particular significance in microaerobic environments, such as water wells (Taylor et al., 1997).

Furthermore, it is important to note that iron may be associated with organic matter, with which it forms organic-metallic complexes. This is especially critical for heterotrophic iron-oxidising bacteria. Since it is presumed, that these bacteria absorb organically bounded iron or chelated iron, the carbon source will be used and the iron hydroxide is released as a waste product; iron(III) precipitation may be an unintended effect. Those bacteria belong to the genera *Leptothrix* and *Siderocapsa* (Röske and Uhlmann, 2005). The formation of aqueous DOC-iron(II) complexes can also effect iron(II) oxidation rates since chelated iron(II) is more readily oxidised.

Chemolithoautotrophic iron-oxidising bacteria like *Gallionella* can use the energy released during the iron(II) oxidation for biomass production, less energy is released, resulting in an enormous amount of iron precipitates (Hallbeck and Pedersen, 1991).

Recent investigations have revealed a wide diversity of iron-oxidising bacteria in both natural habitats and drinking water systems. In addition to known genera, such as *Leptothrix*, *Pedomicrobium*, *Pseudomonas* and *Hyphomicrobium*, many isolates are associated with taxa for which iron deposition has not been described to date (Szewzyk et al., 2011).

Two further physiological groups of iron-oxidising bacteria exist: those that couple iron oxidation and nitrate reduction in anaerobic environments (nitrate-dependent; e.g., *Acidovorax* and *Aquabacterium*; Straub et al., 2004) and anaerobic photosynthetic iron-oxidisers, which mostly belong to the family *Rhodobacteraceae* (Imhoff et al., 2005). Iron(II) can serve as an electron donor in several steps in anaerobic nitrogen cycling.

Under anoxic conditions, iron(III) can be used as terminal electron acceptor for iron(III)-reducing bacteria; dissimilatory iron reduction by neutrophilic bacteria from *Geobacteraceae*, *Shewanella* spp. and hyperthermophilic microorganisms has been widely reported (e.g., Lovley et al., 2004). Furthermore, clogged wells in anaerobic zones can also be caused by sulphate-reducing bacteria, which, if organic material is available, reduce sulphates to sulphides (when excreted, sulphides react with iron to form iron sulphide deposits; Lu et al., 2016; van Beek, 1989).

In the last 10 years, only a few studies have addressed bacterial-mediated iron-clogging within groundwater-fed systems, and within water wells in particular, in relation to the microbial composition and hydrochemical parameters. The relationship between the chemical-mediated iron-clogging of supply wells and hydrochemistry was investigated by Bustos Medina et al. (2013), but that study did not include a microbial analysis. Furthermore, Lerm et al. (2011) investigated the influence of bacteria on the reliability and operational lifetime of a geothermal plant in correlation to the minerals precipitated. Navarro-Noya et al. (2013) analysed the bacterial communities of several drinking water wells according to physicochemical conditions, but those wells were not vulnerable to iron-clogging. Only Wang et al. (2014) have addressed the microbial community of clogging materials and groundwater samples from dewatering wells in conjunction with physicochemical parameters; however, that study mainly focused on acidophilic sampling sites. When the pH is below 4.0, iron(II) is stable, even in the presence of oxygen.

Nevertheless, to the best of my knowledge, there has been no attempt to compare bacterial-mediated iron-clogging across technically distinct groundwater abstracting sites in relation to hydrochemical parameters. In this study, the diversity, composition and quantification of specific bacterial groups directly involved in iron pipe deposit formation and dissolution have been investigated.

The use of species-specific, quantitative PCR (qPCR) enabled the identification of relevant changes within the different water wells. The qPCR was utilised in order to monitor the following bacterial groups: total *Bacteria*, *Rhodoferrax ferrireducens*, *Geothrix fermentans*, *Crenothrix polyspora* and *Gallionella* spp.. Additionally, 16S rDNA-based techniques as DGGE, supported by clone library construction and 454-pyrosequencing were used to observe alterations in the bacterial community composition that resulted from well operation.

Our current understanding of both key biochemical and hydrochemical processes and of the diversity of microbes involved in iron-clogging is still insufficiently comprehensive in terms of most groundwater-fed systems.

Therefore, several technical groundwater-fed systems were investigated, according to the dominant bacterial population involved in iron-clogging. The selection of four sampling sites allowed for a comparison regarding this global

problem. All sites were vulnerable to iron-clogging and characterised by reduced specific capacities due to biofilm formation.

The following sites were investigated:

- I) Drinking water well pumps in Berlin were examined during routine maintenance of their submersible pumps. The assessment focused on the biofilm formation around the pumps' filter screens.
- II) A drinking water catchment system, equipped with subsurface groundwater treatment for iron and manganese removal was evaluated. This system is located in far eastern Russia. Samples were taken during different abstraction phases and from biofilms obtained from technical equipment.
- III) Dewatering wells, located at two opencast mines, named Hambach and Garzweiler, in the Rhenish lignite mining region, were investigated, and samples were taken from both the groundwater and the biofilms on the water well equipment.
- IV) A lab-scale reactor with a natural ochrous formation was investigated to determine whether chemical and hydromechanical regeneration procedures affect bacterial populations.

Identifying those parameters that control the bacterial community structure might contribute to preventing or reversing clogging processes in technical groundwater-fed systems.

Aim of the study

The purpose of this study was to analyse and compare the bacterial populations of ochrous biofilms and groundwater samples taken from various technical groundwater-fed systems in answer the following questions:

- I) Which bacteria are involved in causing iron-clogging in water wells?
- II) Can these bacteria be used as an indicator of iron-clogging in water wells?
- III) What do these bacteria prefer in terms of environmental conditions?

In order to answer these questions, ochrous and water samples obtained from groundwater wells associated with iron-clogging and located at four separate sites were investigated. Each sampling site is characterised by distinct technical and hydrochemical conditions. The bacterial populations from all of the sampling sites were characterised and compared using several biomolecular methods; the results were correlated with the hydrochemical parameters from the surrounding water.

2 Materials and methods

2.1 Chemicals and instruments

All chemicals used were of at least molecular biology grade. Table 1 summarizes the chemicals used, including their suppliers.

Table 1. Chemicals used.

Chemical	Supplier
4',6-diamidino-2-phenylindole (DAPI)	Carl Roth GmbH & Co. KG, Karlsruhe, Germany
4-aminobenzoic acid	Sigma-Aldrich, Steinheim, Germany
Acrylamide:bis-acrylamide 37.5:1	Carl Roth GmbH & Co. KG, Karlsruhe, Germany
Agar-agar	Becton, Dickinson and Company, Sparks, USA
Agarose	Biozym Scientific GmbH, Oldendorf, Germany
AIXTRACTOR 2.0®	Cleanwells GbR, Rottweil, Germany
Ammonium chloride	Sigma-Aldrich, Steinheim, Germany
Ammonium iron(II) sulfate hexahydrate	Merck KGaA, Darmstadt, Germany
Ammonium persulphate	Carl Roth GmbH & Co. KG, Karlsruhe, Germany
Aquagran®	EUROQUARZ, Ottendorf-Okrilla, Germany
Boronic acid	Carl Roth GmbH & Co. KG, Karlsruhe, Germany
Calcium pantothenate	Merck KGaA, Darmstadt, Germany
Cobalt(II) chloride hexahydrate	Merck KGaA, Darmstadt, Germany
Copper(II) chloride dihydrate	Merck KGaA, Darmstadt, Germany
Cyanocobalamin	Sigma-Aldrich, Steinheim, Germany
D+ biotin	Sigma-Aldrich, Steinheim, Germany
D+ calcium pantothenate	Sigma-Aldrich, Steinheim, Germany
Disodium hydrogen phosphate	Sigma-Aldrich, Steinheim, Germany
Ethidium bromide	Carl Roth GmbH & Co. KG, Karlsruhe, Germany
Ethylenediaminetetraacetic acid (EDTA)	Carl Roth GmbH & Co. KG, Karlsruhe, Germany
Formamide	Carl Roth GmbH & Co. KG, Karlsruhe, Germany
Gel loading dye	Carl Roth GmbH & Co. KG, Karlsruhe, Germany
Glycerol ≥98 %	Carl Roth GmbH & Co. KG, Karlsruhe, Germany
Iron(II) chloride tetrahydrate	Merck KGaA, Darmstadt, Germany
Magnesium chloride	Carl Roth GmbH & Co. KG, Karlsruhe, Germany
Manganese(II) carbonate	Merck KGaA, Darmstadt, Germany
Manganese(II) chloride dihydrate	Merck KGaA, Darmstadt, Germany
Manganese(II) sulfate	Merck KGaA, Darmstadt, Germany
Nickel(II) chloride hexahydrate	Merck KGaA, Darmstadt, Germany

Chemical	Supplier
Nicotinic acid	Sigma-Aldrich, Steinheim, Germany
Nitrilotriacetic	Carl Roth GmbH & Co. KG, Karlsruhe, Germany
Oxalic acid	Sigma-Aldrich, Steinheim, Germany
Potassium chloride	Carl Roth GmbH & Co. KG, Karlsruhe, Germany
Potassium dihydrogen orthophosphate	Carl Roth GmbH & Co. KG, Karlsruhe, Germany
Pyridoxamines	Sigma-Aldrich, Steinheim, Germany
Sodium chloride	Carl Roth GmbH & Co. KG, Karlsruhe, Germany
Sodium hydroxide	Merck KGaA, Darmstadt, Germany
Sodium molybdate dihydrate	Merck KGaA, Darmstadt, Germany
SYBR Green I 10.000x	Invitrogen, Life Technologies GmbH, Darmstadt, Germany
50x Tris-acetate-EDTA (TAE) buffer	Carl Roth GmbH & Co. KG, Karlsruhe, Germany
Tetramethylethylenediamine (TEMED)	Carl Roth GmbH & Co. KG, Karlsruhe, Germany
Thiamine Hydrochloride	Sigma-Aldrich, Steinheim, Germany
Trisodium citrate dihydrate	Merck KGaA, Darmstadt, Germany
Urea	Carl Roth GmbH & Co. KG, Karlsruhe, Germany
Yeast extract	Carl Roth GmbH & Co. KG, Karlsruhe, Germany
Zinc chloride	Sigma-Aldrich, Steinheim, Germany

Table 2 summarizes the instruments used.

Table 2. Instruments used.

Name	Type	Vendor
Autoclave	5075 ELV	tuttnauer Systec, Breda, the Netherlands
Cell disruptor	Fast Prep 24	MP Biomedicals Europe, Illkirch, France
Centrifuge	Mikro 200R	Andreas Hettich GmbH & Co. KG, Tuttlingen, Germany
Chromatograph	Agilent 7890 A	Agilent Technologies, Moscow, Russia
Clean bench	Heraeus, Hera Safe	Kendra Laboratory Products GmbH, Langenselbold, Germany
Crucible melter	Rotomelt	Linn High Term, Eschenfelden, Germany
INGENYphorU System	INGENYPHORU	Ingeny International B.V., Goes, the Netherlands
Electronic balance	L610	Satorius GmbH, Göttingen, Germany
Electrophoresis chamber	Mini-Sub Cell GT	Bio- Rad Laboratories GmbH, München, Germany
Fibre furnace		Linn High Term, Eschenfelden, Germany
Gel documentation station	Dark Hood DH50	Biostep, Jahnsdorf, Germany
Microscope	Axioplan 2	Carl Zeiss Microscopy GmbH, Jena, Germany
	CLSM TCS SP5 II	Leica Microsystems GmbH, Wetzlar, Germany
Microwave	MW 13146W	Amica International GmbH, Ascheberg, Germany
Nanodrop	Nanodrop 2000c	Thermo Fischer Scientific, Waltham, USA
PCR hood	UVC/ T-M-AR	Kisker Biotech GmbH & Co. KG, Steinfurt, Germany
pH meter		Hanna Instruments Deutschland GmbH, Kehl am Rhein, Germany
Photometer Nanocolor	500D	MACHEREY-NAGEL GmbH & Co. KG, Düren, Germany
Photometer Nanocolor	PF12 Nr.526	MACHEREY-NAGEL GmbH & Co. KG, Düren, Germany
Pipettes	2 µl, 10 µl, 20 µl, 200 µl, 1000 µl	Eppendorf GmbH, Wesseling-Berzdorf, Germany

Name	Type	Vendor
		Gilsen Inc., Middleton, USA
Press	20t	Herzog, Osnabrück, Germany
real-time PCR cycler	Rotor-Gene 6000-5 Plex	Qiagen, Venlo, the Netherlands
Thermocycler	PeqStar 96 Universal gradient	Peqlab Biotechnologie GmbH, Erlangen, Germany
Total Organic Carbon Analyzer	TOC-VE	Shimadzu, Tokyo, Japan
Vacuum pump		Vacuubrand GmbH & Co KG, Wertheim, Germany
Vortex	Vortex Genie 2	Heidolph Instruments GmbH & Co. KG, Schwabach, Germany
WWT multiparameter analyzer		Wissenschaftlich-Technische Werkstätten GmbH, Weilheim, Germany
X-ray fluorescence analyser	PW 2400 WDXRF Spectrometer	PANalytica, Almelo, the Netherlands
454-Genome Sequencer	454-Genome Sequencer-FLX system	Roche, Branford, US

2.2 Software

Table 3 shows the computer programs and their developers.

Table 3. Computer programs.

Software	Software developer
BioNumerics versions 5.2 / 8.1	Applied Maths, Sint-Martens-Latem, Belgium
SigmaPlot version 13	Systat Software GmbH, Erkrath, Germany
R version 3.0.0	R Core Team
Rotor-Gene Software package version 1.7	Qiagen, Venlo, the Netherlands
SuperQ and Uniquant software	PANalytica, Almelo, the Netherlands

2.3 Consumables

Table 4 summarizes the consumables used including filters, kits, ladders and Master Mixes.

Table 4. Consumables used.

Material	Vendor
100 bp Marker	Roboklon GmbH, Berlin, Germany
3 in 1 - Basic DNA Kit	Roboklon GmbH, Berlin, Germany
Aquaquant for total iron	Merck KGaA, Darmstadt, Germany
Cellulose nitrate filter (0.2 µm, 0.4 µm), Ø 47 mm	Sartorius AG, Göttingen, Germany
DGGE Marker II	Wako Chemical Industries Ltd., Osaka, Japan
NANOCOLOR® Ammonium 3	MACHEREY-NAGEL GmbH & Co. KG, Düren, Germany
NANOCOLOR® Manganese	MACHEREY-NAGEL GmbH & Co. KG, Düren, Germany
PCR / DNA Clean-Up DNA Kit	Roboklon GmbH, Berlin, Germany
Perpetual Taq Master Mix (2x)	Roboklon GmbH, Berlin, Germany
SG qPCR Master Mix (2x)	Roboklon GmbH, Berlin, Germany
Soil DNA Purification Kit	Roboklon GmbH, Berlin, Germany
Taq PCR Master Mix (2x)	Roboklon GmbH, Berlin, Germany
VISOCOLOR® ECO Iron 2	MACHEREY-NAGEL GmbH & Co. KG, Düren, Germany

Material	Vendor
VISOCOLOR® ECO Iron 2	MACHEREY-NAGEL GmbH & Co. KG, Düren, Germany
VISOCOLOR® ECO nitrate	MACHEREY-NAGEL GmbH & Co. KG, Düren, Germany
VISOCOLOR® ECO nitrite	MACHEREY-NAGEL GmbH & Co. KG, Düren, Germany

2.4 Oligonucleotides

All oligonucleotides were synthesized by Biomers.net and purified by HPLC. For primers, 100 µM stock solutions were made with PCR water and stored at -20 °C. The sequences of all primers are listed in Table 5 and Table 6.

Table 5. Primer pairs used for PCR, including the name of the primer, sequence, size and annealing temperature.

Target	Primer	Sequence 5' – 3'	Product Size [bp]	Annealing temp. [°C]	References
<i>Bacteria</i>	p2	ATT ACC GCG GCT GCT GG	193	65-55	(Muyzer et al., 1993)
	p3	CGC CCG CCG CGC GCG GCG GGC GGG GCG GGG GCA			
		CGG GGG GCC TAC GGG AGG CAG CAG			
<i>Bacteria</i>	63f	CAG GCC TAA CAC ATG CAA GTC	1324	58	(Marchesi et al., 1998)
	1387r	GGG CGG WGT GTA CAA GGC			

Table 6. Primer pairs used for qPCR, including the name of the primer, sequence, size and annealing temperature.

Target	Primer	Sequence 5' – 3'	Product Size [bp]	Annealing temp. [°C]	References
<i>Bacteria</i>	Uni338F_RC	ACT CCT ACG GGA GGC AGC	571	60,4	(Lu et al., 2013)
	Uni907R	CCG TCA ATT CMT TTG AGT TT			(Lane et al., 1985)
<i>Rhodospirillum rubrum</i>	RdoR_RC	GAC CTG CAT TTG TGA CTG YA	312	58	(Lu et al., 2013)
	Uni907R	CCG TCA ATT CMT TTG AGT TT			(Lane et al., 1985)
<i>Geothrix fermentans</i>	Gx. 193F	GAC CTT CGG CTG GGA TGC TG	255	58	(Coates and Achenbach, 2001)
	Gx. 448R	AGT CGT GCC ACC TTC GT			
<i>Gallionella</i> -like group	628F	GBM AGG CTA GAG TGT AGC	370	51	(Wang et al., 2011)
	998R	CTC TGG AAA CTT CCT GAC			(Wang et al., 2009)
<i>Crenothrix polyspora</i>	Creno139f	TAG TGG GGG ACA ACG TGT	199	59	(Stoecker et al., 2006)
	EUB338	GCT GCC TCC CGT AGG AGT			(Amann et al., 1990)

2.5 Bacterial strains

In this thesis, DNA from pure cultures of *Rhodospirillum rubrum* T118 (DSM 15236, type strain) (Finneran et al., 2003) and *Geothrix fermentans* H-5 (DSM 14018, type strain) (Coates et al., 1999) were used.

2.6 Media and solutions

The media and solutions used are listed in Table 7 to Table 15. The heat-sensitive solutions were filter sterilized (Table 9 and Table 11).

Table 7. *Leptothrix* strain media 2 (LSM2 media) (modified after Mulder and van Veen, 1963).

Content	Amount
Demineralized water	1000 ml
Ammonium chloride	0.3 g
Difco agar	15 g
Manganese(II) carbonate	2 g
Yeast extract	1 g
Iron ammonium sulfate solution	2 ml
Trace element solution SL9	2 ml
Vitamin solution	2 ml
pH 7.2	

Table 8. H₂O-media (*Leptothrix* strain media 2) (modified after Mulder and van Veen, 1963)

Content	Amount
Demineralized water	1000 ml
Difco agar	15 g
Manganese(II) carbonate	2 g
Iron ammonium sulfate solution	2 ml
Trace element solution SL9	2 ml
Vitamin solution	2 ml
pH 7.2	

Table 9. Vitamin solution (Fuchs and Schlegel, 2007).

Content	Amount
Demineralized water	500 ml
4-aminobenzoic acid	5 mg
D+ biotin	1 mg
Cyanocobalamin	10 mg
Nicotinic acid	10 mg
D+ calcium pantothenate	2,5 mg
Pyridoxamines	25 mg
Thiamine hydrochloride	5 mg

Table 10. Trace element solution SL9 (Tschech and Pfennig, 1984).

Content	Amount
Demineralized water	500 ml
Nitilotriacetic	12.8 g
Iron(II) chloride tetrahydrate	2.0 g
Zinc chloride	70 mg
Manganese(II) chloride dihydrate	80 mg
Boronic acid	6 mg
Cobalt(II) chloride hexahydrate	190 mg
Copper(II) chloride dihydrate	2 mg
Nickel(II) chloride hexahydrate	24 mg
Sodium molybdate dihydrate	36 mg
Demineralized water	ad 1000 ml
pH 6	

Table 11. Iron ammonium sulphate solution (Mulder and van Veen, 1963).

Content	Amount
Demineralized water	20 ml
Trisodium citrate dihydrate	3 g
Ammonium iron (II) sulfate hexahydrate	4 g

Table 12. 1x phosphate-buffered saline (PBS) solution.

Content	Amount
Sodium chloride	8 g
Potassium chloride	0.2 g
Disodium hydrogen phosphate	1.44 g
Potassium dihydrogen orthophosphate	0.24 g
Demineralized water	ad 1000 ml
pH 7.4	

Table 13. Orange G solution.

Content	Amount
50xTAE	2 ml
Orange G	0.15 g
Glycerol (99 %)	60 ml
Milli-Q water	ad 100 ml

Table 14. Ethidium bromide solution.

Content	Amount
Ethidium bromide solution (10 mg ml ⁻¹)	50 µl
Milli-Q water	ad 1000 ml

Table 15. SYBR Green I solution.

Content	Amount
50xTAE	15 ml
SYBR Green I (10.000x)	75 µl
Milli-Q water	ad 750 ml

2.7 Sampling sites, sampling and chemical water analysis

Ochrous biofilms and water samples were collected between May 2011 and May 2014 from four technical groundwater-fed system sites. All sampling sites were vulnerable to iron-clogging.

2.7.1 Drinking water well pumps in Berlin

The drinking water wells are located at various well galleries in Berlin, Germany, and the water samples were taken from four different well galleries (Figure 1). The catchment area of the Stolpe waterworks is located northwest of Berlin. Drinking water is obtained by means of groundwater extraction. Therefore, Havel water is dammed on the Havel meadows, as water seeps through the soil. The Tegel waterworks, which are located in the northern of Berlin, extract pre-cleared surface water from the Tegeler See. The Kaulsdorf and Friedrichshagen waterworks, which are located in the eastern part of Berlin, supply drinking water directly from groundwater.

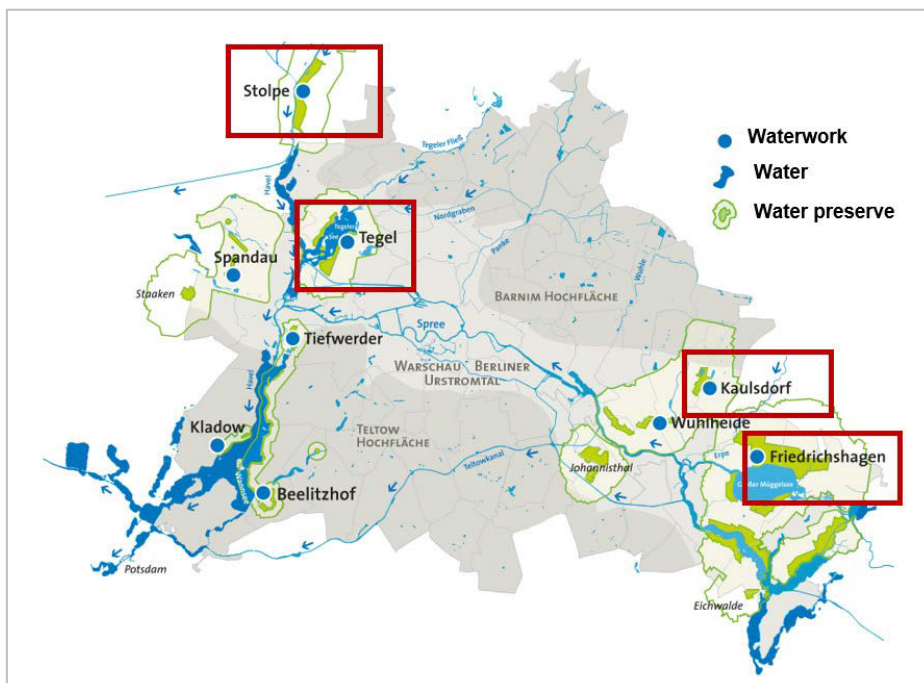


Figure 1. Map of water galleries in Berlin (source 21.8.2015 <http://www.bwb.de/content/language1/html/941.php>). Red frames mark sampling sites (water galleries).

Ochrous biofilms from the pumps' suction strainer of 26 drinking water wells were investigated during routine maintenance of their submersible pumps (Table A 1). Approximately 1 to 10 g of biofilm sample were taken from each pump, if ochrous biofilm surrounded the pumps inlet. An ochrous grade of at least 1 cm thickness surrounding their pumps' suction strainer was considered as a clogged well, while less than 1 cm thickness was classified as non-clogged. The water wells investigated were then grouped into clogged (12 samples) and non-clogged (14 samples) well groups.

Different water chemistry parameters were provided by Berliner Wasserbetriebe (BWB) (Table 16). Physicochemical water parameters were determined on-site for temperature, pH, oxygen and conductivity via a WWT multi-parameter analyser (Table 2) immediately after the ochrous samples were taken.

Table 16. Methods of different hydrochemical parameters.

Parameter	Method
Dissolved organic carbon (DOC)	DIN EN 1484 (HO3)
Iron	ICP-OES (W) DIN EN 11885 (E22)
Nitrate	IC (W) DIN EN ISO 10304-1/2
Manganese	ICP-OES (W) DIN EN 11885 (E22)
Ammonium	NH ₄ -N, photometrical (W) DIN 38406-E05-1
Phosphate	IC (W) DIN EN ISO 10304-1/2
Sulphate	IC (W) DIN EN ISO 10304-1/2

2.7.2 Water catchment system in Russia

The sampling site is located in the far east of Russia, near the Amur River, close to the Chinese border (Figure 2). During the time in which samples were taken, the water catchment area consisted of four sections (1st, 2nd, 3rd and 4th sections), with 12 water wells each as well as four aeration tanks for the respective section. However, wells of the 2nd, 3rd and 4th sections were not in operation during sampling. Since running-in of wells from the 1st section, the performance of these water wells has continuously declined.



Figure 2. Location of the water catchment system area, near the Amur River from which samples were taken. Map data copyright OpenStreetMap contributors (2015) and available from www.openstreetmap.org (Braun et al., 2016).

The water catchment area is equipped with an in-situ subsurface iron- and manganese removal system, as described previously by Van Halem et al. (2011). The pumped groundwater originated from a 48-m-deep aquifer and the distance between the wells is approximately 100 m. The aerated water which consisted of a mixture of the well water from different pumping wells, was obtained from an aeration tank, wherein a portion of abstracted water was enriched with oxygen. The aerated water was then injected to the groundwater by means of water wells creating a subsurface oxidation zone around the wells. One cycle consists of an injection period of 1.500 to 1.700 m³ water (infiltration phase) followed by an abstraction volume of 3.400 to 4.300 m³ water (abstraction phase). Both cycles are separated by a three hour resting period. A technical description of this method has been published by Grischek et al. (2013).

In order to analyse the bacterial populations in association with the decreased abstraction volume, three different sampling campaigns were considered. A total number of 42 water and biofilm samples were analysed.

Sampling campaign one (SC I) included 31 water samples taken from 21 water wells, which derived from four different well sections (1st, 2nd, 3rd and 4th). Due to the fact that the infiltrated water originates from the aeration tank, a further five water samples, with biofilm flocs, were taken from the aeration tank of the 1st section. In total, the microbial communities of 36 samples were analysed in SC I. The well sections started operation at different time points, although wells

of the 2nd, 3rd and 4th sections were not in operation and were thus used as the outgroup (AG), referring to water wells that did not have a decrease in abstraction volume. Water samples were taken from operating wells of the 1st section at two different abstraction stages, i.e. at the beginning of the abstraction phase (AF) or at the end of the abstraction phase (EF).

Sampling campaign two (SC II) included five water samples from water well 1101 (1st section), taken at different abstraction times (the beginning, 3rd, 4th, 5th and end phases) in order to analyse the dynamics of the bacterial populations during well management.

Sampling campaign three (SC III) focused on three samples taken from well 1105 (1st section), both biofilm samples taken before regeneration with hydrogen peroxide solution and one water sample was taken after regeneration procedure in order to analyse the effect of the hydrogen peroxide solution, on the microbial community composition.

Table A 2 provides an overview of sampling campaigns and the well infrastructure. During the sampling period, 40 ml water of each water sample (in total 37 samples) were taken, and several grams of each biofilm sample (in total 5 samples) were directly removed from the wall of the aeration tank and from well pumps.

Physicochemical water parameters as temperature, pH, oxygen, redox potential and conductivity were determined by means of a WWT multi-parameter analyser (Table 2) immediately before samples were taken. Additionally, concentrations of nitrate, nitrite, ammonium and manganese, as well as the amounts of iron(II) and iron(III) by using the corresponding test kits (Table 4), were measured photometrically by means of digital photometer (Table 2). DOC was measured using a total organic carbon analyser (Table 2). The concentration of ammonium was determined according to the Russian Standards and Technical Regulations RD 52.24.512-2012, using an Agilent chromatograph (Table 2). Table A 3 lists the samples used, along with the associated hydrochemistry analyses.

2.7.3 Dewatering wells at two opencast mining areas

The dewatering wells are located at two opencast mines, named Hambach and Garzweiler, in the Rhenish lignite-mining area (Figure 3). The Garzweiler opencast mine is located west of Grevenbroich, and its coal is found 40 to 210 m below the Earth's surface. The Hambach opencast mine is located in the Düren and Erft counties, in the centre of the Rhenish lignite-mining area; it is currently 370 m deep. In opencast mining, groundwater levels must be continuously reduced in order to ensure the safety of mining operations; abstraction of the groundwater from different aquifers is controlled by means of filters at various geological layers. Due to the operating water level in the well some wells had aerated and some wells had non-aerated filter screens (Figure 4).

In order, to investigate if aerated and non-aerated filter screens affect the structure, diversity, composition, and quantity of bacterial populations, water samples from wells equipped with aerated and non-aerated filter screens were collected. A total of 34 water samples (150 ml each) were taken from opencast mines in Garzweiler (five aerated and 14 non-aerated) and Hambach (four aerated and 11 non-aerated). Additionally, biofilm samples were obtained from six ochrous-encrusted pumps.

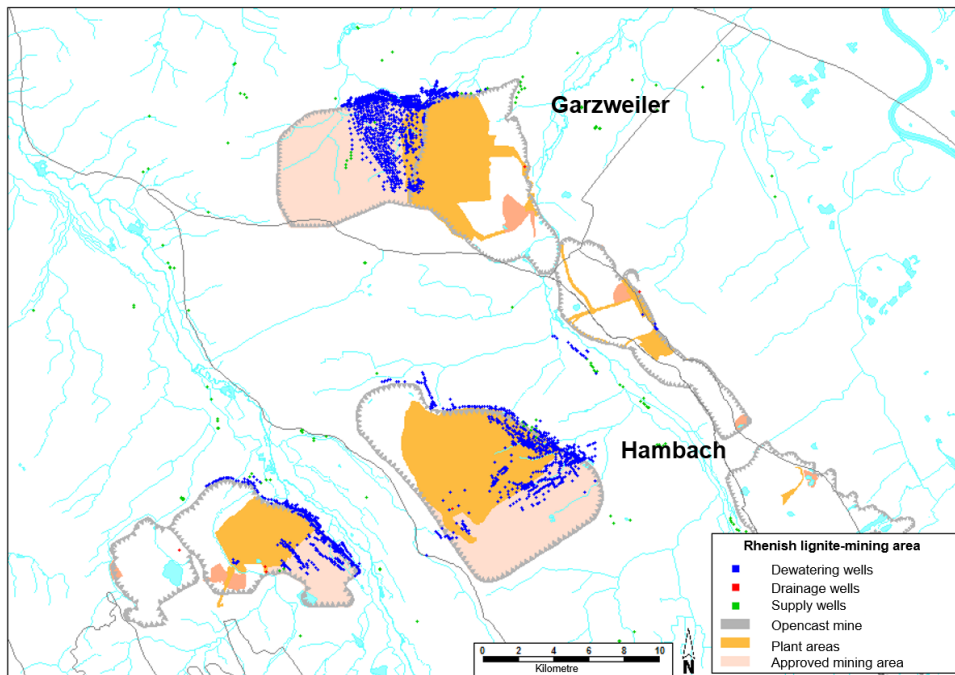


Figure 3. Map of the Rhenish lignite-mining area, with dewatering wells represented by blue dots. (Map was provided by RWE Power AG).

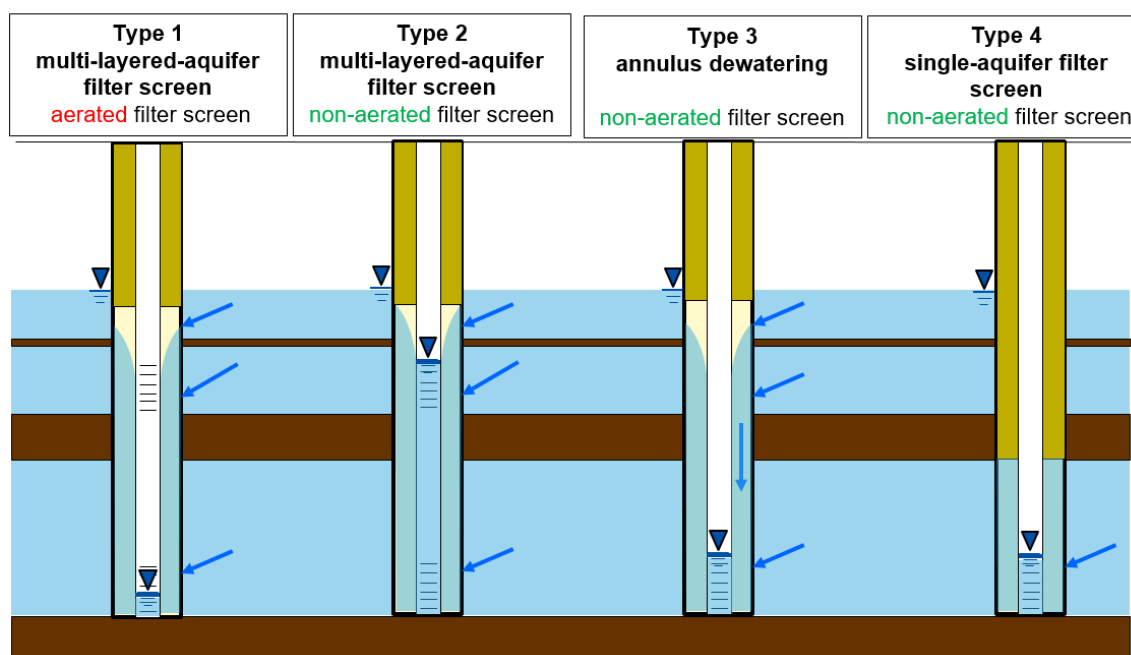


Figure 4. Different types of dewatering well filter screens. (Map was provided by RWE Power AG).

In order to support the biological data, different chemical water parameters were provided by RWE (Table 17). Physicochemical water parameters were determined on-site (pH, redox potential and electrical conductivity) via a WWT multi-parameter analyser (Table 2). Table A 4 provides an overview of the sampling points, their specifications and water chemistry.

Table 17. Methods of different hydrochemical parameters.

Parameter	Method
Temperature	DIN 38404 C 4
Oxygen	DIN 38408 G 22
Iron	DIN EN ISO 11885
Nitrate	DIN EN ISO 10304
Manganese	DIN EN ISO 11885
Ammonium	PA 201
Sulphate	DIN EN ISO 10304
Phosphate	DIN EN ISO 6878

2.7.4 Lab-scale reactor with natural ochrous formation

A lab-scale reactor designed by Hochschule für Technik und Wirtschaft Dresden (HTW) was composed of several columns, which were filled with filter sand. The columns were flushed with natural groundwater obtained from a groundwater test point at the HTW. The iron-clogging of filter sand samples, which were derived from the columns of the lab-scale reactor, was investigated to determine whether chemical and hydromechanical regeneration procedures affect the structure, diversity, composition, and quantity of bacterial populations. In total, the bacterial populations of two test series, with a total of seven columns, in three or four parallel running columns, were investigated. Biofilms were taken from different depths (every 5 to 25 cm) within each column, and two groundwater samples were taken. A total of 26 samples was analysed using biomolecular methods. A particular column was always chosen to represent the control column, without any pretreatment or any kind of regeneration.

All columns consisted of filter sand (Aquagran®) with a pore size of 1 to 2 mm, a length of 50 cm and a diameter of 10 cm. The filter sand originally had a concentration of $0.42 \text{ mg g}^{-1} \text{ Fe}_2\text{O}_3$. The groundwater was pumped directly to the laboratory by means of a submersible pump. After passing through a particle filter, a portion of the groundwater was removed. The remaining water flow passed a non-return valve and distributor before the columns were charged, in parallel, with groundwater. Columns operated in an upflow regime (Figure 5).



Figure 5. A) Picture of the lab-scale reactor with three columns. B) Column with ochrous biofilm.

The test series differed in the regeneration procedures used and the duration of treatment time using oxygenated groundwater.

Test series one (TS I) was carried out between September 2012 and June 2013. Three columns operate in parallel; columns one (S1) and four (S4) operate for 47 and 41 days, respectively. Thereafter, S1 was stored for 120 days, while S4 was stored for 91 days; this was done in order to produce an ageing effect for the ochrous formation as a storage result. Column S1 was immediately regenerated after storage by means of chemical and mechanical regeneration, using three consecutive cycles. One regeneration cycle consisted of four to five stages of hydromechanical and chemical treatment.

First, hydromechanical regeneration was carried out, therefore groundwater was used to flush the column from top to bottom for a period of 60 minutes ($Q = 2.5 \text{ l min}^{-1}$); thereafter, chemical regeneration was performed, using a concentration of 30 g l^{-1} AIXTRACTOR 2.0®, a pH-neutral water well rehabilitation agent with an iron-dissolving component (sodium dithionite), for 45 minutes ($Q = 2.5 \text{ l min}^{-1}$). The last step was always a hydromechanical regeneration. Subsequently, S1 was flushed for 100 days and was then removed from the lab-scale reactor. By comparison, S4 was flushed for seven days and then regenerated by five cycles (see above) of hydromechanical and chemical treatment. In addition, S4 was once again flushed with groundwater for 74 days, followed by a regeneration

procedure that consisted of three cycles and operated again for 23 days. Column six (S6) operated for 169 days with groundwater as a control column, without any treatment.

Test series two (TS II) was carried out between February and July 2014; four columns operated in parallel. In order to release the contained iron, the filter sand of columns five (S5) and eight (S8) was pretreated with AIXTRACTOR 2.0® for 24 hours, whereas the filter sand of columns two (S2) and four (S4) was not pretreated. S2 and S5 ran with groundwater for 57 and 46 days, respectively, before regeneration, whereas S4 and S8 served as the control columns and thus did not undergo regeneration. Figure 6 illustrates the two test series.

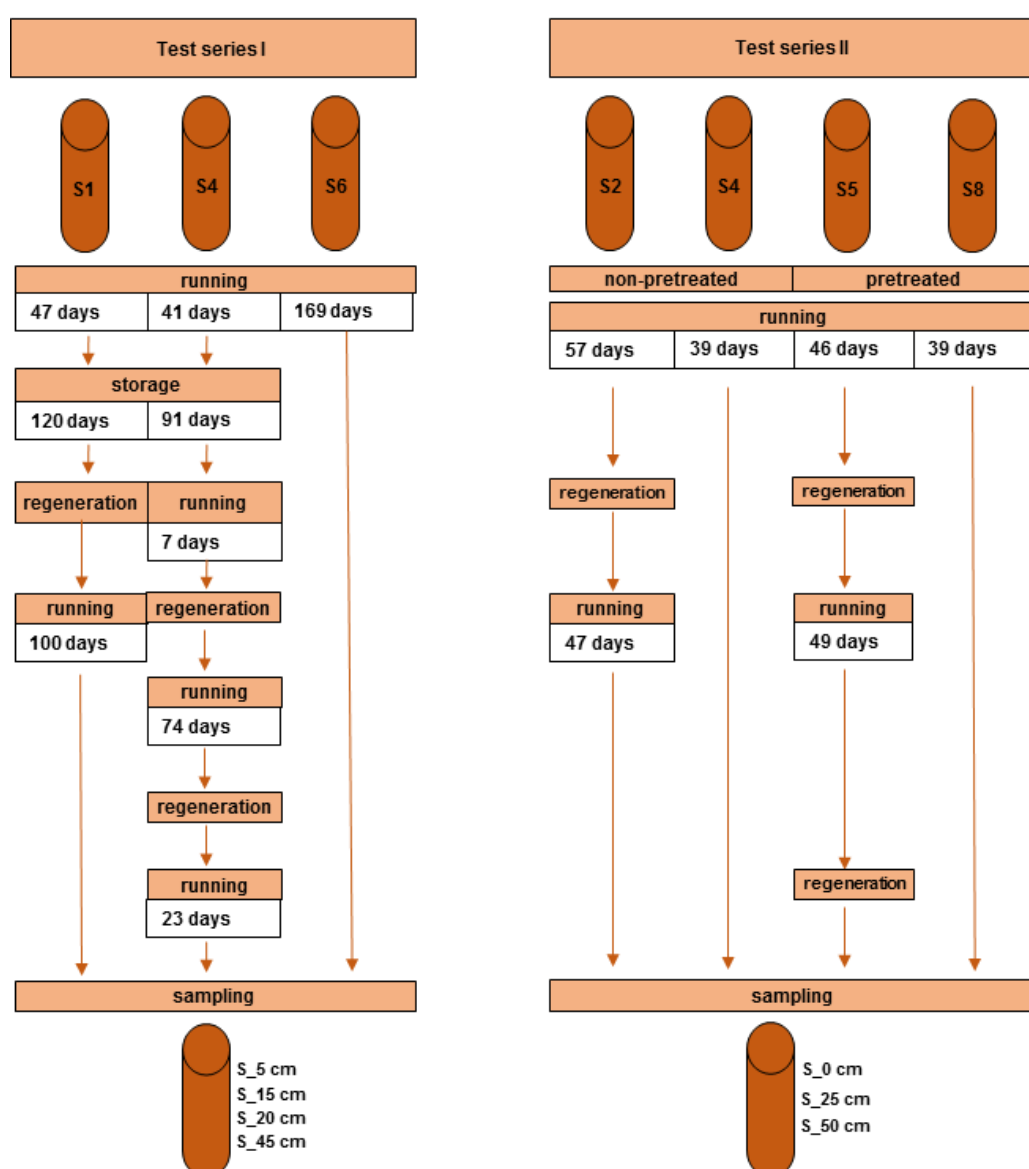


Figure 6. Scheme of lab-scale reactor test series I and II.

Prior to columns flushing, the parameters electrical conductivity, dissolved oxygen, pH and temperature were measured in influent and effluent using a WWT multi-parameter analyser (Table 2). Total iron concentration of groundwater samples was determined using the Aquaquant test (Table 4). The iron content of filter-sand samples from test series II was measured at 5-15 cm, 30-35 cm and 35-45 cm depth by means of flame atomic absorption spectrometry (FAAS). The hydraulic conductivity coefficient (k_f -value) was calculated according to Darcy's law. The values of all parameters were provided by HTW Dresden. All test series, columns, hydrochemical parameters and regeneration types are summarized in Table A 4.

2.8 Isolation of iron-depositing bacteria

In order to isolate iron-depositing bacteria, ochrous samples of 1 g were serially decimally diluted from 10^{-1} to 10^{-4} ml with 1x PBS (Table 12) and 100 μ l of each dilution were plated on LSM2 media (Table 7) and H₂O media (Table 8).

Plates were incubated at room temperature for two to three weeks until dark or reddish-brown colonies developed. Colonies were picked with sterile toothpicks and subcultured until pure cultures originated. Cell morphology and purity were monitored using a phase-contrast microscope (Table 2). Iron and manganese deposition activity of the isolates was verified by dissolving the colonies with oxalic acid (10 %) in order to avoid incorrect classification as a result of pigmentation as described by Schmidt et al. (2014).

2.9 DNA extraction

Prior to DNA extraction, water samples were filtered using a polycarbonate filter with a pore size of 0.2 μ m (Table 4). Ochrous samples and bacterial cell material were respectively homogenized for 1 min; thereafter, 0.25 g of the homogenized ochrous or bacterial cell samples was taken for DNA extraction.

The filters, homogenized ochrous samples or bacterial cell material were then used for total DNA extraction, respectively by means of Soil DNA Purification Kit

(Table 4), according to the manufacturer's instructions. The DNA was finally eluted with 70 μ l elution buffer.

2.10 Amplification of the 16S rRNA gene and clone library construction

The total community DNA from water, ochrous samples or isolated strains was amplified using primer pair 63f and 1387r (Table 5), to ensure nearly complete 16S rRNA gene amplification. Master Mix composition and PCR programs are shown in Table 18 and Table 19. PCR products were visualized on an 1 % agarose gel and photographed with a gel documentation system (Table 2). 8 μ l of each PCR reaction was mixed with 2 μ l gel loading dye (Table 1). The gel ran at 100 V for 60 min in 0.5 x TAE buffer (Table 1); thereafter, it was stained with ethidium bromide (10 mg ml⁻¹) for 10 min. 16S rDNA amplicons from the ochrous and water samples were chosen for further community analysis by means of clone library construction. Cloning and sequencing services were performed by Macrogen (Seoul, South Korea), with primer M13F. For each sample, 48 to 96 clones, depending on genetic diversity of each sample were obtained. Sequencing of the 16S rRNA gene of the isolated strains was done in both primer directions in order to obtain almost the complete 16S rDNA sequence.

Table 18. PCR Master Mix composition for primer pair 63f and 1387r.

Reagent	Volume	Final concentration
PCR water	21 μ l	
<i>Taq</i> PCR Master-Mix (ready-to-use)	25 μ l	1x
Primer 63f	1.5 μ l	0.6 μ M
Primer 1387r	1.5 μ l	0.6 μ M
Template DNA	1 μ l	
Total volume	50 μ l	

Table 19. PCR program for primer pair 63f and 1387r.

Initial denaturation	95 °C	120 sec	
Denaturation	95 °C	20 sec	
Annealing	58 °C	30 sec	33 cycles
Extension	72 °C	120 sec	
Final extension	72 °C	1200 sec	
Hold	8 °C	∞	

2.11 Sequence analysis performed by BioNumerics software

The sequence chromatograms of the amplified 16S rRNA gene derived from bacterial clones and isolates were trimmed, according to the manufacturer's quality filter, using BioNumerics software 8.2 (Table 3) followed by manually controlling and trimming in order to form high-quality sequences. Sequences were clustered into operational taxonomic units (OTUs) by 97 % sequence similarity, using the Needleman-Wunsch algorithm with a CLUSTW similarity calculation in order to create multiple alignments. Distance-based evolutionary trees were constructed using UPGMA clustering and the Kimura 2-parameter correction. Bootstrap analysis was performed using a round of 1.000 samplings. Furthermore, OTUs were identified using the RDP Naïve Bayesian rRNA Classifier, Version 2.6 (Wang et al., 2007), and the NCBI database (Altschul et al., 1990), using the nucleotide collection database, excluding uncultured/environmental sample sequences. For the BLAST algorithm, a megablast, based on the Greedy-algorithm (Zhang et al., 2000), was chosen.

2.12 Amplification of the V3 fragment from the 16S rRNA gene

For the amplification of the 16S rRNA gene, the universal primer pair p2 and p3 (Table 5) was used, which is located in the conserved sequence area that covers the variable V3 region. The amplification program and Master Mix composition were adapted according to Muyzer et al. (1993) as summarized in Table 20 and Table 21. A final extension of 30 min at 72 °C was added in order to prevent the

formation of double bands (Janse et al., 2004). PCR reaction was conducted as described in chapter 2.10. The amplified PCR products were cleaned using the PCR/DNA clean-up kit (Table 4), then the DNA concentration was measured using a NanoDrop spectrometer (Table 2). For each sample, a concentration of 10 ng μl^{-1} was used in order to generate genetic fingerprints by conducting the denaturing gradient gel electrophoresis (DGGE) analysis (Table 2).

Table 20. Master Mix composition for primer pair p2 and p3.

Reagent	Volume	Final concentration
PCR water	21 μl	1x
Perpetual <i>Taq</i> PCR Master-Mix (ready-to-use)	25 μl	
Primer p2	1.5 μl	
Primer p3	1.5 μl	0.6 μM
Template DNA	1 μl	
Total volume	50 μl	

Table 21. PCR program for primer pair p2 and p3.

Initial denaturation	96 °C	5 min	
Denaturation	94 °C	1 min	
Annealing	65 °C	1 min	-0.5 °C and 20 cycles
Extension	72 °C	1 min	
Denaturation	94 °C	1 min	
Annealing	55 °C	1 min	15 cycles
Extension	72 °C	1 min	
Finale extension	72 °C	30 min	
Hold	8 °C	∞	

2.13 Denaturing gradient gel electrophoresis (DGGE) of V3 region of the 16S rRNA gene

In order to compare bacterial diversity and structure of different ochrous and water samples, DGGE analysis was performed. The INGENYphorU system (Table 2) was used to perform the DGGE analysis according to manufacturer's instructions, preparing an 8 % polyacrylamide gel. The resolving gels were made from stock solutions 0 % and 80 % with a chemical denaturing gradient that ranged from 40 % to 65 %.

The PCR products (V3 region) were adjusted to a volume of a final concentration of 10 ng μl^{-1} with PCR water; in addition, 5 μl of 6x Orange G DNA loading dye (Table 13) per well was added to the sample. The DGGE marker II (Table 4) was loaded in the two outer lanes and the middle lane of each gel. Electrophoresis was performed at a constant voltage of 100 V for 18 h and at a temperature of 60 °C. After electrophoresis, both gels were stained for 15 min with 1x SYBR Green I solution (Table 15); they were then destained with Milli-Q water for 10 min, followed by gel visualisation and documentation (Table 2).

Table 22. Composition of DGGE stock solutions.

Reagent	Amount	
	0 % solution	80 % solution
Acrylamide/bis-acrylamide [ml]	60	60
50x TAE (pH 8.3) [ml]	6	6
Urea [g]	0	100.8
Formamide (de-ionized) [ml]	0	96
ad Milli-Q water [ml]	300	300

Using the BioNumerics software package (5.2), the DGGE profiles were analysed for similarities by means of digital image analysis and were subjected to a series of steps that were intended to allow the comparison of multiple gel images. Thus, each lane was normalised to the reference marker run in each gel. DGGE profiles were initially optimised for each calculated cluster analysis by the estimation of comparison settings (position tolerance (%) and optimisation (%)). Relatedness of microbial communities was determined using the Dice coefficient in order to allow the performance of pairwise calculations of the bands that were shared

between samples. The similarity matrix of patterns was calculated using the unweighted-pair group method, applying average linkages (UPGMA).

In addition, DGGE patterns from all sampling sites were analysed and compared according to their range-weighted richness (*Rr*) and functional organisation (*Fo*). Furthermore, for groundwater samples derived from different abstraction phases, the dynamics (*Dy*) that reflected the specific rate of species that came to significant dominance, were determined. These *Rr*, *Fo* and *Dy* values were calculated as described by Marzorati et al. (2008).

2.14 Preparation of standards and quantification of 16S rRNA gene copies (qPCR)

The number of bacterial gene copies of the 16S rRNA gene in the total genomic DNA of water and ochrous biofilm samples was calculated using quantitative PCR (qPCR), which was performed with a Rotor-Gene real-time PCR cycycler (Table 2). All qPCR assays were performed using a SG qPCR Master Mix (Table 4); the Master Mix composition is listed in Table 23. The specific programs for each amplification are shown in Table 24 to Table 28.

The decimal dilution series of PCR products of the *Rhodoferrax ferrireducens* and *Geothrix fermentans* 16S rRNA gene (63f and 1387r) were used as a standard for bacterial qPCR analysis, respectively. For the quantification of the 16S rRNA gene from *Gallionella* spp. and *Crenothrix polyspora*, plasmid DNAs of bacterial clones were provided by MacroGen. The target copy number for DNA standard was calculated, assuming a molecular mass of 660 Da for dsDNA, using the following equation (Smith et al., 2006):

$$CN_{ST} = \frac{N_A * c_{ST}}{MW} * \frac{1}{1000}$$

CN_{ST} = Gene copies of standard μl^{-1}

N_A = Avogadro's constant ($6.023 \times 10^{23} \text{ mol}^{-1}$)

c_{ST} = Measured concentration of standard (PCR product) ($\text{g } \mu\text{l}^{-1}$)

MW = Molecular weight of standard (base pairs * molecular mass) (g mol^{-1})

Gene copy numbers were measured in a range of 10^2 to 10^8 gene copies μl^{-1} . Template DNA was tenfold diluted in order to minimise polymerisation problems caused by e.g., humic substances or iron hydroxides in samples. Each sample was tested in duplicate for each run. Non-DNA containing samples were used as no template control (NTC). To ensure the accuracy of the qPCRs, a melt curve analysis (55-99°C) was performed at the end of the qPCR in order to specify primer annealing. Quantification was performed using standard curves obtained from the amplification profiles of known concentrations of the respective standard. PCR efficiency and r^2 was calculated using the Rotor-Gene software package (Table 3). The final concentrations of gene copies ml^{-1} or g^{-1} were calculated using the following equations:

$$CN_{OS} = GC_{OS} * df * ef * 4$$

CN_{OS} = Gene copies g^{-1} ochrous sample

GC_{OS} = Gene copies μl^{-1} (calculated by the Rotor-Gene software package)

df = DNA dilution factor

ef = DNA elution factor after extraction

$$CN_{WS} = \frac{GC_{WS} * df * ef}{V_{WS}}$$

CN_{OS} = Gene copies ml^{-1} water sample

GC_{WS} = Gene copies μl^{-1} (calculated by the Rotor-Gene software package)

df = DNA dilution factor

ef = DNA elution factor after extraction

V_{WS} = Volume of extracted water sample (ml)

Table 23. Master Mix composition of qPCR assay.

Reagent	Volume	Final concentration
PCR water	9 µl	
SG qPCR Master-Mix (ready-to-use)	12.5 µl	1x
Primer forward	0.75 µl	0.6 µM
Primer reverse	0.75 µl	0.6 µM
Template DNA	2 µl	
Total volume	25 µl	

Table 24. qPCR for universal primer pair Uni907R and Uni338F_RC.

Initial denaturation	95 °C	2 min	
Denaturation	95 °C	20 s	
Annealing	60,4 °C	30 s	40 cycles
Extension	72 °C	1 min	

Table 25. qPCR for *Rhodoferrax ferrireducens* primer pair RodoR_RC and Uni907R.

Initial denaturation	95 °C	2 min	
Denaturation	95 °C	20 s	
Annealing	58 °C	30 s	40 cycles
Extension	72 °C	1 min	

Table 26. qPCR for *Gallionella*-like group primer pair 628F and 998R.

Initial denaturation	95 °C	2 min	
Denaturation	95 °C	20 s	
Annealing	51 °C	20 s	45 cycles
Extension	72 °C	45 s	

Table 27. qPCR for *Crenothrix polyspora* primer pair Creno 139f and EUB338.

Initial denaturation	95 °C	2 min	
Denaturation	95 °C	40 s	
Annealing	59 °C	30 s	45 cycles
Extension	72 °C	40 s	

Table 28. qPCR for *Geothrix fermentans* primer pair 448R and 193F.

Initial denaturation	95 °C	3 min	
Denaturation	95 °C	20 s	
Annealing	58 °C	20 s	45 cycles
Extension	72 °C	30 s	

In addition, analysis of the Hellinger-transformed gene copy data of all qPCR assays (Table 6), was done in order to determine the differences in microbial gene copy numbers between samples via Principle component analysis (PCA), using the R package VEGAN. Additionally, redundancy analysis (RDA) was utilized to quantify the variance in gene copy numbers that arose as a result of environmental factors. The statistical model was specified via backward-stepwise selection by function *ordistep*. The significance of the parameters investigated within the selected model was assessed by means of 10^4 restricted permutations. The statistical analysis of differences between groups was assessed by analysis of variance (ANOVA), using the *adonis* function.

2.15 454-pyrosequencing

Amplification of the variable V1-V3 region of the 16S rRNA gene was done using primer pair 28F/519R and 454-pyrosequencing was performed on a 454-Genome Sequencer-FLX system (Table 2) by Research and Testing Laboratories (Texas, USA), as described by Dowd et al. (2008).

The analysis of the 454-pyrosequencing results, including biostatistics and bioinformatics, was performed by omicstoview.consulting GbR (Kiel, Germany). Preprocessing and quality filtering of the data was performed employing MOTHUR version 1.32.1. as described by Stratil et al. (2013). The exclusion of

low quality and short reads (≤ 200 bp) was performed as previously described by Braun et al. (2016). Sequences were then clustered into OTUs by 97 % sequence similarity, using MOTHUR's average neighbour algorithm.

Multivariate statistics and data analysis were performed in R (Table 3). Alpha diversity was calculated by Shannon index; indicator species analysis was performed using the R package *indicspecies*, v1.6.5.

2.16 Elemental composition of ochrous samples

Measurement of loss-on-ignition (LOI) and x-ray fluorescence (XRF) was performed at TU Berlin (Institute for Applied Geosciences, Department of Hydrogeology).

Ochrous samples were dried in an incubator at 35 °C for five days. Thereafter, the dried samples were finely ground using a disc mill. LOI and x-ray fluorescence analyses were performed for several ochrous samples derived from the drinking water wells in Berlin, as presented in Table A 1.

2.16.1 Loss-on-ignition

In order to estimate the LOI of the ochrous samples taken from the Berlin groundwater wells, LOI was measured using a fibre furnace (Table 2). In the furnace, approximately 1 g of each dried sample was ignited at 1000 °C for an hour; LOI was calculated as the percentage difference to the dry weight.

2.16.2 X-ray fluorescence analysis

Dried samples of 7 g were required to measure the concentration of trace elements (at ppm level) and major elements (up to 100 %) in the ochrous samples. The production of powder-compressed tablets was done by means of a press (Table 2), and the preparation of orodispersible tablets was carried out using a crucible melter (Table 2) at 1200 °C. X-ray fluorescence analysis was performed using a PW 2400 sequential WDXRF spectrometer (Table 2), equipped with SuperQ and Uniquant software (Table 3).

3 Results

3.1 Chemical and biomolecular investigations of ochrous biofilms originating from pumps of drinking water wells

The drinking water wells were located at various water galleries in Berlin, Germany (Figure 1). In order to perform biomolecular analyses of the bacterial populations' inhabiting ochrous biofilms of pumps from these drinking water wells, a total of 17 biofilm samples were taken. The water wells investigated were grouped into clogged (12 samples) and non-clogged (5 samples) categories, depending on their ochrous grade. Wells with an ochrous grade of at least 1 cm thickness around their pumps' suction strainer were considered as clogged (Figure 7 A), while those with less than 1 cm thickness were classified as non-clogged (Figure 7 B). A further nine water wells, that were classified as non-clogged could only be used for chemical analysis of their water due to the fact that no biofilm formation was present around their pumps (Chapter 2.7.1).



Figure 7. The pump inlets of drinking water wells in Berlin. (A) Deposits of at least 1 cm thickness (classified as clogged wells) and (B) thin deposits (classified as non-clogged wells).

3.1.1 Hydrochemistry of the drinking water wells

A total of 26 water wells served as subjects for chemical water analyses; of these, 12 water wells were classified as clogged and 14 as non-clogged. The water characteristics of the drinking water wells investigated are listed in Table A 1.

Within the wells, the mean water temperature was 11.3 ± 1.3 °C for clogged wells and 10.9 ± 5.5 °C for non-clogged wells. The pH values of both clogged and non-clogged wells varied from 7.3 to 7.6. Furthermore, electrical conductivity ranged from 782.8 ± 120.3 $\mu\text{S cm}^{-1}$ to 787.8 ± 8.3 $\mu\text{S cm}^{-1}$ for clogged and non-clogged wells, respectively. Dissolved oxygen concentrations and redox potential were only determined for clogged wells, yielding a mean of 0.2 ± 0.2 oxygen mg l^{-1} and a redox potential of $-47.3 \pm \text{mV}$. The DOC ranged from 2.1 to 6.6 mg l^{-1} for clogged wells, while a mean value of 4.4 mg l^{-1} was observed for non-clogged wells. Furthermore, iron(II), total iron and nitrate showed comparable mean concentrations in clogged and non-clogged wells, at 1.2 mg l^{-1} , 1.2 mg l^{-1} and 0.4 mg l^{-1} , respectively. Higher values for ammonia, manganese, phosphate and sulphate were found in non-clogged wells (Table A 1).

3.1.2 Denaturing gradient gel electrophoresis profiling of the bacterial communities of drinking water wells

The DGGE method was used to compare the large number of samples derived from the various pumps and to obtain an overview of the bacterial genetic diversity and variation within the samples. The DGGE analysis of the 16S rDNA amplicons from 17 ochrous samples revealed highly diverse bacterial communities of the ochrous biofilms, as indicated by a high number of bands in the range of 23 to 45 present in each lane. The DGGE patterns of all samples showed the presence of a number of stronger bands and a large number of less intense bands (Figure 8). The DGGE patterns from the wells of the same water galleries resulted in different DGGE profiles. Band-based similarity calculations clearly showed two clusters of approximately 80 % similarity; however, no correlation between the microbial patterns of clogged and non-clogged wells could be inferred.

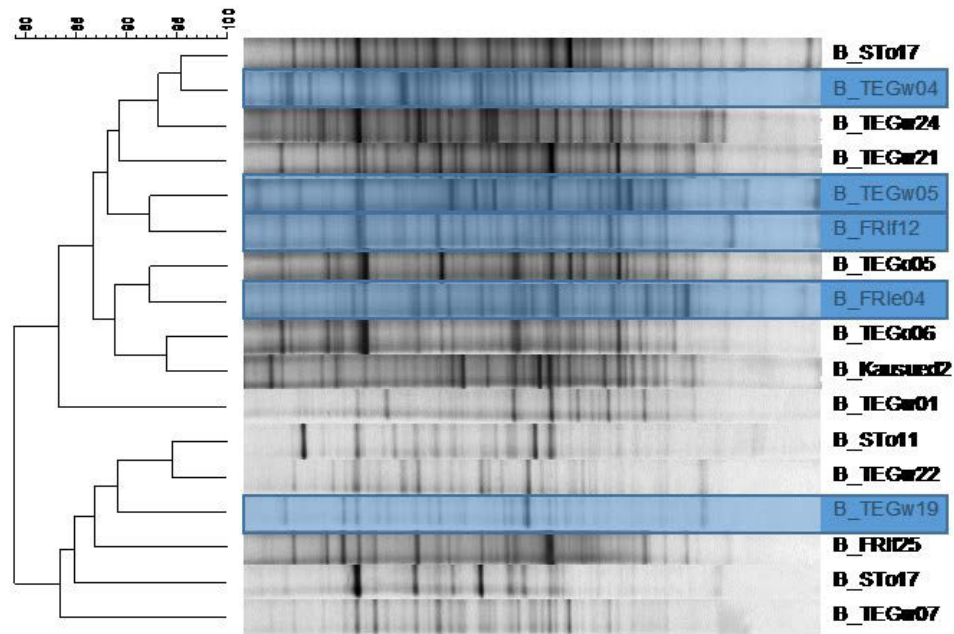


Figure 8. Dendrogram constructed with bacterial community fingerprints of biofilm samples obtained from drinking water wells in Berlin. This dendrogram is based on the Dice coefficient and the UPGMA cluster analysis. The scale bar indicates the similarity of community profiles [%] between non-clogged wells (marked with blue frames) and the clogged well group.

An additional parameter for evaluating the bacterial community composition based on DGGE analysis is the functional organisation (*Fo*) of the microorganisms that are most fitting to the environmental-microbiological interactions. In order to graphically represent the structure of the bacterial communities obtained from drinking water wells, Pareto-Lorenz (P-L) evenness curves were constructed. Figure 9 shows, 17 P-L curves based on the DGGE patterns of the pump biofilms. For both groups, a medium *Fo* was detected, as 20 % of the bands (number-based) corresponded with an average of 40 to 70 % of the cumulative band intensities. Here, the most fitting species are dominant and present in high numbers, while the majority (the remaining 80 % on the x-axis) are present in lower quantities. No differences could be determined on the vertical 20 % P-L line line between the clogged and non-clogged pumps; thus, *Fo* was highly comparable between the two groups.

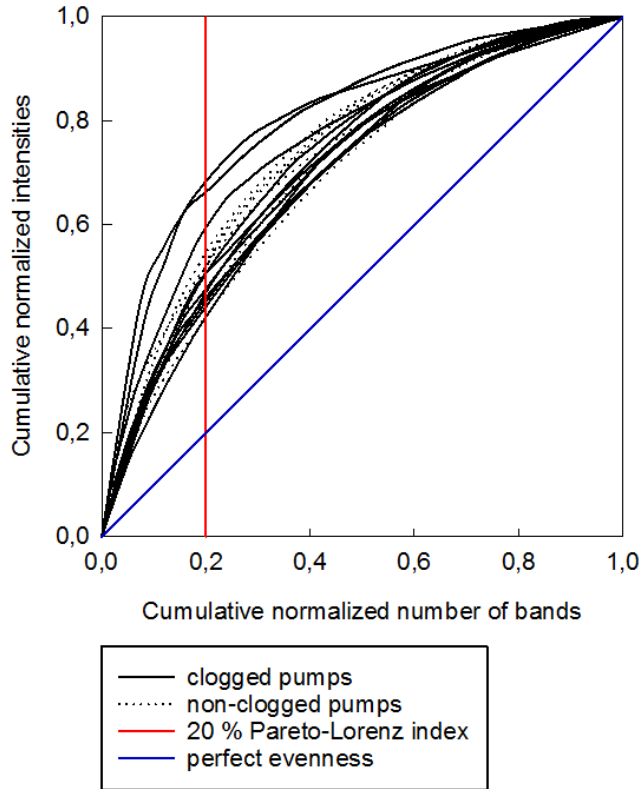


Figure 9. Comparison of the P-L distribution curves based on the DGGE profiles of the bacterial communities of clogged and non-clogged drinking water well pumps in Berlin.

Additionally, the range-weighted richness (R_r) was calculated by the distribution (number) of bands in one lane and correlated with the denaturing gradient percentage of the gel (25 %). The R_r -values of the bacterial communities of both the clogged and non-clogged pumps are illustrated in Figure 10. The mean R_r of the clogged wells was 221.9 ± 97.6 , while that of the non-clogged wells was 275.6 ± 106.2 .

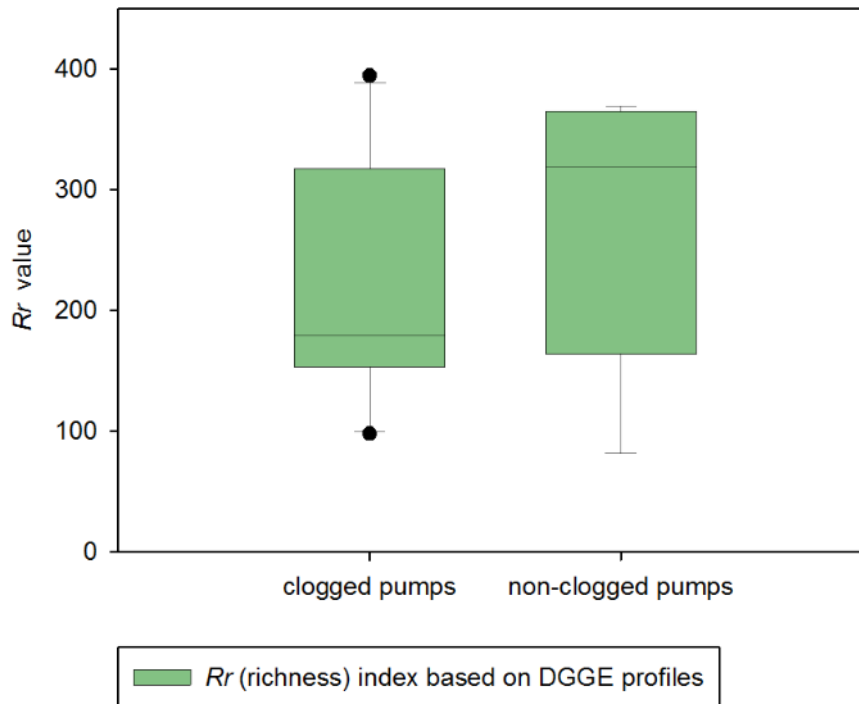


Figure 10. Boxplot of R_r -values based on DGGE profiles of samples taken from clogged and non-clogged drinking water well pumps in Berlin. Dots are outlier.

3.1.3 Bacterial population analysis of drinking water well samples by 16S rRNA gene clone libraries

Two samples deriving from DGGE cluster one and two from cluster two were chosen for clone library construction of the 16S rRNA gene (Chapter 2.10) in order to analyse the composition of the bacterial communities of both the clogged and non-clogged wells. For each sample, 96 clones were obtained, which were respectively classified as either clogged or non-clogged.

The quality check (Chapter 2.11) left 57 sequences from the group non-clogged drinking water wells, which were assigned to a total of 46 OTUs; however, 89 sequences were left from the group of clogged wells and could be assigned to 69 OTUs. The relative abundance of OTUs at the phylum and genus levels is depicted in Figure 11. OTUs with high homology to the phylum *Proteobacteria* were the most abundant group in both sample types (75 % in clogged and 61 % in non-clogged wells), followed by *Bacteroidetes* (6 % in clogged and 15 % in

non-clogged wells), *Acidobacteria* (1 % in clogged and 7 % in non-clogged wells) and uncl. *Bacteria* (18 % in clogged and 13 % in non-clogged wells). Within the *Proteobacteria* phylum, the class *Deltaproteobacteria* was predominant. In addition, the phyla *Actinobacteria* and *Firmicutes* could only be detected in non-clogged wells.

Furthermore, the top 10 OTUs at the genus level of both the clogged and non-clogged groups were evaluated and showed fewer differences. The top OTUs of both groups were primarily associated with the iron-reducing genus *Geobacter* and the heterotrophic *Pseudomonas* and *Brevundimonas* genera. However, the top 10 OTUs represented only 35 % of the total bacterial communities of each well group. Other OTUs (the remaining percentage) were characterized by only one sequence per OTU.

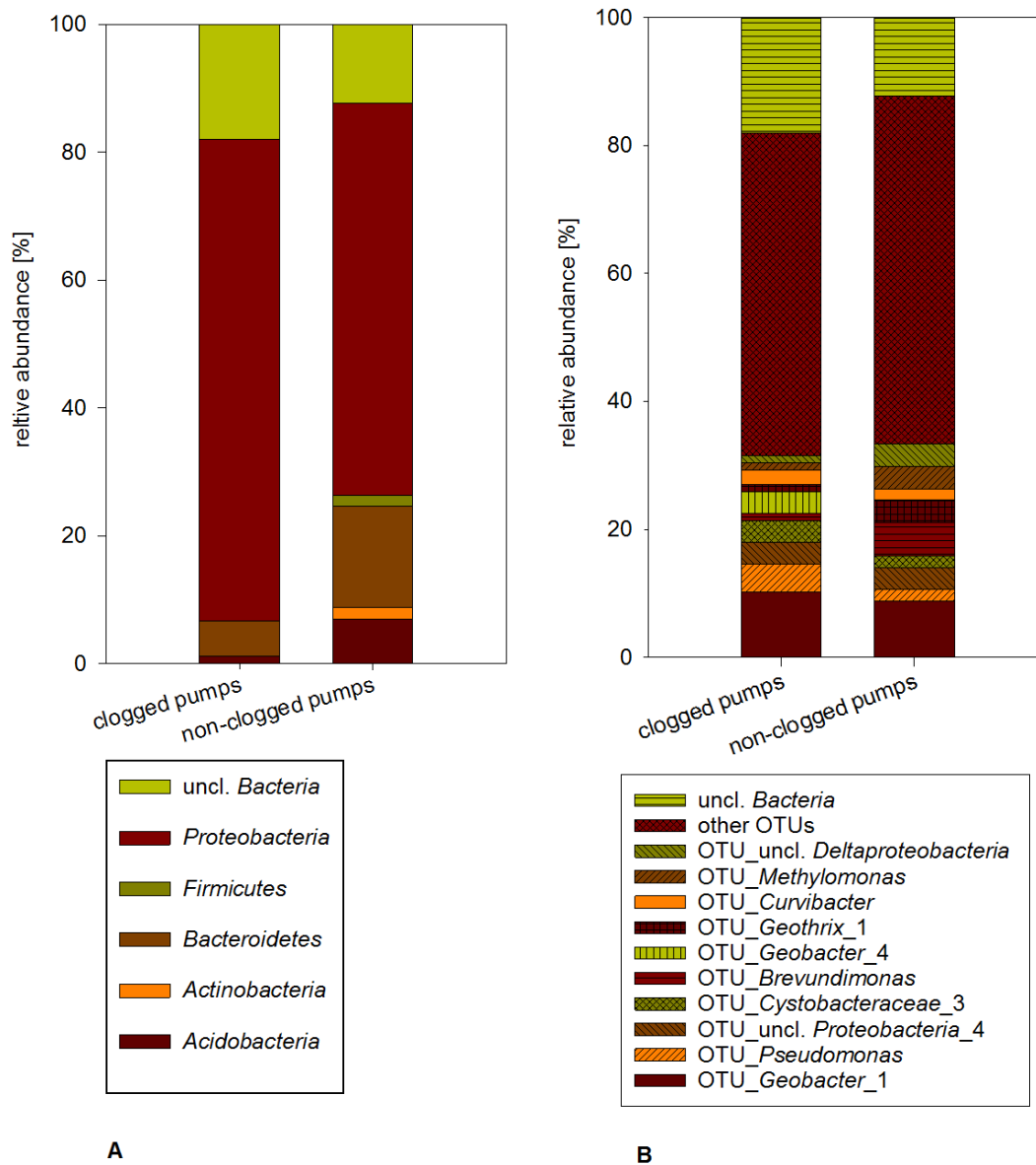


Figure 11. Plots of 16S rRNA clone libraries at (A) the phylum level and (B) the top 10 OTUs (at the genus level) of the microbial communities of the biofilm samples obtained from clogged and non-clogged drinking water well pumps in Berlin.

3.1.4 Quantification of 16S rRNA gene copies from ochrous biofilms taken from clogged and non-clogged drinking water wells

The number of bacterial gene copies of the 16S rRNA gene in the total genomic DNA of 17 ochrous samples was calculated by using quantitative PCR (qPCR). The specific primers for each amplification and program are listed in Table 6 and Table 25 to Table 28.

The quantitation reports obtained from qPCR runs always had a certain reaction efficiency of 80 to 95 %, as well as a required r^2 value of >0.99 . The melt curve

analysis at the end of each run showed, dependent on fragment size, overlapping peaks at a consistent temperature and a second, lower peak of the negative control, which was due to the remaining primers in the reaction.

Real-time PCR showed major differences in the numbers of 16S rRNA gene copies of the investigated bacterial groups (Figure 12). The gene copy numbers of the 16S rRNA gene g^{-1} in all of the investigated bacterial groups were higher in clogged wells than in non-clogged wells, with the exception of the assay that targeted the iron-reducing group *Geothrix fermentans*. The *Bacteria* gene copy number in clogged wells revealed a mean of $1.8 \times 10^{10} \text{ g}^{-1}$, in contrast to the 3×10^9 gene copies g^{-1} detected in the non-clogged wells. Specific quantification of iron-oxidising *Gallionella*-related genes revealed that this group was highly abundant in clogged wells; the average gene copy number was $9.5 \times 10^9 \text{ g}^{-1}$. Gene copies related to *Rhodoferrax ferrireducens* were the second-most abundant group detected in the ochrous biofilm samples taken from the various drinking water wells. *Rhodoferrax*-related gene copies had an average number of $6.2 \times 10^9 \text{ g}^{-1}$ in clogged wells and a lower number of $6.54 \times 10^8 \text{ g}^{-1}$ in non-clogged wells. In order to quantify the number of methanotrophic bacteria, the genus *Crenothrix* was chosen; the *Crenothrix* assay showed the highest deviation between clogged ($1.3 \times 10^8 \text{ g}^{-1}$) and non-clogged wells ($3.2 \times 10^6 \text{ g}^{-1}$).

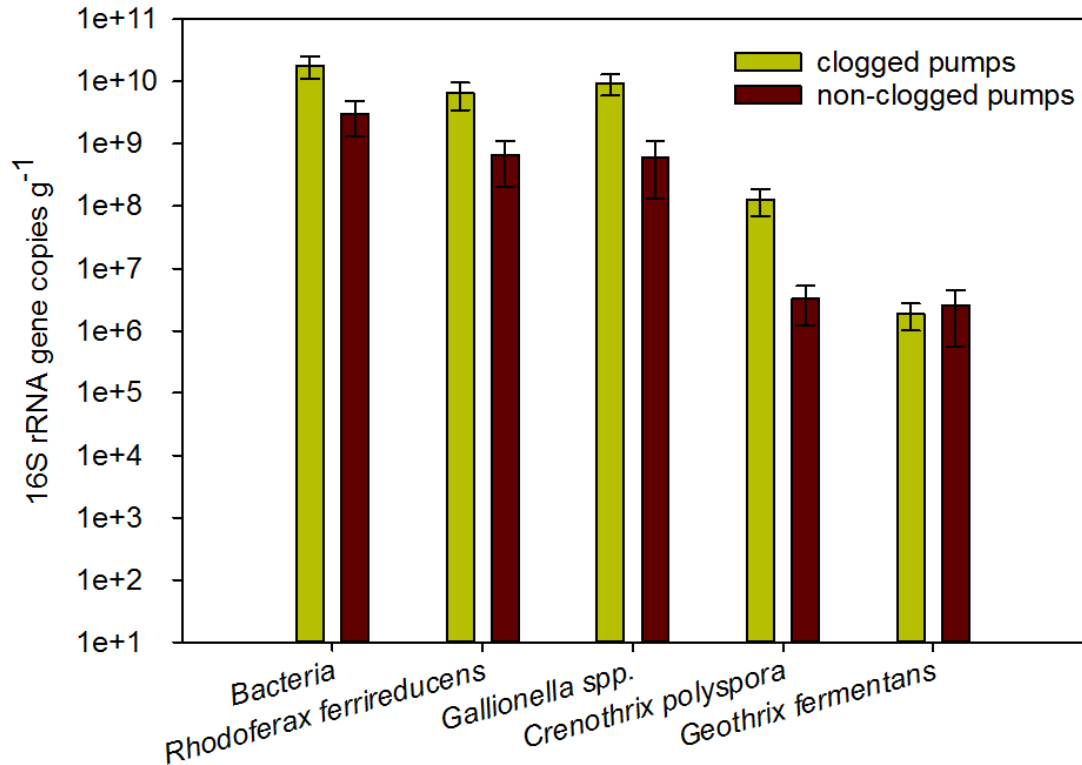


Figure 12. Plot of 16S rRNA gene copies of ochrous biofilms taken from clogged and non-clogged pumps, targeting *Bacteria*, *Rhodoferrax ferrireducens*, *Gallionella* spp., *Crenothrix polyspora* and *Geothrix fermentans*. Error bars represent the standard error.

Furthermore, correlation analysis, based on the gene copy data of all of the qPCR assays, was conducted via principle component analysis (PCA) in order to determine the differences in microbial gene copy numbers between the clogged and non-clogged pumps.

Additionally, redundancy analysis (RDA) was applied to explain the variance of the gene copy data by investigating the environmental factors that affected these two groups; the findings thereof are illustrated in

Figure 13. The results indicated no significant differences between the two groups. The model explained a fairly large portion of the variance ($r^2=32\%$) by DOC. Of all the analysed parameters, only DOC demonstrated the ability to affect the variance in bacterial abundance between the clogged and non-clogged wells ($p\text{-value}_{\text{DOC}} = 0.05$); a higher sample number is needed to verify significance.

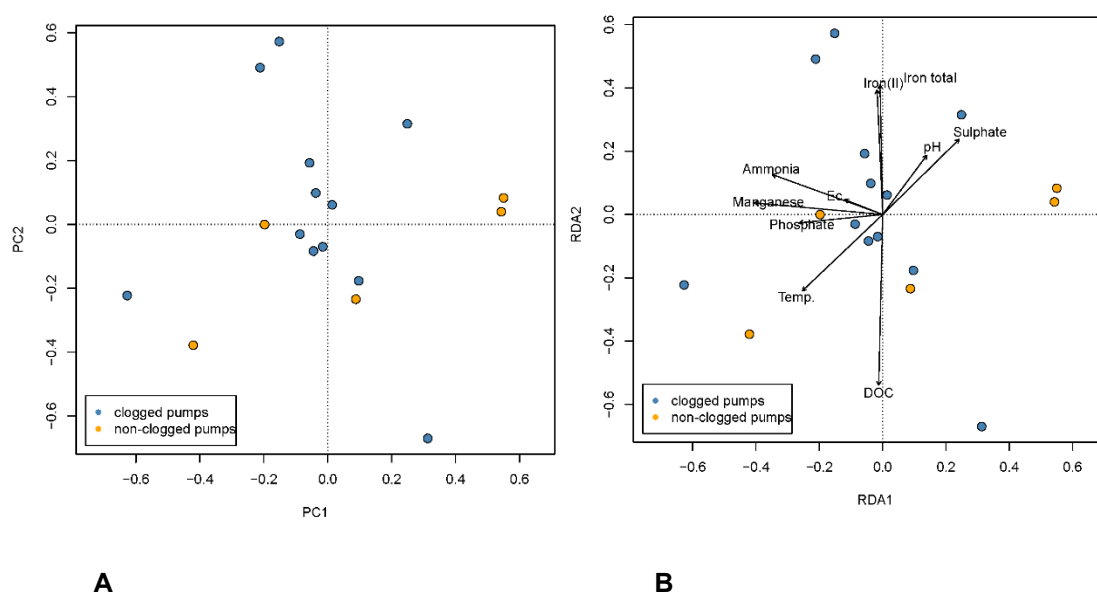


Figure 13. Graphical representations of A) PCA and B) RDA. The PCA represents the differences in the quantities of several bacterial groups between the clogged and non-clogged groups, while the RDA model depicts the influence of environmental factors on the two microbial groups. The lengths and direction of the arrows indicate importance and the correlation of environmental variables to the bacterial communities.

3.1.5 Loss-on-ignition and x-ray fluorescence analysis of ochrous samples from drinking water wells

The LOI of nine ochrous samples from the drinking water wells were measured; in addition, wavelength dispersive XRF analysis was used to perform both qualitative and quantitative analysis of a large number of compounds in the ochrous samples. The results of the LOI and XRF are shown in Figure 14; LOI ranged from 25.4 to 29.1 %. The most abundant element in the ochrous samples was Fe_2O_3 , with a range of 52.6 to 70.72 %. Other compounds present in the ochrous samples were P_2O_5 , SiO_2 and CaO ; B_TEGw_01 had, when compared to the other ochrous samples, a high Ba abundance of 10.8 %. No comparison could be made between the clogged and non-clogged pump groups due to the absence of ochrous biofilms from non-clogged wells.

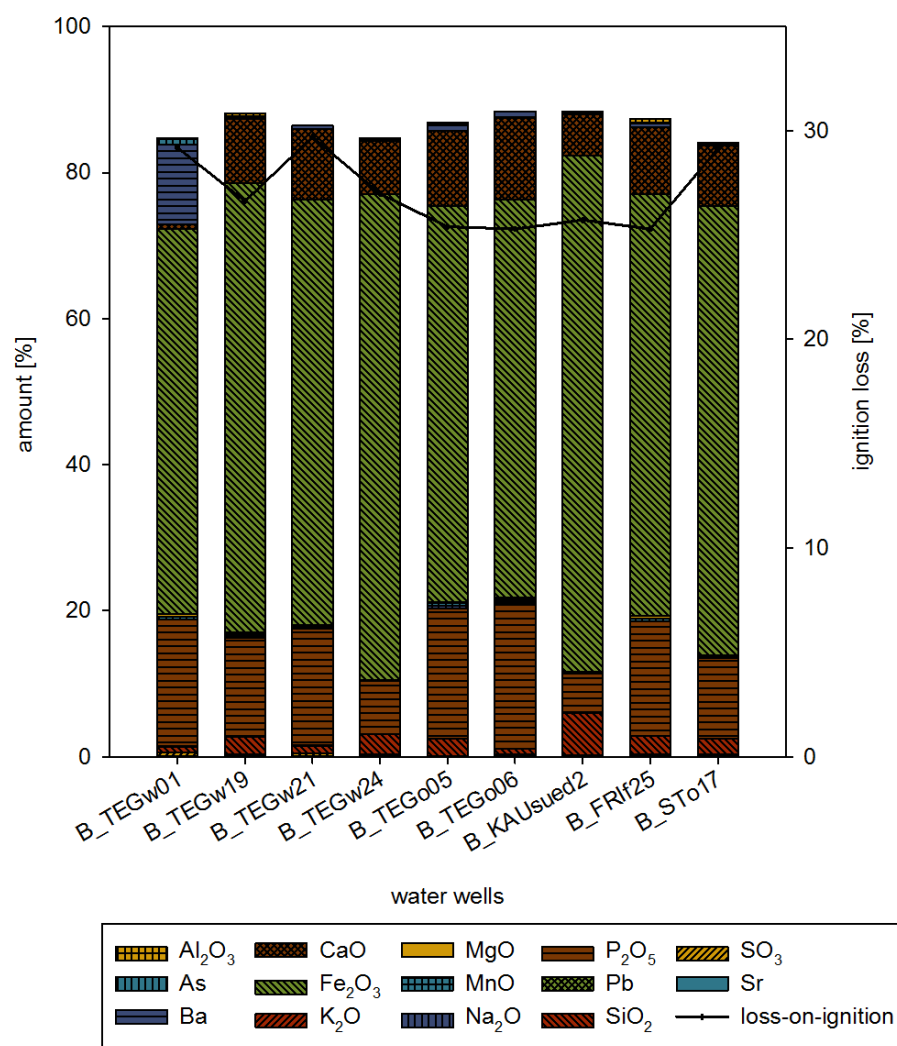


Figure 14. XRF analysis and LOI of nine ochrous samples obtained from drinking water wells in Berlin.

3.2 Chemical and biomolecular investigations of water and biofilm samples from the water catchment area in Russia

The sampling site is located in the far east of Russia, near the Amur River and the water catchment area investigated is equipped with an in-situ subsurface iron and manganese removal system that produces drinking water. In order to analyse the bacterial populations associated with the decreased abstraction volume of the water wells, three different sampling campaigns (Chapter 2.7.2) were considered; thus, a total number of 42 water and biofilm samples were recorded. Table A 2 provides an overview of sampling campaigns and the well infrastructure.

3.2.1 Hydrochemistry of the water catchment area according to sampling campaigns

Table A 3 lists the samples used, along with the associated hydrochemistry analyses.

Sampling campaign I

The SC I contained samples from four sections (1st, 2nd, 3rd and 4th sections) and the aeration tank of the 1st section. Water samples were taken from operating wells of the 1st section at two different abstraction stages, i.e. at the beginning of the abstraction phase (AF) or at the end of the abstraction phase (EF).

The reduction of specific well yield within wells of the 1st well cluster (AF and EF) ranged from 40.4 to 75.7 %. Within the 1st well-cluster, the mean pH at the AF was 7.6, while at EF, a more acidic pH of 6.4 was determined; the mean pH value of the wells from the outgroup was 5.7, and the aeration tank samples had a pH of 6.3. The mean water temperature within the wells at the AF was 6.3 °C, while that of the wells at EF was 5.9 °C; the same temperatures were found for the outgroup samples, the samples taken from the aeration tank and the samples taken from AF. Due to the infiltration of oxygenated groundwater being managed, the dissolved oxygen concentrations were higher at the beginning of each abstraction phase, while, at the end, almost no oxygen could be detected; however, traces of oxygen could be detected in the outgroup samples. Conductivity measurements in the aeration tank and at EF revealed higher values

compared to AF. Due to the subterrestrial removal of iron and manganese, the concentrations of iron(II), iron(III) and manganese in all of the processing wells and the aeration tank were lower than 0.1 mg l^{-1} , except for sample 1101D_EF, wherein 0.3 mg l^{-1} of manganese was observed. Wells of the 3rd and 4th sections (AG), for which subterrestrial removal had not been previously performed, showed concentrations of iron(II) and iron(III) between 11.8 and 31.9 mg l^{-1} . No iron(II) could be detected in the aeration tank.

In the AF, EF and aeration tank samples, ammonia and nitrite concentrations were $<0.02 \text{ mg l}^{-1}$ and $<0.005 \text{ mg l}^{-1}$, respectively, while, within the outgroup samples, the ammonia and nitrite concentrations were 0.12 and 0.7 mg l^{-1} , respectively. Nitrate concentrations ranged between 3.0 and 6.2 mg l^{-1} in all of the processing wells, while the nitrate concentrations in the outgroup samples ranged from 6.2 to 0.2 mg l^{-1} . The DOC varied from 0.7 to 4.3 mg l^{-1} ; The DOC of the outgroup samples ranged from 0.2 to 1.9 mg l^{-1} . The DOC was not determined in the aeration tank.

Sampling campaign II

The SC II was performed in order to analyse the bacterial community dynamics in well 1101 during different abstraction phases. At the beginning of the abstraction phase, the pH was 7.54 ; by the fourth abstraction phase, the pH had decreased to 6.34 and, at the end of the abstraction stage, it had stabilized at 6.44 . The temperature ranged from 6 °C to 6.3 °C. Due to the infiltration of aerated water, the oxygen concentration at the beginning of the abstraction phase was than higher; it decreased from 11.93 to 0.08 mg l^{-1} at the end of the abstraction phase. Water conductivity increased with the volume of abstracted water, while concentrations of iron(II), iron(III), nitrite and ammonia remained stable during the different abstraction phases. Nitrate concentration varied from 4.9 to 5.4 mg l^{-1} and the manganese concentration increased in association with the growing abstraction volume.

3.2.2 Denaturing gradient gel electrophoresis profiling of the bacterial communities of the water catchment area

DGGE analysis served as the first molecular tool used to compare 48 samples obtained from the groundwater catchment area and to obtain an overview of the bacterial diversity and variation found within the samples.

Sampling campaign I

The DGGE analysis of 16S rDNA fragments from all of the samples revealed highly diverse communities in each sample, as presumed by the high number of bands present in each lane. The band-based similarity calculation clearly revealed two distinct clusters with approximately 82 % similarity, corresponding to the beginning and end of each abstraction phases, while analysis of the outgroup samples revealed four distinct clusters (55 %, 72 %, 72 % and 78 %), indicating the presence of a non-homogeneous bacterial community in the groundwater; sample 1105A_EF is an outlier (Figure 15). Within the cluster that contained the operating wells, most of the fingerprint patterns had a similarity of about 82 % and formed a cluster of bacterial communities at the beginning of the abstraction phase. The fingerprints at the end of the abstraction phase were less similar to each other and formed only one cluster of five fingerprints.

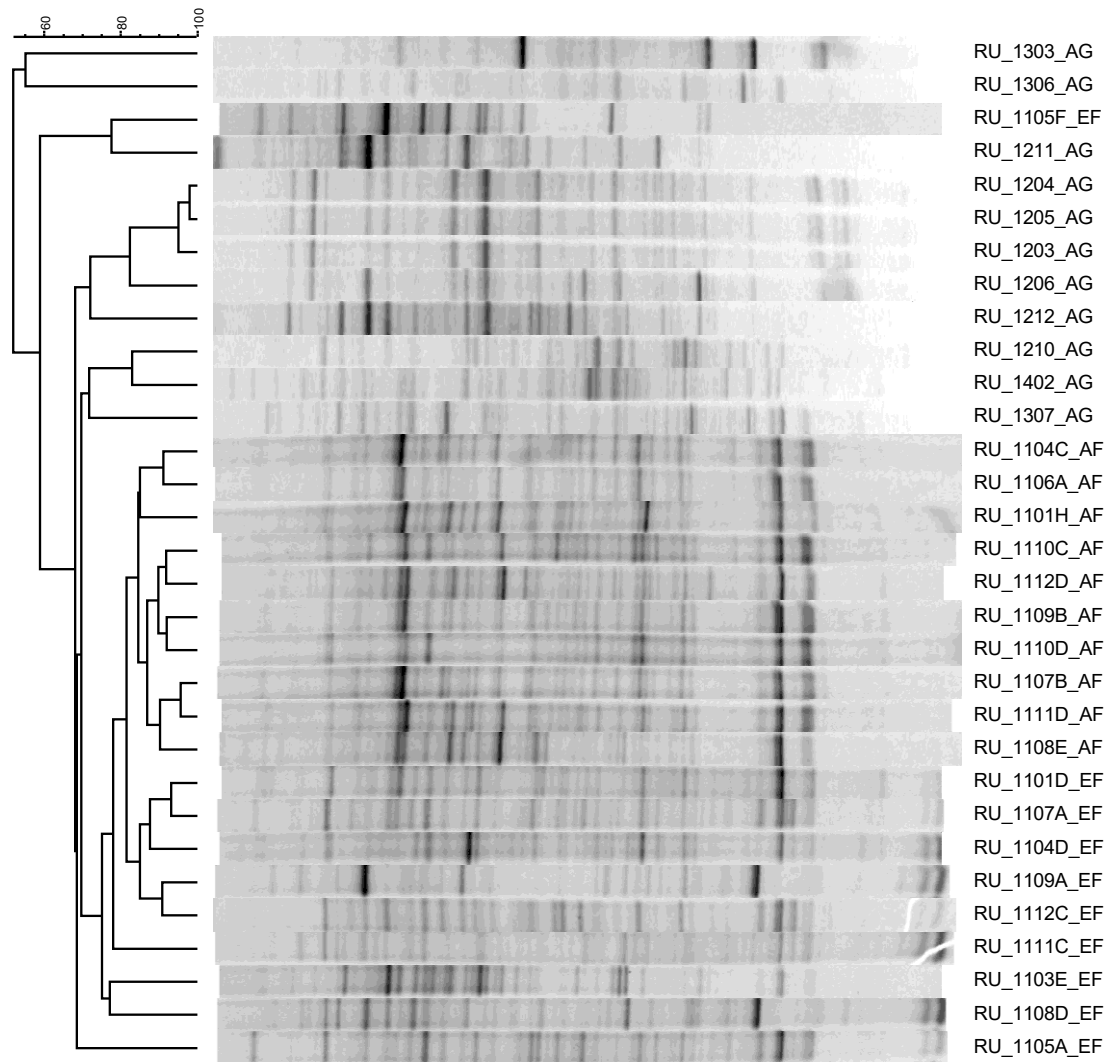


Figure 15. Dendrogram constructed with the bacterial community fingerprints of the water samples. The dendrogram is based on the Dice coefficient and the UPGMA cluster analysis. The scale bar indicates the similarity of community profiles [%] between AG (outgroup samples), AF (samples taken at the beginning of the abstraction phase) and EF (samples taken at the end of the abstraction phase).

The band-based similarity calculation clearly revealed two distinct clusters with 78 % similarity, corresponding to two biofilm samples from different time points and a water sample (Figure 16). The fingerprints of RU_KH and RU_FLB_1 were less similar to each other, showing similarities of 58 % and 54 %, respectively; representing a non-homogeneous bacterial community in the first section's aeration tank. RU_FLB_2, the sample taken last, showed the highest number of bands, indicating an increase of the bacterial diversity in the aeration tank.

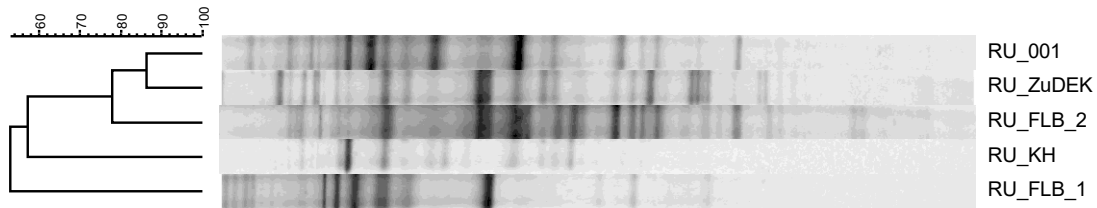


Figure 16. Dendrogram constructed with the bacterial community fingerprints of samples from the aeration tank. The dendrogram is based on the Dice coefficient and the UPGMA cluster analysis. The scale bar indicates the similarity of community profiles [%]: RU_001 (biofilm; 23.02.2013), RU_KH (biofilm; 22.03.2012), RU_ZuDEK (water; 17.12.2012), RU_FLB_2 (biofilm; 14.06.2013) and RU_FLB_1 (water; 17.05.2013).

Sampling campaign II

Band-based similarity was calculated for samples from different abstraction phases of well 1101. Bacterial fingerprints analysis showed two distinct clusters with 74 % similarity to each other. Within the two clusters, one, consisting of two fingerprints taken at the beginning and the end of the abstraction phase, revealed a similarity of 88 % (Figure 17; blue frame). Within the second cluster, the bacterial communities of the 4th and 5th abstraction phases were more similar to each other than that of the 3rd abstraction phase. Bacterial community structure changed within abstraction phases.

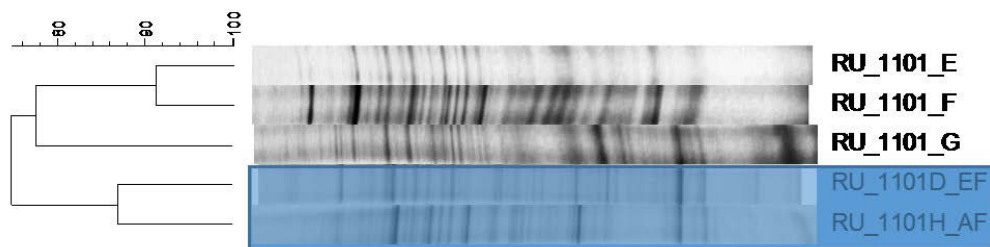


Figure 17. Dendrogram constructed with the bacterial community fingerprints of samples from well 1101 taken during different abstraction phases. The dendrogram is based on the Dice coefficient and the UPGMA cluster analysis. The scale bar indicates similarity of community profiles [%]: RU_1101H_AF (beginning of abstraction phase; blue frame), RU_1101_F (3rd abstraction phase), RU_1101_G (4th abstraction phase), RU_1101_E (5th abstraction phase) and RU_1101_D (end of abstraction phase; blue frame).

Sampling campaign III

The fingerprints of biofilm samples taken before the regeneration procedure showed a similarity of only 72 % to each other. The bacterial community derived from the water sample taken after regeneration had a similarity of only 62 % to the biofilm samples (Figure 18).

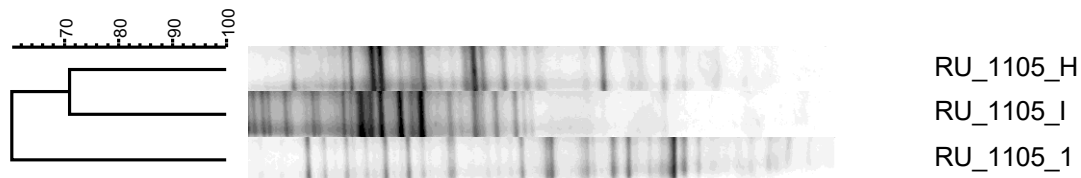


Figure 18. Dendrogram constructed with the bacterial community fingerprints of samples from well 1105 before and after regeneration. The dendrogram is based on the Dice coefficient and the UPGMA cluster analysis. The scale bar indicates similarity of community profiles [%]: RU_1105_H and _I (biofilm before regeneration procedure) and RU_1105_1 (water sample after regeneration procedure).

Analysis of DGGE patterns

The functional organisation (F_o) of the microorganisms that are most fitting to the environmental-microbiological interactions was calculated for all three sampling campaigns. Figure 19 illustrates the P-L curves of the DGGE patterns of three different sampling campaigns. Figure 19 A) shows that the most fitting species were dominant and present in high numbers, while the majority (the remaining 80 % on the x-axis) were present in decreasingly lower amounts.

No differences can be derived according to the vertical 20 % P-L line between the microbial structure, from the beginning of abstraction phase (mean 60 %), the end of the abstraction phase (mean 53 %) and from the outgroup samples (mean 47 %). Thus, F_o was highly comparable between the three groups. Therefore, these groups can be viewed as forming a balanced community with medium F_o . Figure 19 B) presents the P-L curves of the aeration tank samples, showing a mean similarity of 46 % to the outgroup samples. The P-L curves at the beginning and end of the abstraction process had the same value of 60 %, while the 3rd, 4th and 5th abstraction phases had decreasing values of 40 % (Figure 19 D).

Figure 19 C) illustrates the P-L curve of the bacterial community before and after the regeneration procedure. Minimal differences could be seen within this

sampling campaign III (F_o ranged from 50 % to 40 %). The bacterial communities of all of the sampling campaigns showed a medium F_o .

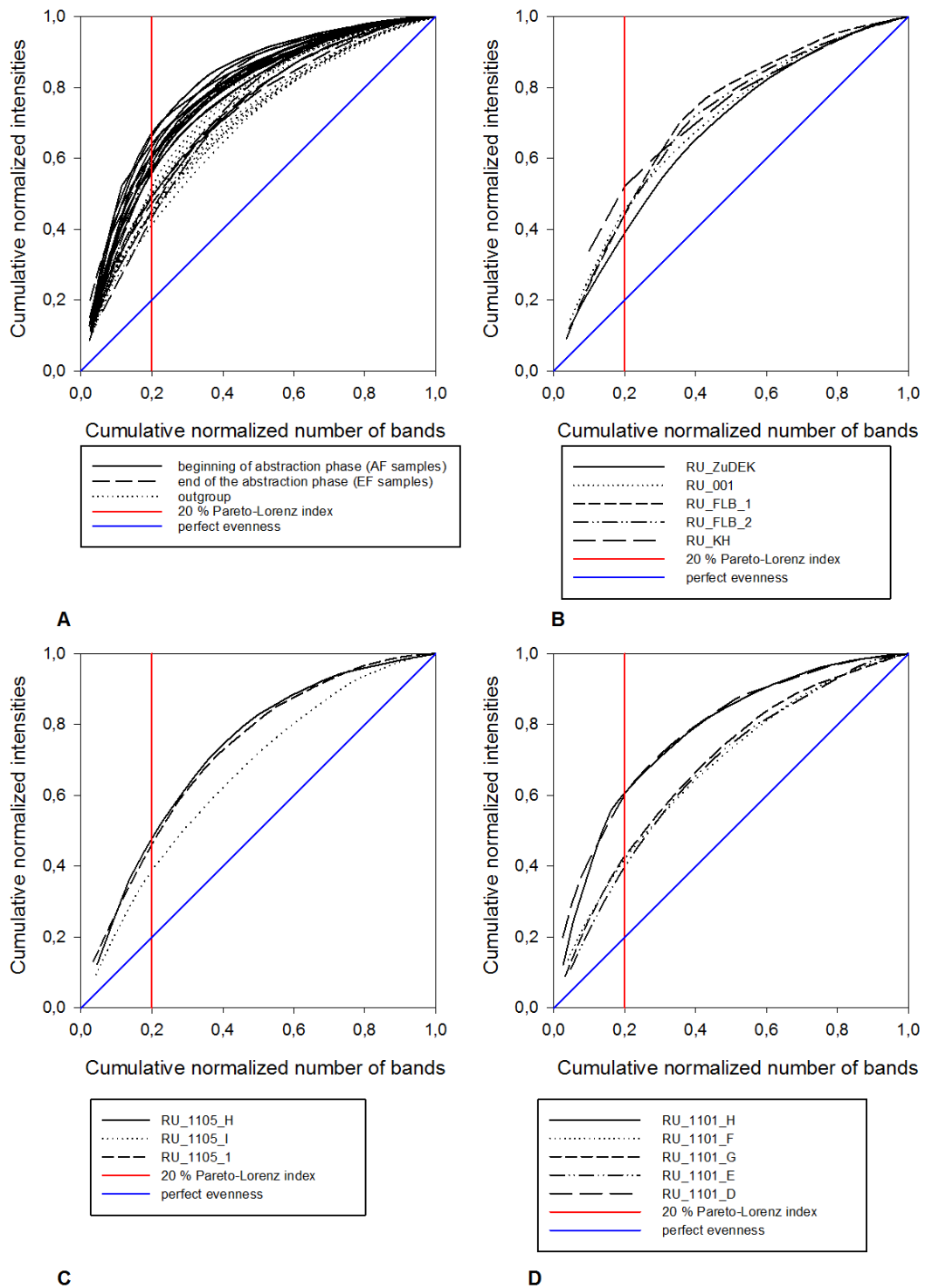


Figure 19. Comparison of the P-L distribution curves based on the DGGE profiles of the various sampling campaigns. (A) Operating wells compared to non-operating wells. (B) Several aeration tank samples. (C) Regeneration samples taken from well 1105. (D) Samples taken from well 1101 during different abstraction phases.

Additionally, the range-weighted richness (R_r) was calculated by the distribution (number) of bands in one lane and correlated with the denaturing gradient percentage of the gel (25 %) required to represent the total diversity. While no differences could be determined by F_o , R_r analysis showed varying values within the sampling campaigns (Figure 20). Following the bacterial community composition as the water flows to the catchment system, the R_r increased from aeration tank samples to the beginning of the abstraction phase and to the end of the abstraction phase; the aeration tank samples showed the lowest R_r value, 47.6 (Figure 20 A). After the regeneration procedure, R_r increased from 58.2 to 122.6 (Figure 20 B). R_r declined from the first to the fifth abstraction phases, while, at the end of the abstraction phase, the diversity, according to the DGGE bands, increased to a value of 223.8 (Figure 20 C).

.

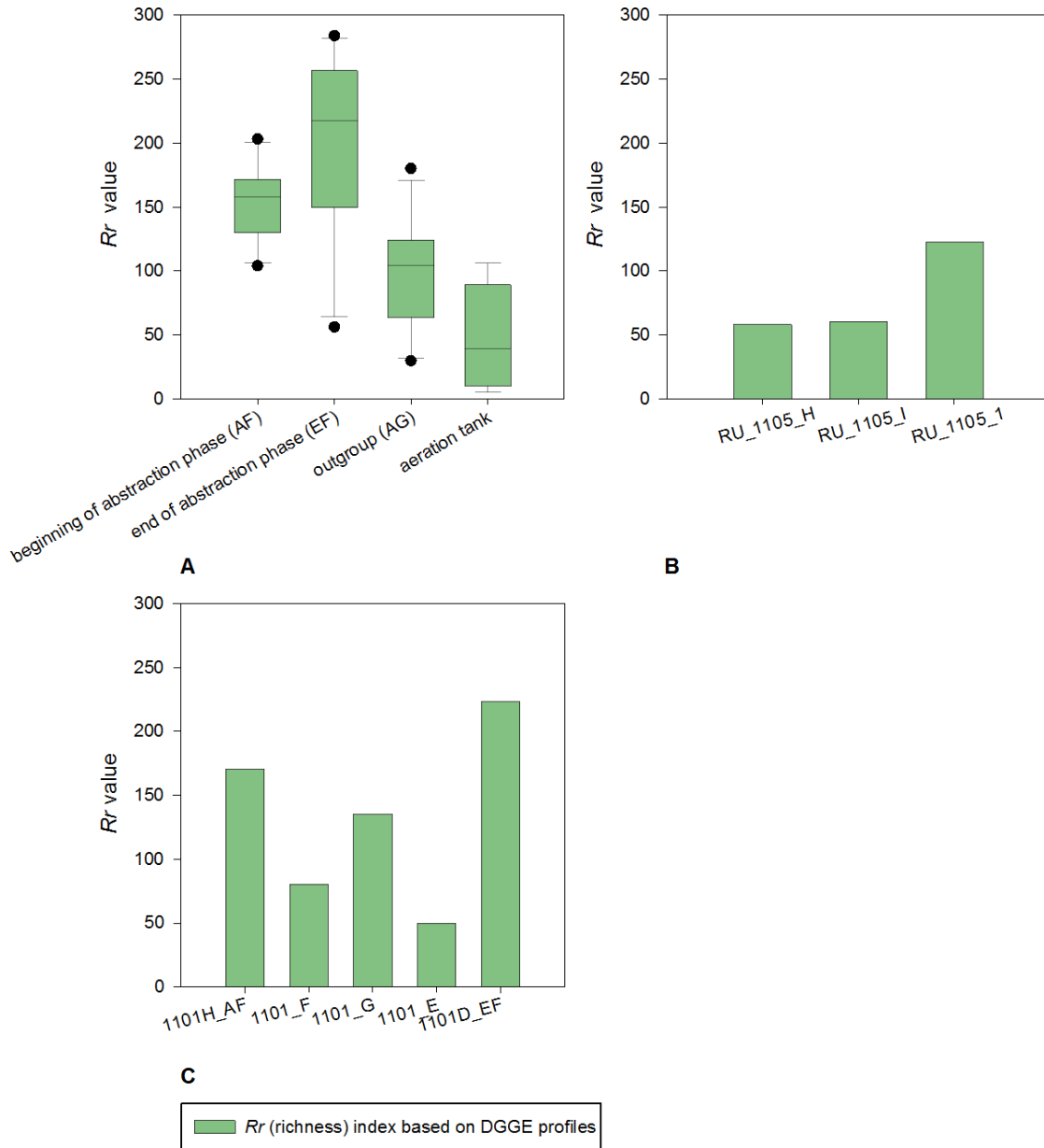


Figure 20. Plots of *Rr*-values based on the DGGE profiles from various sampling designs. (A) Operating wells compared to non-operating wells and several aeration tank samples, (B) samples taken from well 1105 and (C) samples taken during different abstraction phases from well 1101. Dots are outlier.

In addition, the dynamics (*Dy*) reflecting the specific rates at which species came to significant dominance were determined for the groundwater samples obtained during the various abstraction phases of well 1101 (Figure 21); based on the percentage of Pearson correlation similarity, their calculated rate of change was found to be particularly high, at approximately 85 %.

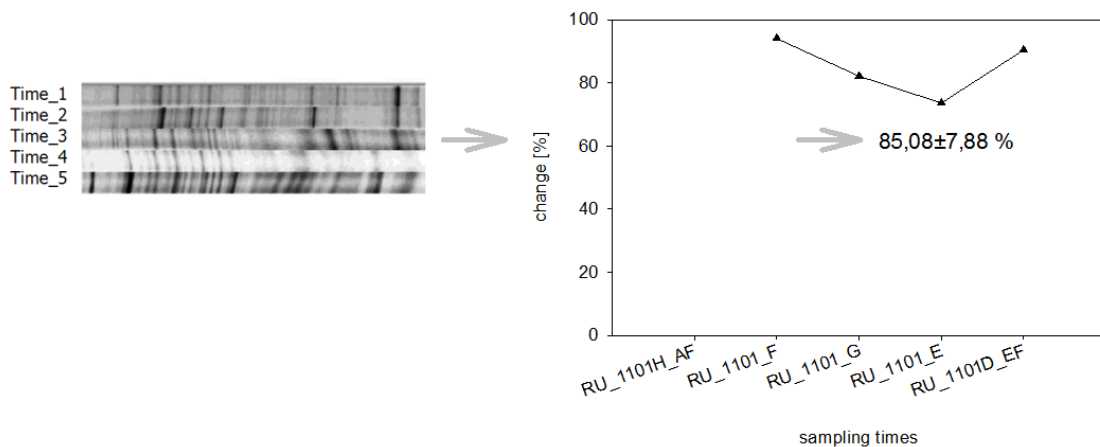


Figure 21. The DGGE profiles, mowing window analysis (MWA) and rate of change values used to determine the dynamics of the bacterial population in different abstraction phases.

3.2.3 Bacterial community analysis by 16S rRNA gene 454-pyrosequencing

Sampling campaign I

Sequencing of the V1 to V3 regions of the 16S rRNA gene of 31 water samples resulted in a total of 2158 OTUs. Only 2.5 % (53/2,158) of the OTUs showed a high abundance (>100 reads), but they represented 67.3 % of all sequences.

The distribution of the relative abundance of phyla in the 1st section samples from AF and EF were different when compared to the phyla of the 2nd section, which consisted almost entirely of *Proteobacteria*. However, samples taken from the 3rd/4th sections were more similar in their phyla composition to the samples taken from AF and EF than to samples of the 2nd well cluster. The relative abundance of OTUs at phylum level is depicted in Figure 22.

OTUs with high homology to the phylum *Proteobacteria* were predominantly abundant in all wells (1st section AF 59.4 %, EF 51.3 %, 2nd section 98.6 % and 3rd/4th sections 38.6 %), followed by *Actinobacteria* (1st section AF 19 %, EF 17.1 %, 2nd section 0.63 % and 3rd/4th sections 19 %), *Bacteroidetes* (1st section AF 5.3 %, EF 5.7 %, 2nd section 0.5 %, 3rd/4th sections 8.7 %) and *Firmicutes* (1st section AF 1.18 %, EF 0.1 %, 2nd section 0.1 %, 3rd/4th sections 10.3 %). The

outgroup samples derived from 2nd and 3rd/4th sections showed major differences in phylum abundance. Within the phylum of *Proteobacteria*, the class of *Betaproteobacteria* was predominant.

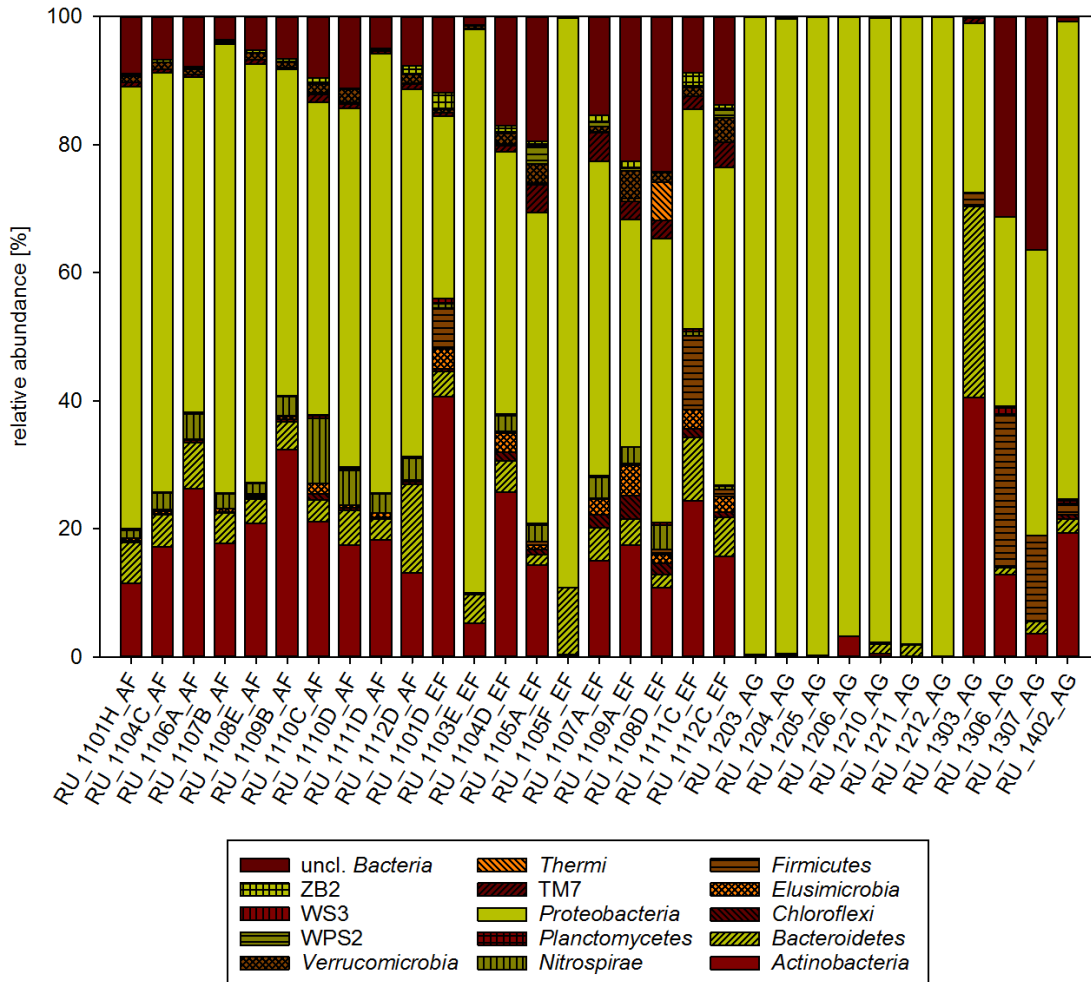


Figure 22. Relative abundance of different phyla present in the water catchment system as estimated by pyrosequencing. Bars indicate the relative abundance of the phylogenetic groups at the phylum level. AF samples (beginning of the abstraction phase, 1st section), EF samples (end of the abstraction phase, 1st section) and AG (outgroup samples, 2nd, 3rd and 4th section).

Additionally, the top 10 OTUs at the genus level were evaluated for all samples and showed significant differences for AF and EF (1st section) samples compared to wells which were not in operation (AG samples) (Figure 23). Samples from the 1st section were significantly associated with the OTU ACK-M1 which belongs to the phylum *Actinobacteria*. The OTU *Rhodoferrax* known as iron-reducing bacteria, could be detected in all samples from the 1st section and be assigned as core OTU. Within the 1st section, differences between AF and EF could be found, as also indicated by indicator analysis (Table 29); the outgroup samples

(2nd and 3rd/4th sections) were associated with significantly different OTUs. OTUs of the 2nd section were almost exclusively related to several *Gallionella* OTUs. Samples from the 3rd/4th sections were not related to the top 10 OTUs; however, the dominant families were *Propionibacteriaceae*, *Staphylococcaceae* and *Micrococcaceae* (data not shown).

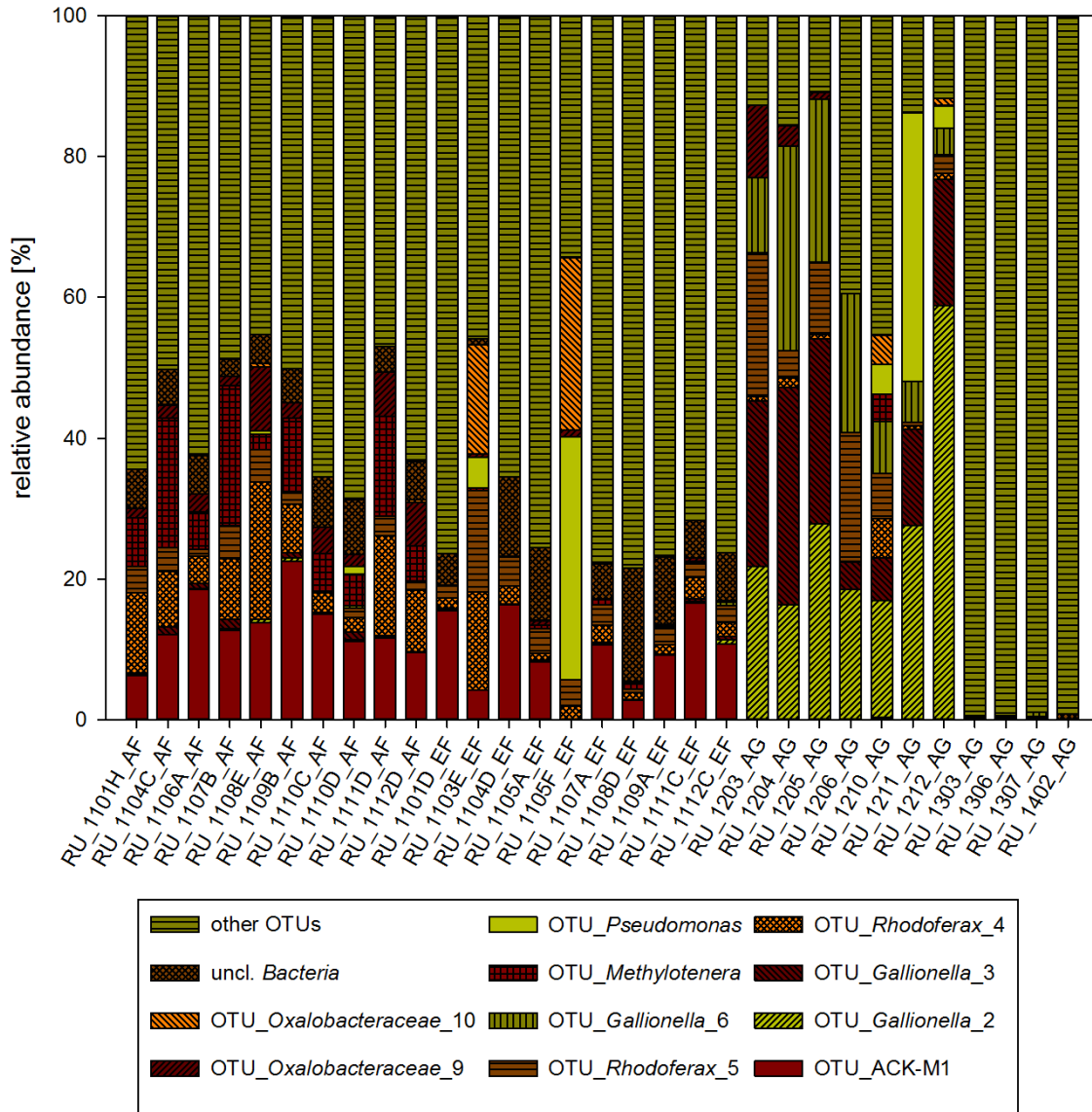


Figure 23. Relative abundance of top the 10 OTUs present in the water catchment system as estimated by pyrosequencing. Bars indicate the relative abundance of the phylogenetic groups at the family and genus levels. AF samples (beginning of the abstraction phase), EF samples (end of the abstraction phase) and AG (outgroup samples).

In addition, a comparative 454 pyrosequencing analysis of the 16S rRNA gene of several samples taken from the aeration tank of the 1st section was performed. Water obtained from the aeration tank was associated with well water due to

infiltration management. The analysis showed that the dominant phylum within the aeration tank was associated to *Proteobacteria* (43.6 to 99.5 %), followed by *Bacteroidetes* (0 to 47.4 %) and *Verrucomicrobia* (0 to 9.7 %) (Figure 24 A). There were major differences between the samples at the family and genus levels. The OTU *Limnohabitans*, a group typically found inhabiting freshwater reservoirs, was the only core OTU; however, it had a low abundance, ranging from 0.3 to 4.5 %. High abundance of the OTU *Flavobacterium* was found in RU_001 and RU_FLB_2, with over 30 % each. The highest abundance of *Pseudomonas*-associated sequences was found in sample RU_FLB_1, while the other samples showed a particularly low abundance of *Pseudomonas*.

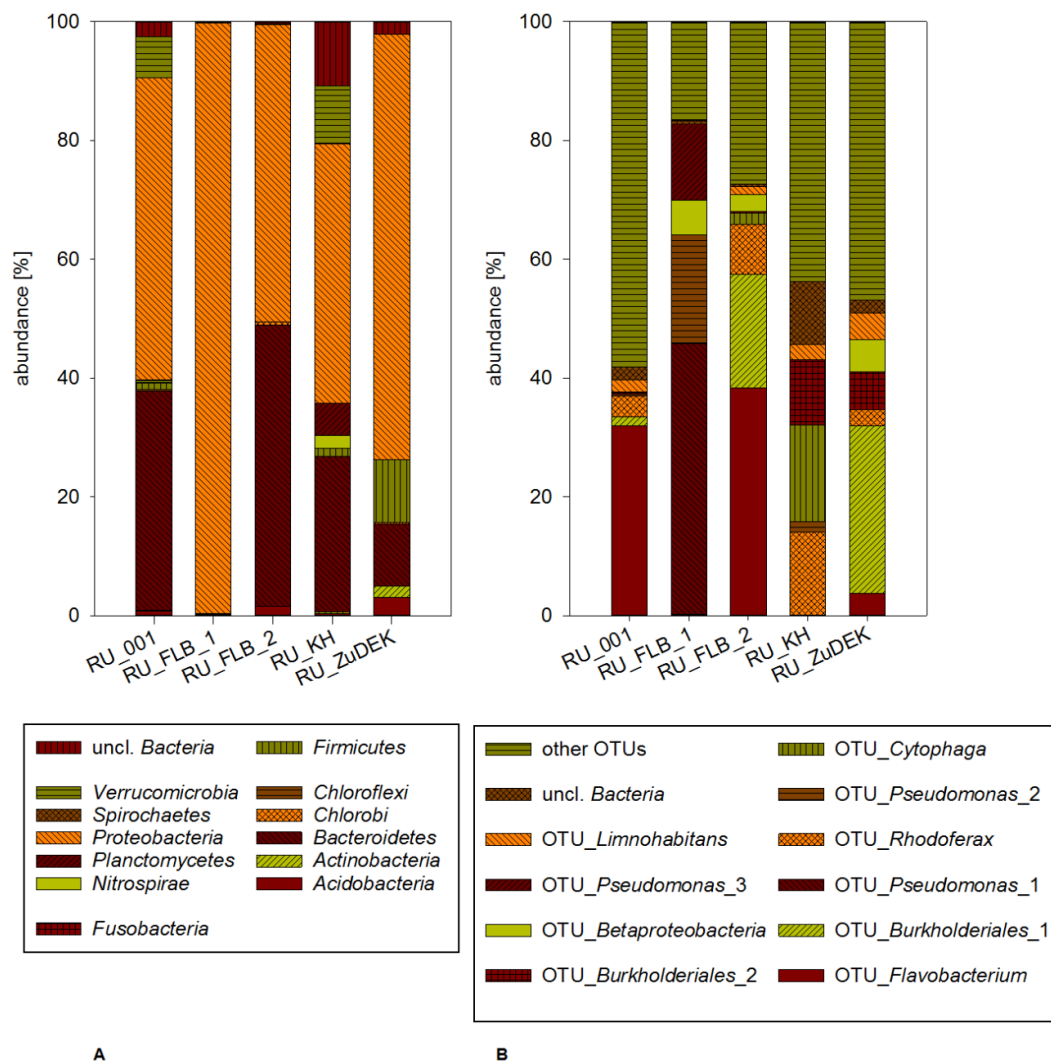


Figure 24. Relative abundance of the bacteria present in the water and biofilm samples taken from the aeration tank, estimated by 454-pyrosequencing. (A) Plot of the relative abundance of different phyla. (B) Plot of the top 10 OTUs. RU_001 (biofilm), RU_KH (biofilm), RU_ZuDEK (water), RU_FLB_2 (biofilm) and RU_FLB_1 (water).

In addition, the alpha diversity of EF, AF (1st section), AG and the aeration tank was calculated using the Shannon index (Figure 25). Additionally, the coverage of OTUs was determined for the samples from each group. Alpha diversity was significantly higher in AF and EF when compared to the AG and aeration tank samples, as already shown by the *Rr*-values calculated based on the number of DGGE bands (Chapter 3.2.2). As indicated by the alpha diversity indices, the top 10 OTUs of each of the outgroup samples (AG) represented 82 % of the entire community. However, the coverage reached for both the AG and aeration tank samples nearly 100 %.

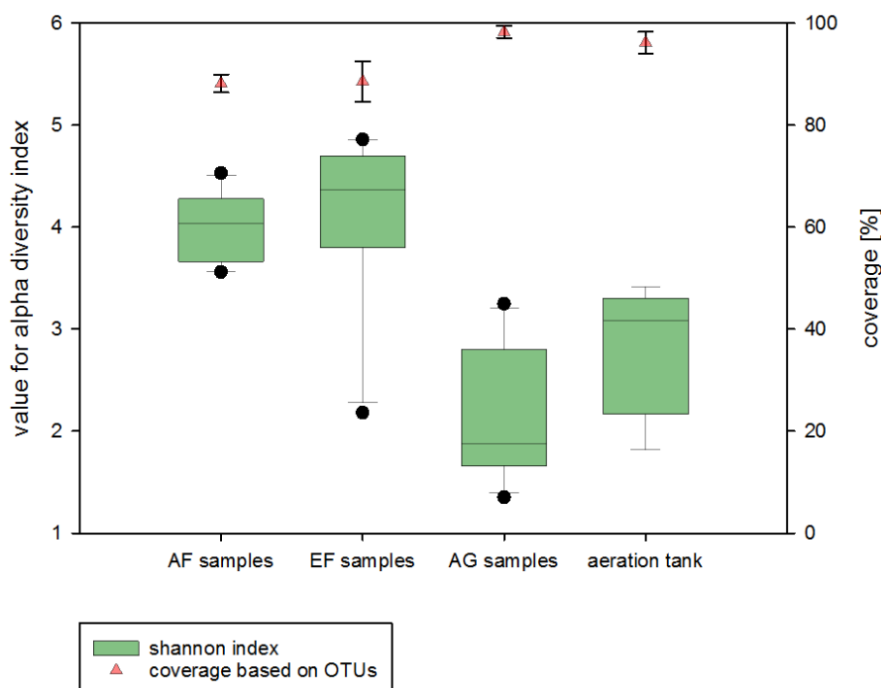


Figure 25. Boxplot of alpha diversity and coverage of samples from the beginning of the abstraction phase (AF), the end of the abstraction phase (EF), outgroup samples (AG) and samples from the aeration tank. Alpha diversity was calculated by Shannon based on the OTUs. Dots are outlier.

The analysis of the bacterial communities of AF, EF and AG served for calculation of indicator groups between wells that were in operation and those that were not. Indicator OTUs, which are analogous to indicator species, are those OTUs that prevail in a certain sample type but are found only infrequently in the sample types used for comparison. The abundance of the methylotrophic OTU

Methylothermobacter was statistically significant at the beginning of each abstraction phase, while no indicator OTUs could be identified at the end of each pumping phase. The *actinobacterial*-cluster ACK-M1 was approved as an indicator OTU for the operating wells of the 1st section, whereas the iron-oxidizing *Gallionella* OTUs were correlated with non-operating wells of the 2nd section (Table 29).

Table 29. Indicator species analysis of the beginning of the abstraction phase (AF), the end of the abstraction phase (EF) and the outgroup (AG, excluding 3rd and 4th sections), used to determine which OTUs were significantly associated with the various operational modes of the drinking water catchment system.

Bacteria (OTU)	AF, mean abundance	Positive samples	EF, mean abundance	Positive samples	AG, mean abundance	Positive samples	p-value
ACK-M1	156	10/10	112	10/10	0	0/11	p<0.005
<i>Gallionella_I</i>	2	1/10	2	1/10	205	10/11	p<0.001
<i>Gallionella_II</i>	6	9/10	1.7	5/10	133	8/11	p<0.001
<i>Gallionella_III</i>	1	3/10	0	0/10	109	8/11	p<0.005
<i>Methylothera</i>	111	10/10	4	9/10	4	1/11	p<0.005

Sampling campaign II

Sequencing of the 16S rRNA gene of five water samples resulted in a total of 194 OTUs. The top 10 OTUs represented 50 to 70 % of all sequences. Analysis of the relative abundance of different phyla in well 1101 during several abstraction phases showed that the abundance of *Actinobacteria* increased with proceeding abstraction volume while the abundance of *Proteobacteria* associated sequences decreased (Figure 26 A). Consequently, the abundance of the *actinobacterial* cluster ACK-M1 increased over time, but with a small decrease at the end of the abstraction phase (Figure 26 B). The second- and third-most abundant OTUs in all samples were sequences associated with the family *Oxalobacteraceae* and the genus *Rhodoferrax*, which decreased after the 3rd abstraction phase (Figure 26 B).

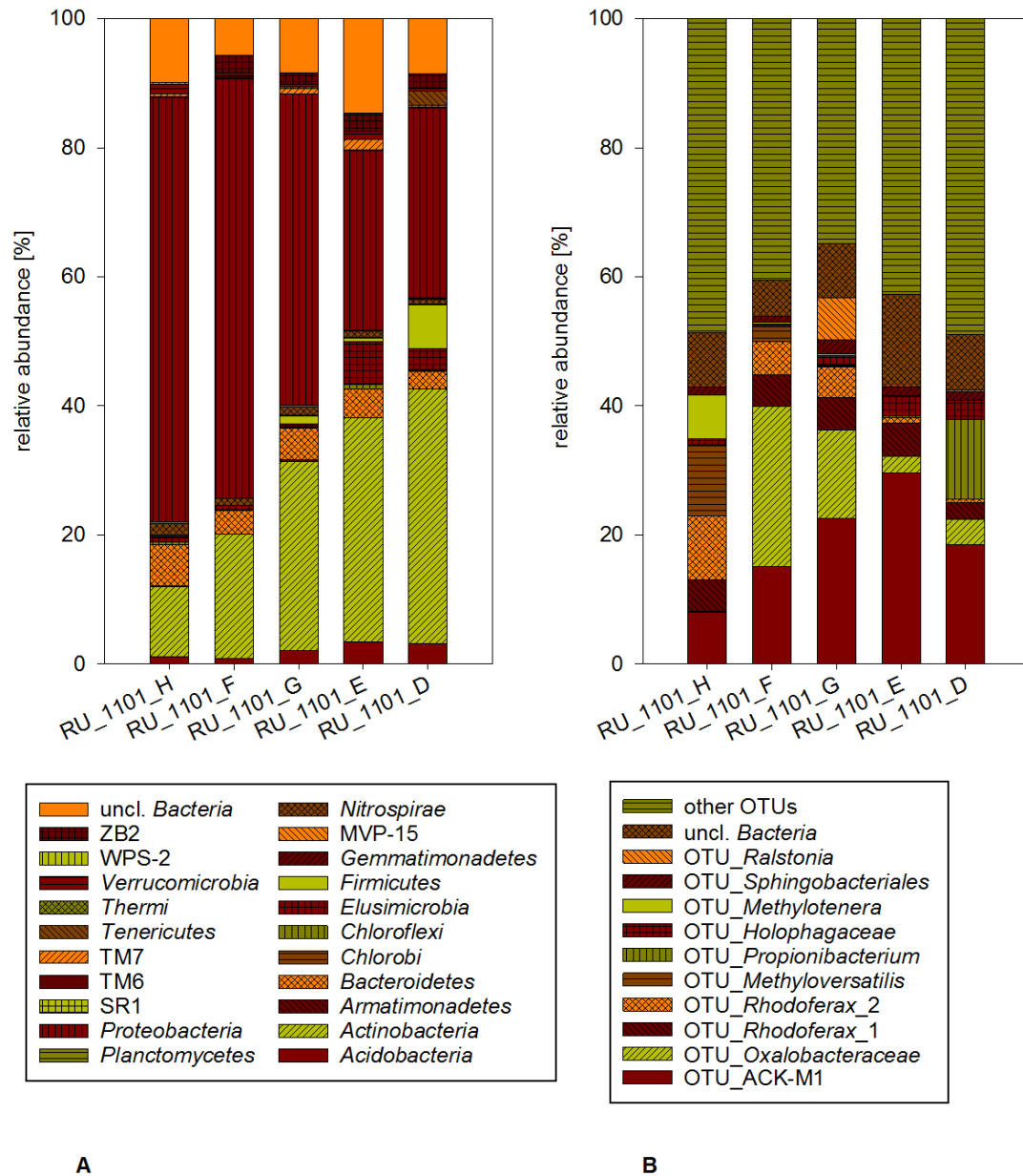


Figure 26. Relative abundance of the bacteria present in water well 1101 during different abstraction phases estimated by pyrosequencing. (A) Plot of the relative abundance of different phyla. (B) Plot of the top 10 OTUs. RU_1101H_AF (beginning of the abstraction phase), RU_1101_F (3rd abstraction phase), RU_1101_G (4th abstraction phase), RU_1101_E (5th abstraction phase) and RU_1101D_EF (end of the abstraction phase).

Alpha diversity, calculated using the Shannon index, revealed an increase after the beginning of the abstraction phase until the 5th abstraction phase; however, at the end of the abstraction process, alpha diversity declined. Additionally, the coverage was determined for each sample. The coverage reached at the beginning and the end of each abstraction phase nearly 90 % (Figure 27), while it remained stable (69.3 to 72.6 %) during the 3rd and 5th abstraction phases.

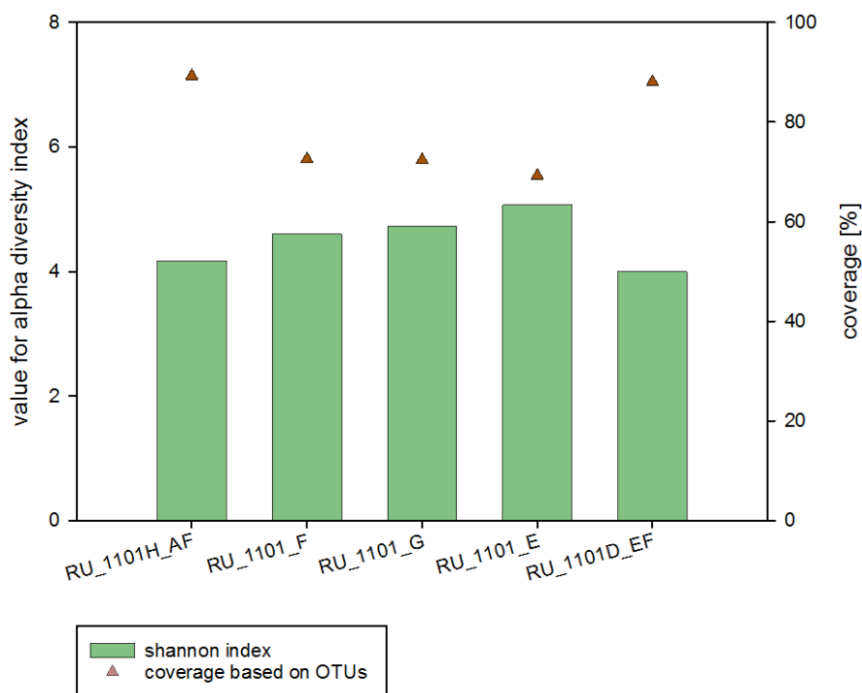


Figure 27. Plot of alpha diversity and coverage based on the OTUs from samples RU_1101H_AF (beginning of the abstraction phase), RU_1101_F (3rd abstraction phase), RU_1101_G (4th abstraction phase), RU_1101_E (5th abstraction phase) and RU_1101D_EF (end of the abstraction phase). Alpha diversity was calculated using Shannon index.

Sampling campaign III

Pyrosequencing of the 16S rRNA genes of three samples obtained from well 1105 resulted in a total of 49 OTUs; the top 10 OTUs represented 70 to 98 % of all sequences. Comparative 454-pyrosequencing analysis of the 16S rRNA genes from the samples taken from well 1105 before regeneration showed that the major sequences were associated with *Proteobacteria* (56.4 to 97.9 %), followed by *Bacteroidetes* (1 to 28 %) and *Actinobacteria* (0 to 11.54 %) (Figure 28 A). After the regeneration procedure *Bacteroidetes* decreased to 1 %. Furthermore, water from well 1105 taken after regeneration (RU_1105_1) presented a distinctly higher number of unclassified sequences in comparison to the biofilm samples. The most dominant OTU in all three samples was *Pseudomonas*. After the regeneration procedure with hydrogen peroxide, no sequences associated with *Flavobacterium* and *Oxalobacteraceae* could be detected (Figure 28 B).

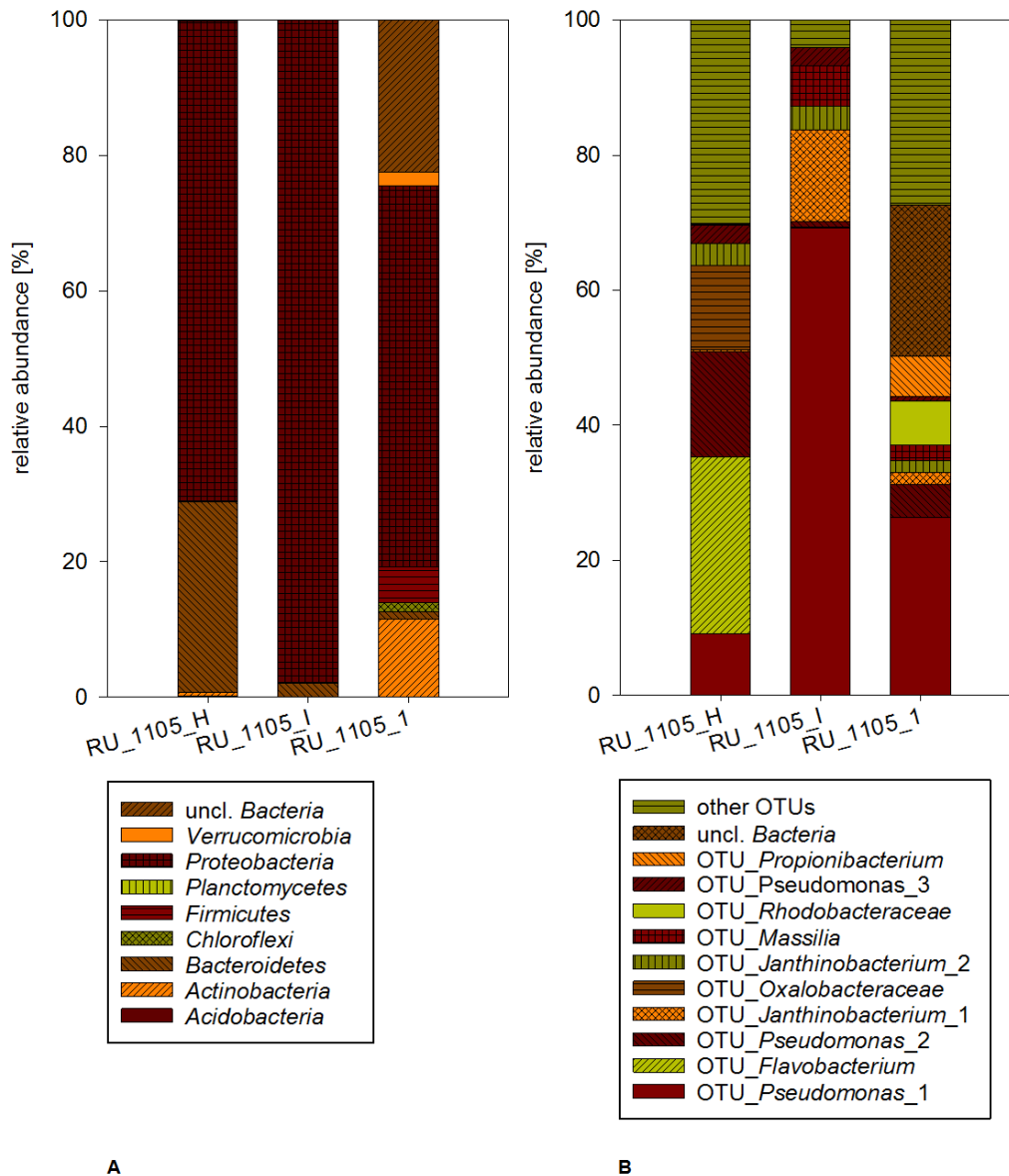


Figure 28. Relative abundance of the bacteria present in the water and biofilm samples taken from well 1105 before and after regeneration estimated by pyrosequencing. (A) Plot of the relative abundance of different phyla. (B) Plot of the top 10 OTUs. RU_1105_H and _I (biofilm before regeneration) and RU_1105_1 (water taken at the end of abstraction phase, after regeneration).

Calculating alpha diversity using the Shannon index revealed that the diversity remained stable after the regeneration procedure. Additionally, the coverage was determined for each sample and reached nearly 100 % for all samples (Figure 29).

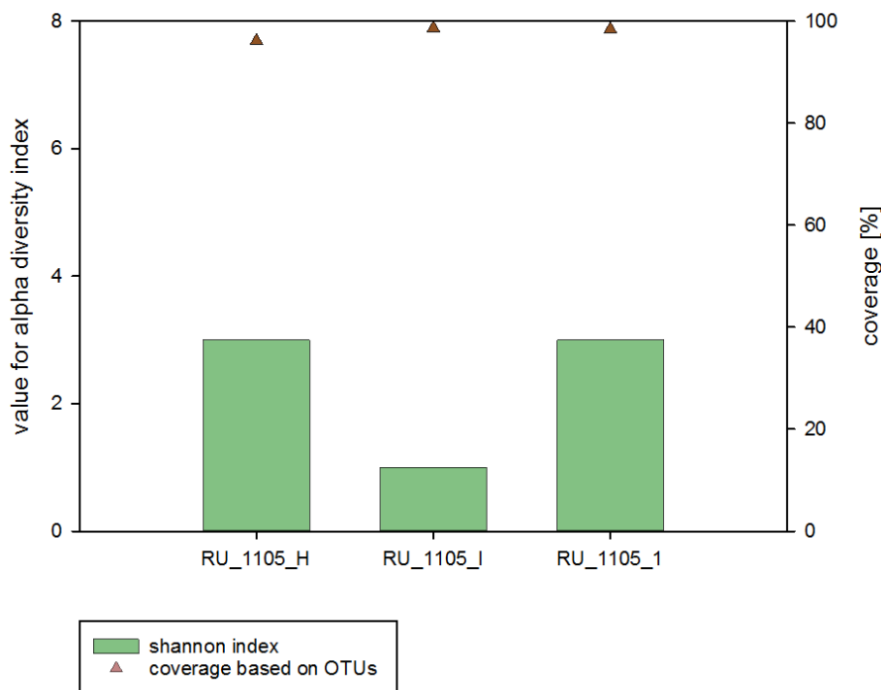


Figure 29. Plot of alpha diversity and coverage based on the OTUs of RU_1105_H and _I (biofilm before regeneration procedure) and water after regeneration. Alpha diversity was calculated using the Shannon index.

3.2.4 Quantification of 16S rRNA gene copies from ochrous and water samples taken from the water catchment area

The quantitation reports produced by the qPCR runs always showed a reaction efficiency of between 80 to 95 %, as well as a required r^2 value of >0.99 . The melt curve analysis conducted at the end of each run showed overlapping peaks at a consistent temperature, depending on fragment size, and a second, lower peak in the negative control, which was due to the remaining primers in the reaction.

Sampling campaign I

Figure 30 A illustrates the abundance of the 16S rRNA gene found in the samples used in SC I, including the beginning of the abstraction phase (1st section, AF), the end of the abstraction phase (1st section, EF) and from the outgroup samples (2nd, 3rd and 4th sections, AG) targeting four different primer pairs, two of which belonged to the top ten OTUs. Figure 30 B represents the biofilm and water

samples taken from the aeration tank of the 1st section. At the beginning of the abstraction phase, an average of 5×10^5 bacterial 16S rRNA gene copies ml^{-1} were detected in the 1st well section, while a decreased number of gene copies of $2 \times 10^4 \text{ ml}^{-1}$ were measured at the end of the abstraction phase. The number of Bacteria gene copies were highly variable between the 2nd and 3rd/4th sections. Within the 2nd section, an increased copy number of 2×10^6 gene copies ml^{-1} was found. The outgroup samples derived from the 3rd/4th sections revealed lower copy numbers of between 2×10^1 to $3 \times 10^3 \text{ ml}^{-1}$.

The infiltrated, aerated water originated from the aeration tank. The highest gene copy numbers of total *Bacteria* were detected in the biofilm samples; the average ranged from 8×10^8 to 3×10^{10} gene copies g^{-1} . The gene copy numbers derived from the water samples taken from the aeration tank revealed an average of between 4×10^7 to 2×10^8 16S rRNA gene copies g^{-1} (Figure 30 B).

Specific quantification of *Rhodoferrax*-related 16S rRNA gene copies, which represent the group of iron reducers, revealed that this group was highly abundant at the beginning of the abstraction phase and in the outgroup samples of the 2nd section, as also indicated by 454-pyrosequencing (Chapter 3.2.3). High gene copy numbers could be detected in samples obtained from the aeration tank, particularly in the biofilm samples, while, in the samples taken from the 3rd and 4th sections, *Rhodoferrax ferrireducens*-related gene copy numbers could not be detected (Figure 30).

Bacterial gene copies related to *Gallionella* spp., representing a group of known iron oxidizers were the second most abundant group detected in the water samples used in this sampling campaign; gene copies of the 16S rRNA gene could be detected in the 1st (AF) and 2nd sections at the highest levels of abundance. High gene copy numbers were also found in aeration tank samples whereas the highest abundance of *Gallionella* gene copies occurred in biofilm samples. No gene copies of *Gallionella* spp. were detected in the samples taken from the 3rd and 4th sections (Figure 30).

The genus *Crenothrix* was chosen to quantify the amount of methanotrophic bacteria. The majority of the 16S rRNA *Crenothrix polyspora* genes were observed in samples derived from the 2nd section (AG), with a mean average of 2×10^4 gene copies ml^{-1} . Samples from the beginning of the abstraction phase contained only low numbers of these copies, ranging between undetectable to

1×10^3 gene copies ml^{-1} as well as low gene copies were revealed in samples taken at the end of the abstraction phase and in the outgroup samples of the 3rd and 4th sections (Figure 30). However, high gene copy numbers of *Crenothrix polyspora* were detected in all of the samples obtained from the aeration tank; the average ranged from 1×10^4 to 3×10^8 gene copies g^{-1} .

Gene copies related to *Geothrix* spp., representing another group of iron-reducing bacteria besides *Rhodoferrax*, could only be detected in the aeration tank samples. The average 16S rRNA gene copy numbers ranged from 6×10^2 to 2×10^5 g^{-1} .

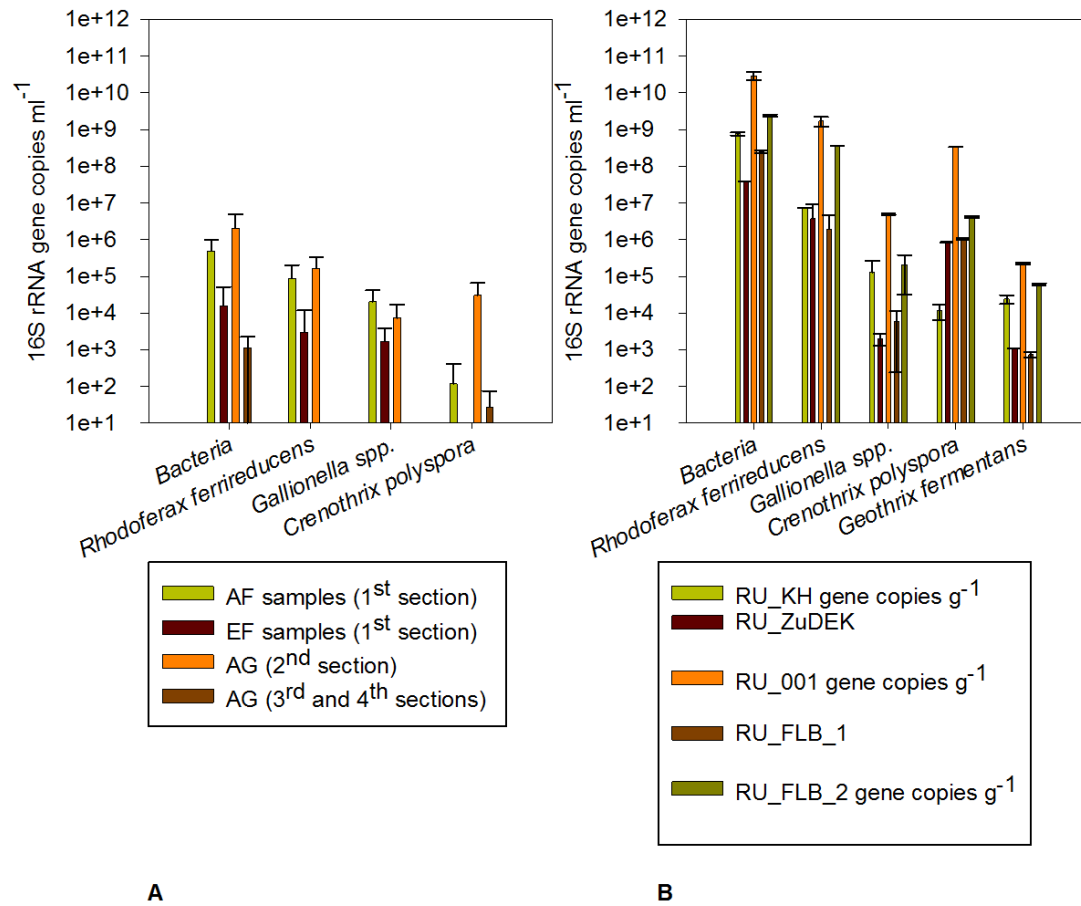


Figure 30. (A) Plot of 16S rRNA gene copies of samples derived from the beginning of the abstraction phase (1st section, AF), from the end of the abstraction phase (1st section, EF) and from wells that were not in operation (2nd, 3rd and 4th sections and AG samples). (B) Plot of 16S rRNA gene copies from five different aeration tank samples. Both plots targeted gene copies of total *Bacteria*, *Rhodoferrax ferrireducens*, *Gallionella* spp. *Crenothrix polyspora* and *Geothrix fermentans*. Error bars represent the standard error.

Sampling campaign II

Figure 31 illustrates the progress of 16S rRNA gene copy numbers during various abstraction phases of well 1101, targeting *Bacteria*, *Rhodoferrax ferrireducens*, *Gallionella* spp. and *Crenothrix polyspora*. All measured gene copies increased considerably after the beginning of the abstraction phase and decreased after the 3rd abstraction phase. At the end of the abstraction phase, only gene copies of *Bacteria* and *Rhodoferrax ferrireducens* could be determined.

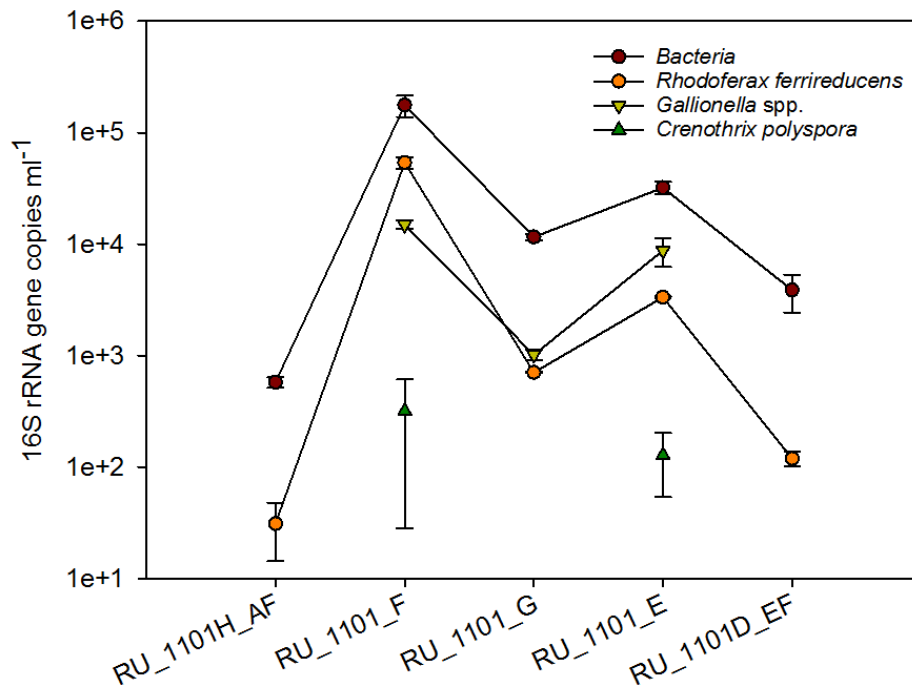


Figure 31. Plot of 16S rRNA gene copies from the water samples obtained from well 1101 during the abstraction process: at the beginning of the abstraction phase (RU_1101H_AF), 3rd abstraction phase (RU_1101_F), 4th abstraction phase (RU_1101_G), 5th abstraction phase (RU_1101_E) and the end of the abstraction process (RU_1101D_EF) targeting gene copies of total *Bacteria*, *Rhodoferrax ferrireducens*, *Gallionella* spp. and *Crenothrix polyspora*. Error bars represent the standard error.

Sampling campaign III

Figure 32 illustrates 16S rRNA gene copies from biofilm samples that were deposited in a pipe connected to well 1105 before the regeneration procedure which used a 38 % hydrogen peroxide solution compared to a water sample at the end of abstraction after regeneration. The 16S rRNA gene copies of *Bacteria* decreased in particular after regeneration, dropping from 2×10^9 ml⁻¹ to 1×10^1 ml⁻¹. The remaining bacterial groups declined by at least three log steps after the

regeneration procedure, particularly the *Rhodoferrax*-associated gene copies that belonged to the top 10 OTUs, estimated by 454-pyrosequencing; *Geothrix*-related gene copies could not be detected at all after regeneration.

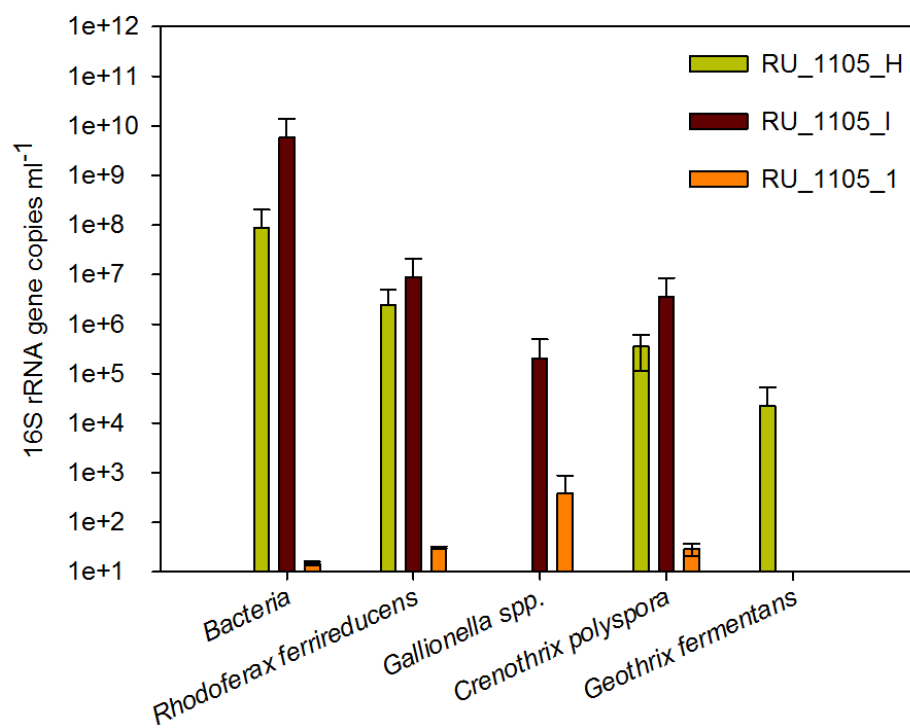


Figure 32. Plot of 16S rRNA gene copies from the samples obtained from well 1105. Biofilms placed within a well pipe before regeneration (RU_1105_H) and (RU_1105_I) as well as a water sample from the end of abstraction phase after regeneration (RU_1105_1) targeting gene copies of total *Bacteria*, *Rhodoferrax ferrireducens*, *Gallionella* spp., *Crenothrix polyspora* and *Geothrix fermentans*. Error bars represent the standard error.

3.3 Chemical and biomolecular investigations of groundwater and biofilm samples taken from dewatering wells at two different opencast mines

A total of 34 water samples were collected from opencast mines in Garzweiler (18 samples) and Hambach (16 samples); water samples were taken from both dewatering wells with aerated and those with non-aerated filter screens (Chapter 2.7.3). Additionally, biofilm samples were taken from six ochrous-encrusted pumps after their removal (Figure 33).

Table A 4 provides an overview of the sampling points and times.



Figure 33. Example of the pumps used at the opencast mines; removal of riser with a pump and deposits on a pump.

3.3.1 Hydrochemistry of two opencast mines

The on-site parameters measured were temperature, dissolved oxygen, pH, electrical conductivity and redox potential; the remaining chemical parameters were determined in the RWE laboratory. Table A 4 provides a complete overview of the wells and chemical parameters.

Among the wells at the Garzweiler opencast mine, major differences could be identified between those equipped with aerated filters and those with non-aerated filters, including electrical conductivity and amounts of dissolved oxygen, iron(II), iron(III) and sulphate. Electrical conductivity was $660.8 \pm 47.0 \mu\text{S cm}^{-1}$ and $511.2 \pm 69.4 \mu\text{S cm}^{-1}$ for aerated and non-aerated filters, respectively. The mean dissolved oxygen concentration value was higher in wells with aerated filters (1.9 mg l^{-1}) when compared to their non-aerated counterparts (0.7 mg l^{-1}). Furthermore, mean values of 3.0 mg l^{-1} iron(II) and 2.05 mg l^{-1} iron(III) were found in wells with aerated filters, as opposed to the values of 1.8 mg l^{-1} iron(II) and 0.4 mg l^{-1} iron(III) found in wells equipped with non-aerated filters. The mean sulphate concentration in water samples taken from wells with aerated filters revealed a value that was five times higher than that of the wells with non-aerated filters.

Among the water samples taken at the Hambach opencast mine, the only major differences found between the wells equipped with aerated and non-aerated filters were the concentration of dissolved oxygen and the amount of iron(III). The mean concentration of iron(III) in wells with aerated filters was 0.4 mg l^{-1} , in contrast with the remaining wells, wherein no iron(III) could be measured. Oxygen concentration was 3.5 times higher in wells with aerated filters.

3.3.2 Denaturing gradient gel electrophoresis profiling of the bacterial communities of opencast mining wells

16S rRNA gene profiling of the bacterial community was performed on the water and ochrous samples in order to investigate their spatial variability.

Hambach opencast mine

Figure 34 shows the microbial genetic comparison of water sample fingerprints from the Hambach opencast mine, composed of samples taken from aerated and non-aerated filters. The DGGE patterns revealed the presence of some stronger bands and a large number of less intense bands; indicating a relatively small number of bacteria dominating the population, while many, less-abundant bacteria represent a diverse background population. A total of five clusters, each of which included a different number of fingerprints, were calculated, but not all

clusters correlated to aerated and non-aerated filters. The fingerprints of cluster one revealed a similarity of 55 % to each other; with the exception of sample H1429, all of these samples were taken from pumps with non-aerated filter screens. The second cluster (60 % similarity) contained five fingerprints from non-aerated wells and one fingerprint from an aerated well. The fingerprints of adjacent wells were similar, but not identical, to each other; adjacent wells can be recognized by consecutive numbers.

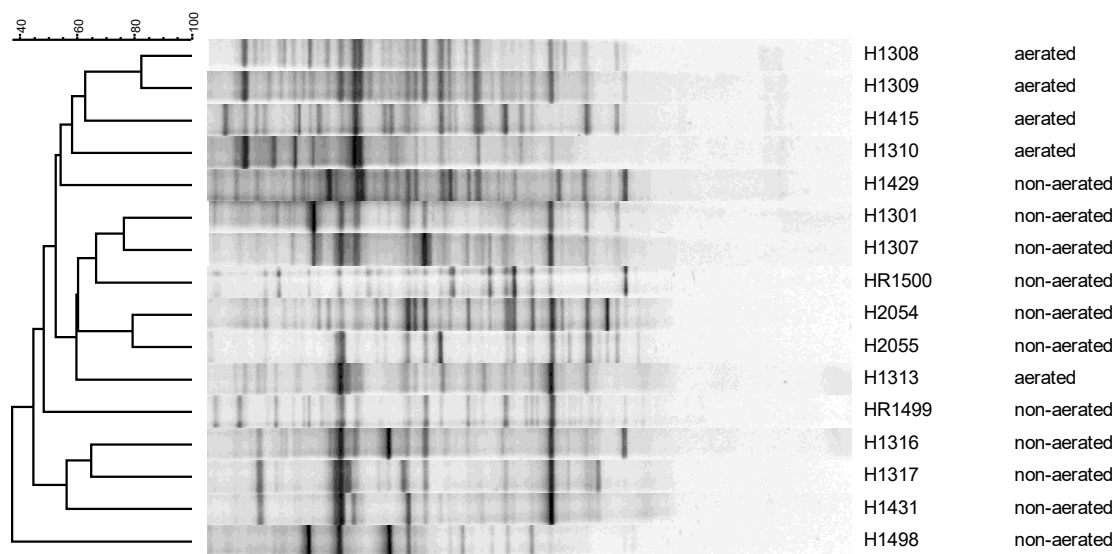


Figure 34. Dendrogram constructed with the bacterial community fingerprints of groundwater samples taken from wells at the Hambach site (indicated by H and HR); The dendrogram is based on the Dice coefficient and the UPGMA cluster analysis. The scale bar indicates the similarity of community profiles [%]: Water samples derived from wells with aerated and non-aerated filters are marked by this terms.

In addition, the genetic diversity of four biofilm samples taken from different well components (e.g., riser and pump) was compared using DGGE fingerprints. The dendrogram revealed two clusters with a similarity of 68 % to each other. The bacterial community derived from the pump resulted in one cluster and the communities from the riser clustered together with similarities of 78 % and 86 %, respectively (Figure 35).

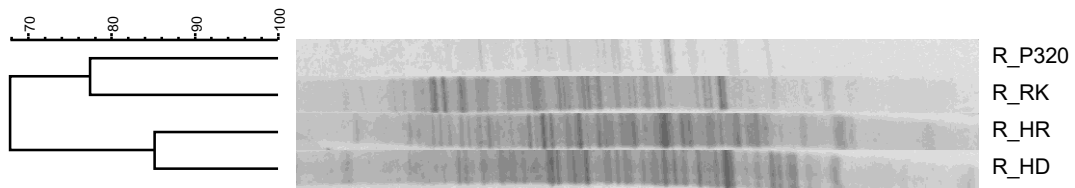


Figure 35. Dendrogram constructed with the bacterial community fingerprints of biofilm samples taken from wells at the Hambach site. The dendrogram is based on the Dice coefficient and the UPGMA cluster analysis. The scale bar indicates the similarity of community profiles [%]: R_P320 (H1424, pump), R_RK (HS1362, flap trap of pump), R_HR (HR1402, riser) and R_HD (HR45, riser).

Garzweiler opencast mine

Figure 36 illustrates the microbial genetic comparison of water sample fingerprints from the Garzweiler opencast mine, comprising samples obtained from aerated and non-aerated filters. The DGGE patterns revealed the presence of some stronger bands and a large number of less intense bands, indicating that only a limited number of dominant species existed. A total of four clusters could be found. No correlation between the bacterial communities inhabiting wells with aerated filters and those without was possible due to the fact that the clusters consisted of fingerprints taken from both filter types. The first cluster consisted of four bacterial fingerprints from wells with non-aerated filters (78 % similarity). The second and third clusters consisted of mixed bacterial fingerprints from both types with 82 % and 83 % similarity, respectively. The bacterial fingerprint from W5827 represented an outgroup (Figure 36).

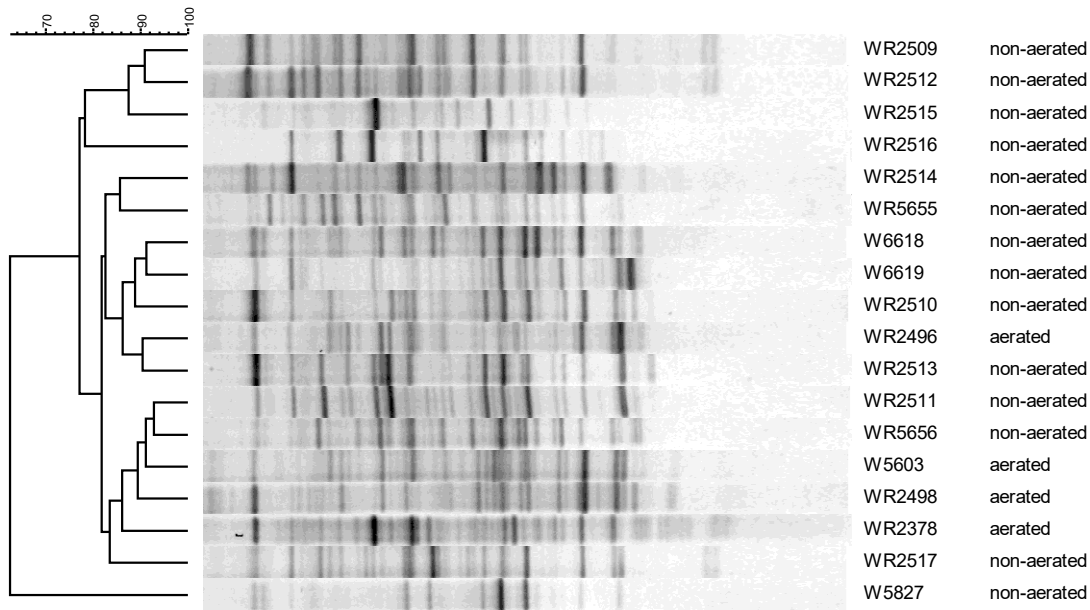


Figure 36. Dendrogram constructed with the bacterial community fingerprints of groundwater samples from wells of the site Garzweiler (indicated by W and WR). The dendrogram is based on the Dice coefficient and the UPGMA cluster analysis. The scale bar indicates the similarity of community profiles [%]: Water samples derived from wells with aerated and non-aerated filters are marked by this term.

In addition, two bacterial fingerprints derived from ochrous samples taken from two different wells at the Garzweiler site were compared: one sample derived from the pump intake and the other from the filter inlet. The bacterial fingerprints had a similarity of 80 % (Figure 37).

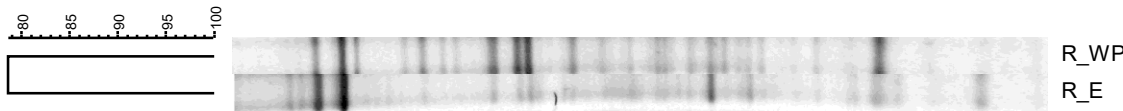


Figure 37. Dendrogram constructed with the bacterial community fingerprints of biofilm samples taken from wells at the Garzweiler site. The dendrogram is based on the Dice coefficient and the UPGMA cluster analysis. The scale bar indicates the similarity of community profiles [%]: R_WP (WR2377, pump intake) and R_E (WR2378, inlet filter).

Analysis of DGGE patterns

In order to graphically represent the structures of the bacterial communities of water samples taken from wells with aerated and non-aerated filter screens, P-L evenness curves were constructed based on the DGGE profiles. Figure 38 A illustrates that the P-L curves for non-aerated wells from the Hambach opencast mine had a higher evenness than those of aerated filters. The bacterial community in the Garzweiler samples had similar P-L indices. Here, the most fitting species are dominant and present in high numbers, while the majority (the remaining 80 % on the x-axis) was present in decreasingly lower amounts. Due to the elevated concentration of some species and the availability of many others, it can be seen as a balanced community with medium *Fo*.

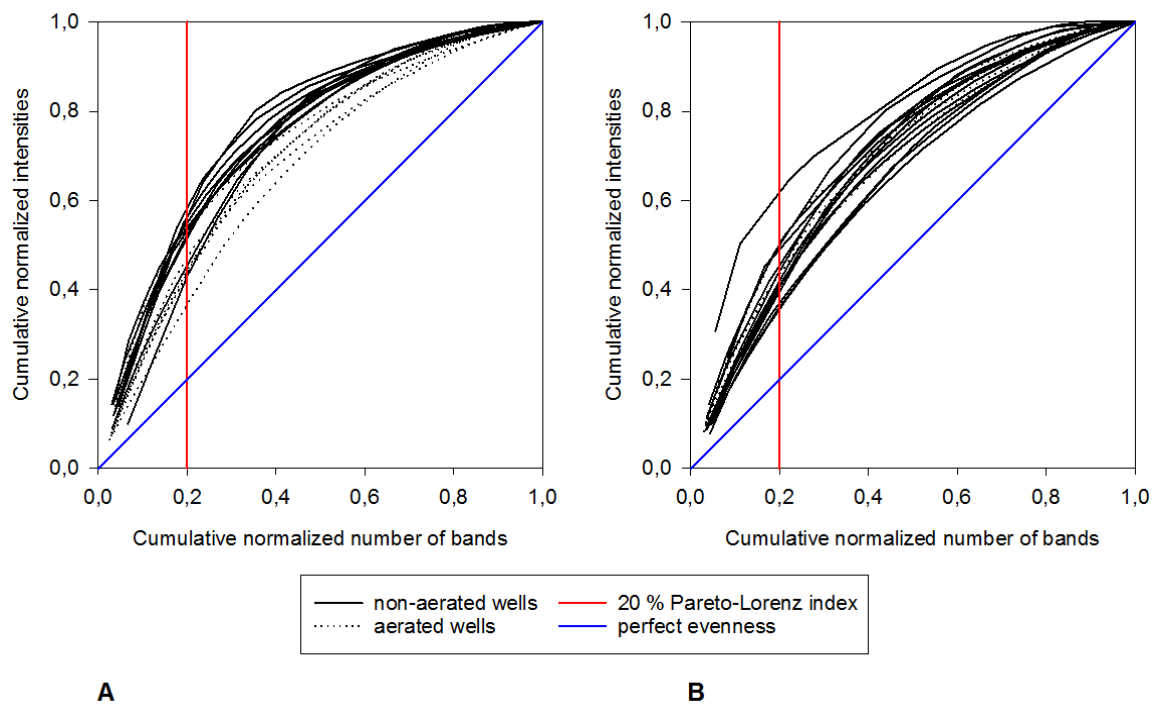


Figure 38. Comparison of the P-L distribution curves based on the DGGE profiles of the water samples derived from wells equipped with aerated and non-aerated filters at Hambach (A) and Garzweiler (B) opencast mines.

Additionally, the P-L curves of the ochrous samples are illustrated in Figure 39. The bacterial community from Garzweiler clearly had higher values ($Fo \sim 50\%$) than those found in the samples taken at Hambach ($Fo \sim 35\%$).

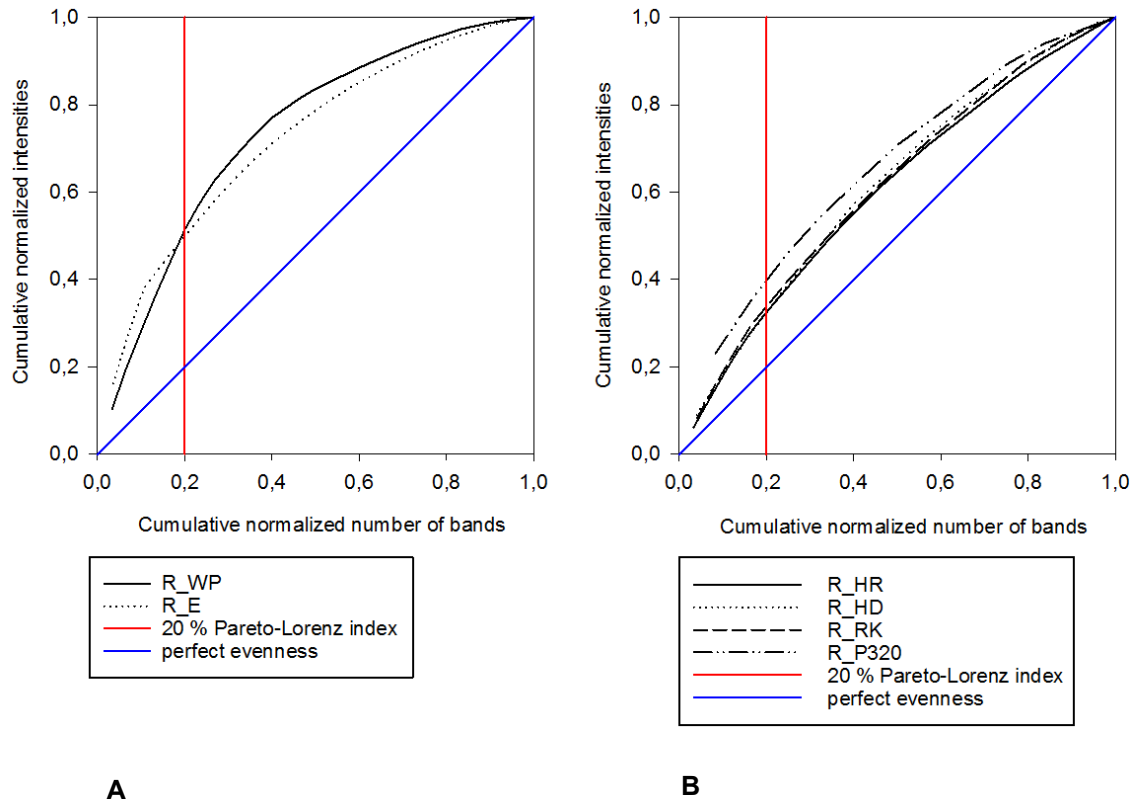


Figure 39. Comparison of the P-L distribution curves based on the DGGE profiles of biofilm samples taken from two opencast mines: (A) Garzweiler: R_WP (WR2377, pump intake), R_E (WR2378, inlet filter) and (B) Hambach: R_P320 (H1424, pump), R_RK (HS1362, flap trap of pump), R_HR (HR1402, riser) and R_HD (HR45, riser).

Additionally, range-weighted richness (R_r) was calculated by correlating the distribution (number) of bands in one lane with the denaturing grade percentage of the gel (25 %) required to represent the total diversity of the water samples; the boxplots are illustrated in Figure 40. For both mines, the mean R_r of non-aerated wells was clearly lower than that of samples derived from aerated wells; however, groundwater samples from the Hambach mine showed higher bacterial R_r values (Figure 40 A).

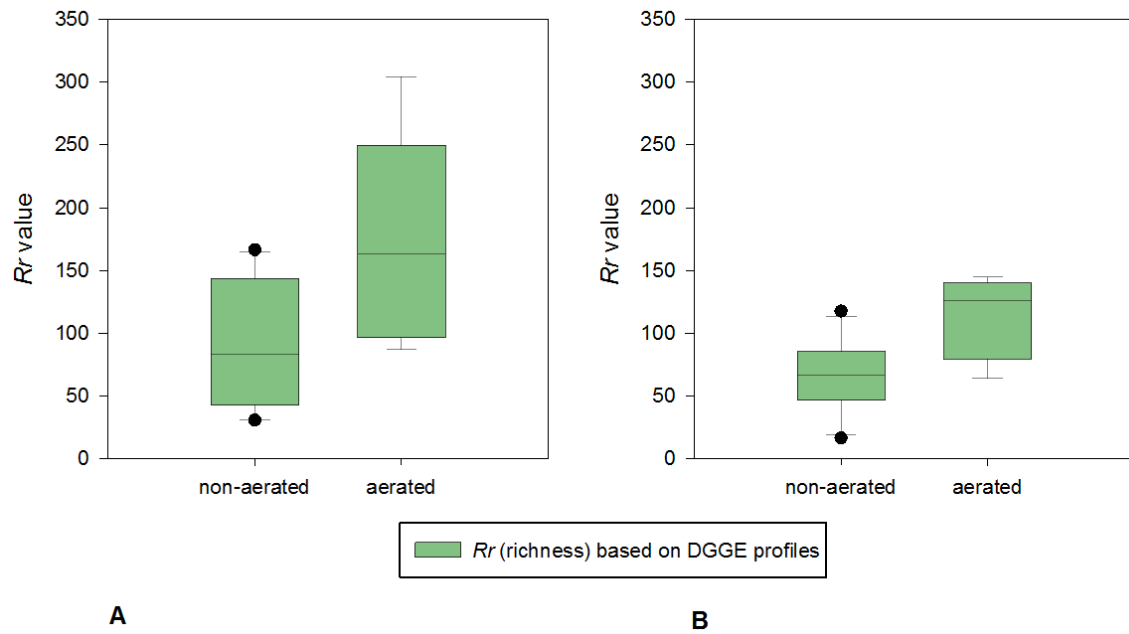


Figure 40. Boxplots of *Rr*-values based on the DGGE profiles of the bacterial community from (A) Hambach and (B) Garzweiler opencast mining wells. Dots are outlier.

Figure 41 presents the bacterial richness of all ochrous samples, showing the highest richness in samples derived from Garzweiler. The lowest richness was clearly found in the sample obtained from the deepest well (R_P320), which had a depth of 320 m.

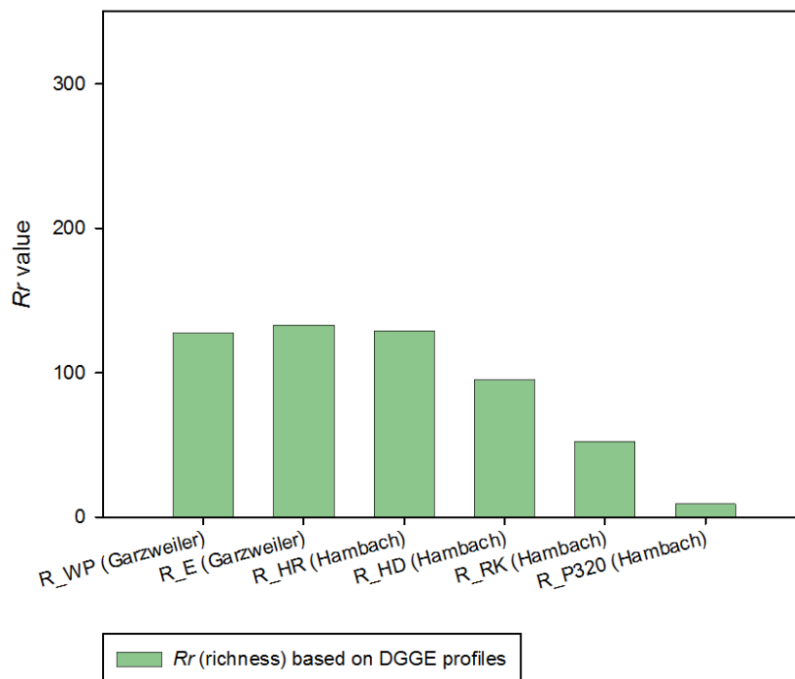


Figure 41. Plot of R_r -values based on the DGGE profiles of the biofilm samples derived from the two opencast mines. R_WP (WR2377, pump intake), R_E (WR2378, inlet filter), R_P320 (H1424, pump), R_RK (HS1362, flap trap of pump), R_HR (HR1402, riser) and R_HD (HR45, riser).

3.3.3 Bacterial population analysis of dewatering well samples by 16S rRNA gene clone libraries

All of the biofilm samples taken from the various dewatering wells were further used for bacterial community analysis by means of clone library construction in order to gain deeper into bacterial community composition. The major bacterial sequences represented in most of the ochrous samples taken from the opencast mining areas were associated with the phyla *Proteobacteria*, *Acidobacteria* and *Bacteroidetes* (Figure 42). No sequences associated with *Actinobacteria*, *Elusimicrobia*, *Gemmatimonadetes* and *Ignavibacteria* could be detected in samples originating from Garzweiler (Figure 42 A).

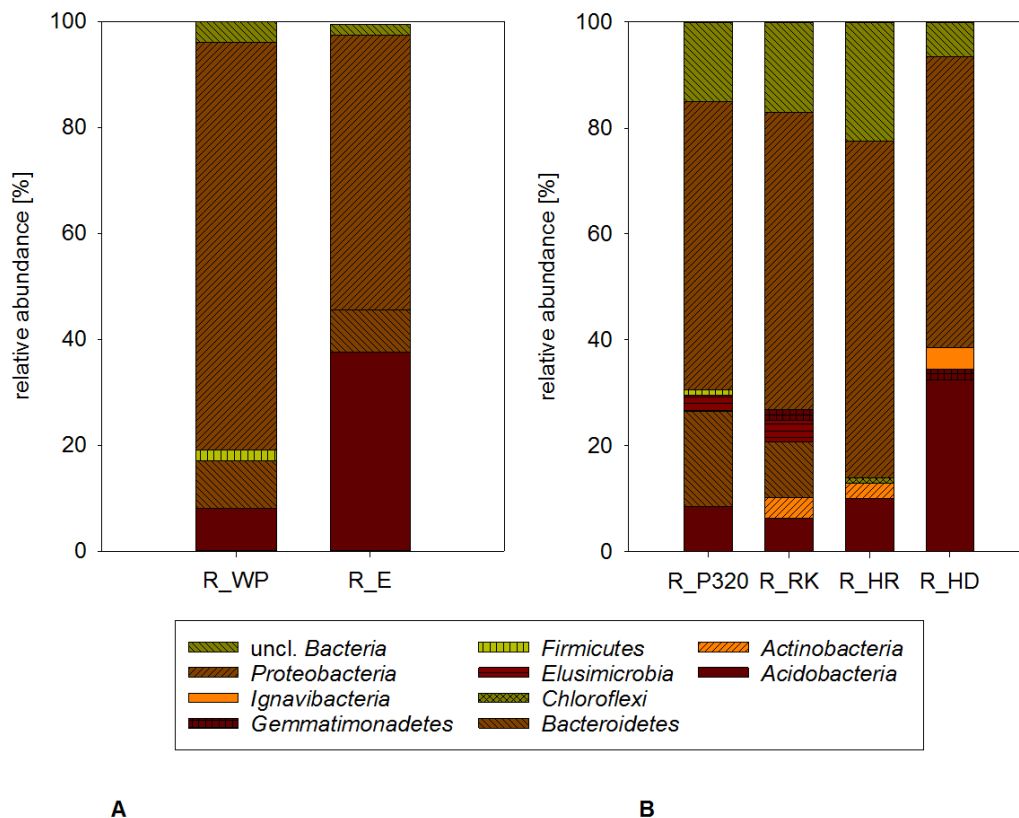


Figure 42. Phylum plots of several ochrous samples taken from water wells at the opencast mines generated by clone library construction. (A) Garzweiler R_WP (WR2377, pump intake), R_E (WR2378, inlet filter) (B) Hambach. R_P320 (H1424, pump), R_RK (HS1362, flap trap of pump), R_HR (HR1402, riser), R_HD (HR45, riser).

Clone library construction showed major differences in the top 10 OTUs of the ochrous samples taken from Hambach and Garzweiler (Figure 43). The top 10 OTUs in the samples from Garzweiler were more similar to each other, as has already been shown by means of DGGE analysis; however, the top 10 OTUs represented only 22 to 32 % of the total OTUs (Figure 43 A). The most dominant OTUs in the Garzweiler samples comprised sequences associated with *Novosphingobium*, which are known for their potential to degrade aromatic compounds, the anaerobic *Holophagaceae*, methanotrophic *Methylococcaceae* and iron-reducing *Geothrix*, which also belongs to the family *Holophagaceae*. The top 10 OTUs of the biofilm samples taken from the Hambach opencast mine showed particular differences in their community structures. Sequences associated with the methano- and methylotrophic *Beijerinckiaceae* and *Geothrix* were the most abundant groups, but could only be found in two of the four samples;

the strictly anaerobic group *Anaeromyxobacter* served as the core OTU in the biofilm samples taken at Hambach.

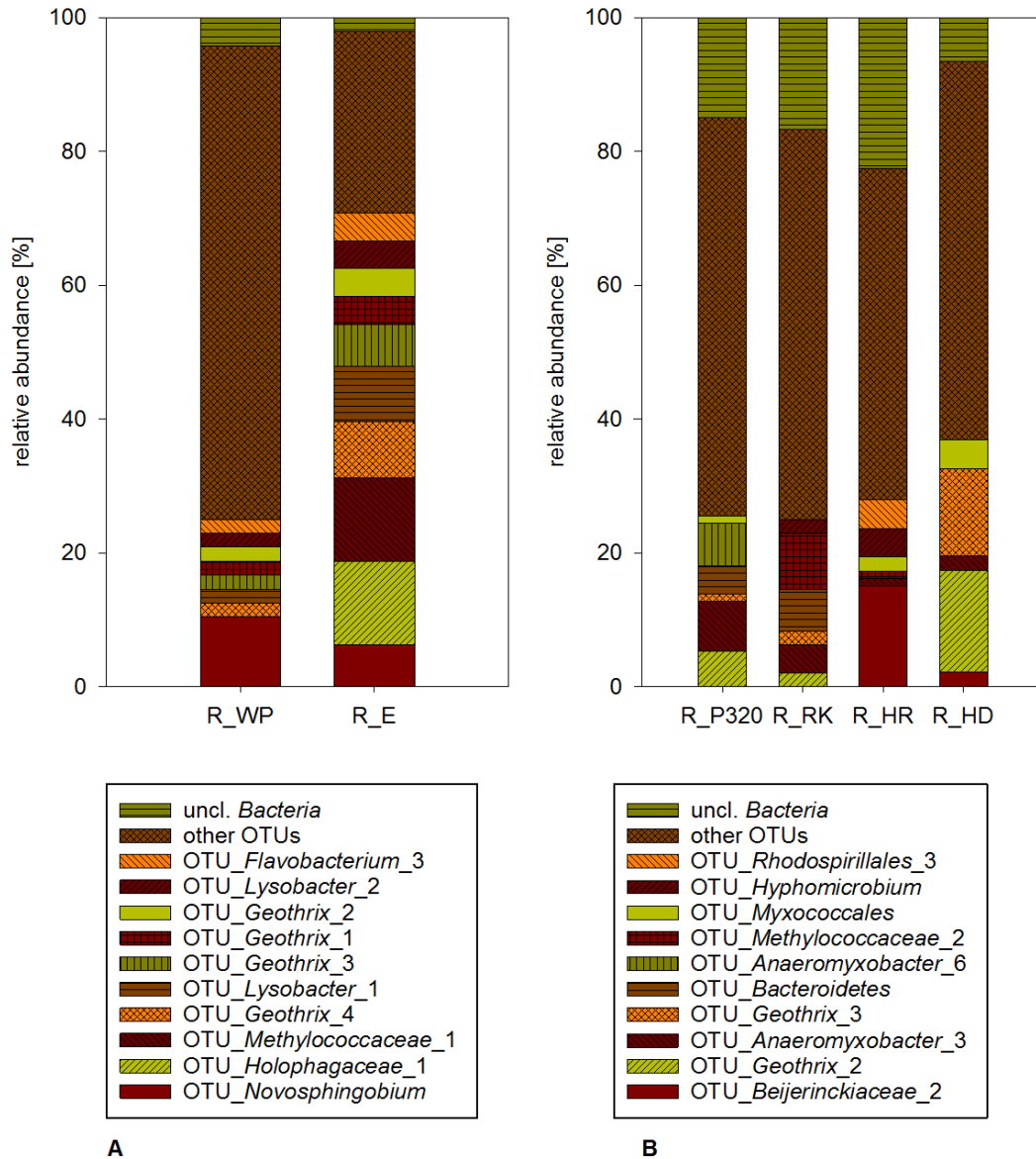


Figure 43. The top 10 OTU plots of the 16S rRNA gene clone libraries of two opencast mines: R_WP (WR2377, pump intake), R_E (WR2378, inlet filter) and B) Hambach R_P320 (H1424, pump), R_RK (HS1362, flap trap of pump), R_HR (HR1402, riser), R_HD (HR45, riser).

3.3.4 Bacterial community analysis of the 16S rRNA gene by 454-pyrosequencing of the opencast mines samples

All of the biofilm samples taken from the various dewatering wells were further used for bacterial community analysis by 454-pyrosequencing in order to gain deeper into bacterial community composition. At the phylum level, there were similar results between the clone library and pyrosequencing findings (Figure 42

and Figure 44). Sequences at the phylum level that were detected by means of clone library construction could also be found by pyrosequencing, with the exception of sequences associated with *Ignavibacteria*. Additionally, pyrosequencing identified 11 further phyla as a result of the higher output of sequences this method offers when compared to clone library construction. The three most abundant phyla belonged to *Proteobacteria* (47 to 84 %), *Nitrospirae* (5 to 22 %) and *Bacteroidetes* (0.7 to 12 %).

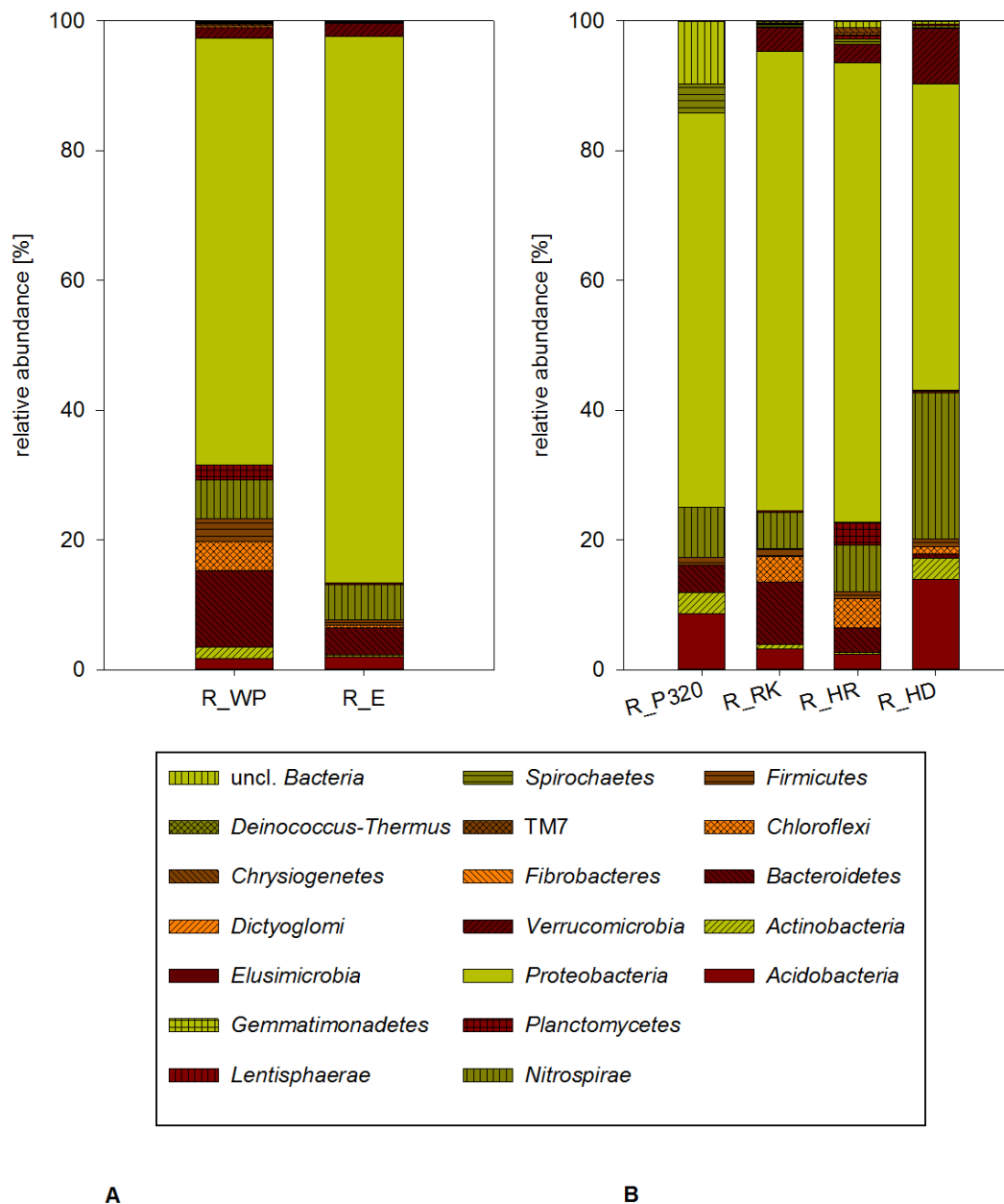


Figure 44. Relative abundance of the bacterial phyla present in the biofilm samples taken from the opencast mining areas, estimated by pyrosequencing: (A) Garzweiler, (B) Hambach.

In addition, the top 10 OTUs at the family and genus levels were calculated, as illustrated in Figure 45; the OTUs *Crenothrix* and *Methylobacter* were the most abundant groups at the Garzweiler site, while the most abundant OTUs at the Hambach site were *Nitrospira*, *Methylococcus* and *Methylobacter*; an exception was sample R_P320, taken at a depth of 320 m, which showed major differences. Sequences associated with *Anaeromyxobacter* served as the core OTUs for the Hambach site, as already shown by means of clone library construction. *Gallionella*-, *Geothrix*- and *Rhodoferrax*-associated OTUs were present in all samples from both sampling sites (Figure 45).

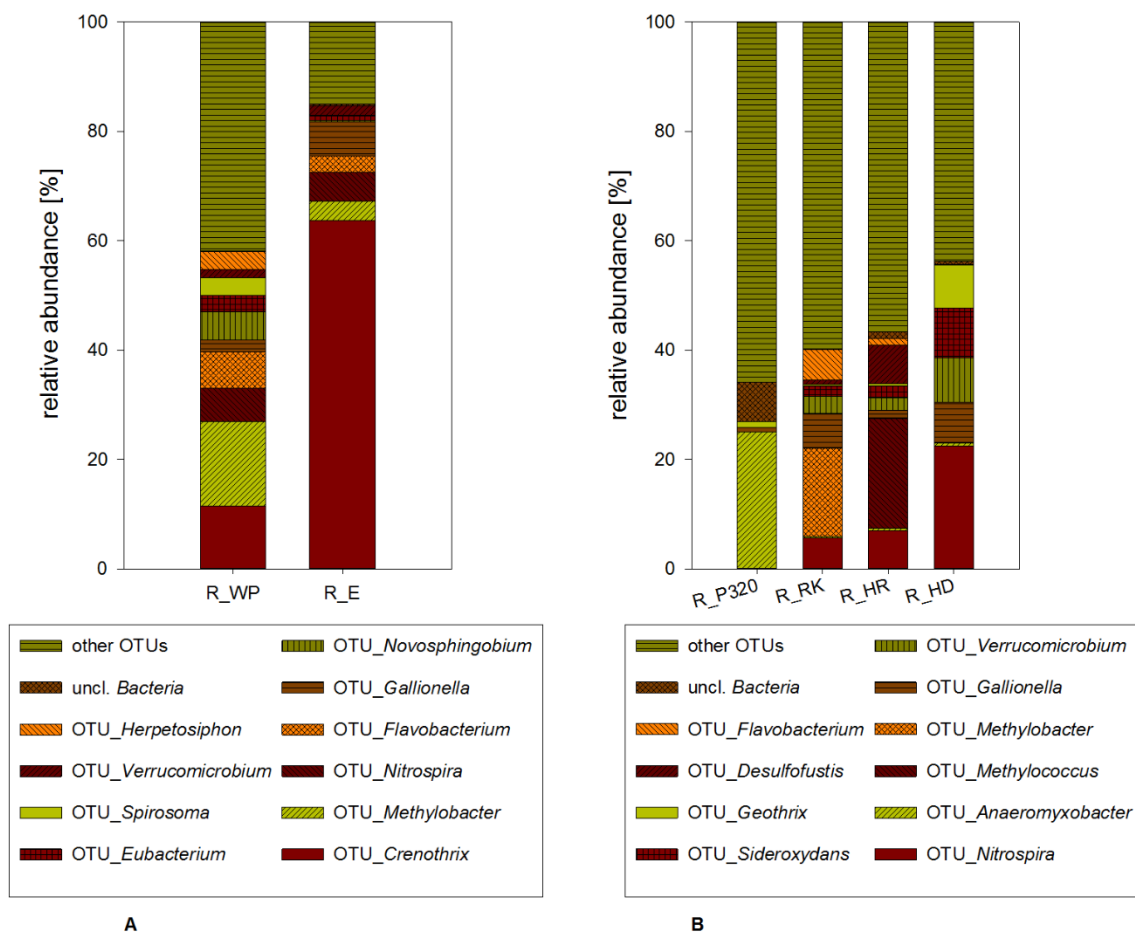


Figure 45. Relative abundance of the top 10 OTUs present in the biofilm samples taken in the opencast mining areas, estimated by 454-pyrosequencing: (A) Garzweiler, (B) Hambach.

3.3.5 Quantification of 16S rRNA gene copies from ochrous and water samples taken from the opencast mines

The quantitation reports produced by qPCR runs always demonstrated a certain reaction efficiency of between 80 to 95 %, as well as a required r^2 value of >0.99 . The melt curve analysis performed at the end of each run showed overlapping peaks at a consistent temperature, depending on fragment size, and a second, lower peak of the negative control, which was due to the remaining primers in the reaction.

The bacterial 16S rRNA gene abundance of the groundwater samples was determined in order to compare the samples taken from wells with aerated filters and non-aerated filters; this analysis was performed using samples obtained from the Hambach and Garzweiler opencast mines (Figure 46). Figure 46 A illustrates the gene copy abundance of four different bacterial groups, which were determined in the Hambach biofilm samples.

On average, 8×10^5 bacterial 16S rRNA gene copies ml^{-1} were detected in wells with aerated filter screens, while the number of gene copies was lower in wells equipped with non-aerated filters. The results of quantitative PCR demonstrated that the *Gallionella*- and *Rhodospirillum rubrum*-related gene copies were more abundant in samples derived from wells with non-aerated filters; *Crenothrix*-related 16S rRNA genes were present in similar numbers in both groups. Figure 46 B shows the bacterial abundance of the water wells located at the Garzweiler opencast mine. All detected groups were higher in those samples derived from wells with non-aerated filter screens; in particular, the *Crenothrix*-associated 16S rRNA gene copies showed the greatest difference between aerated and non-aerated filter screens.

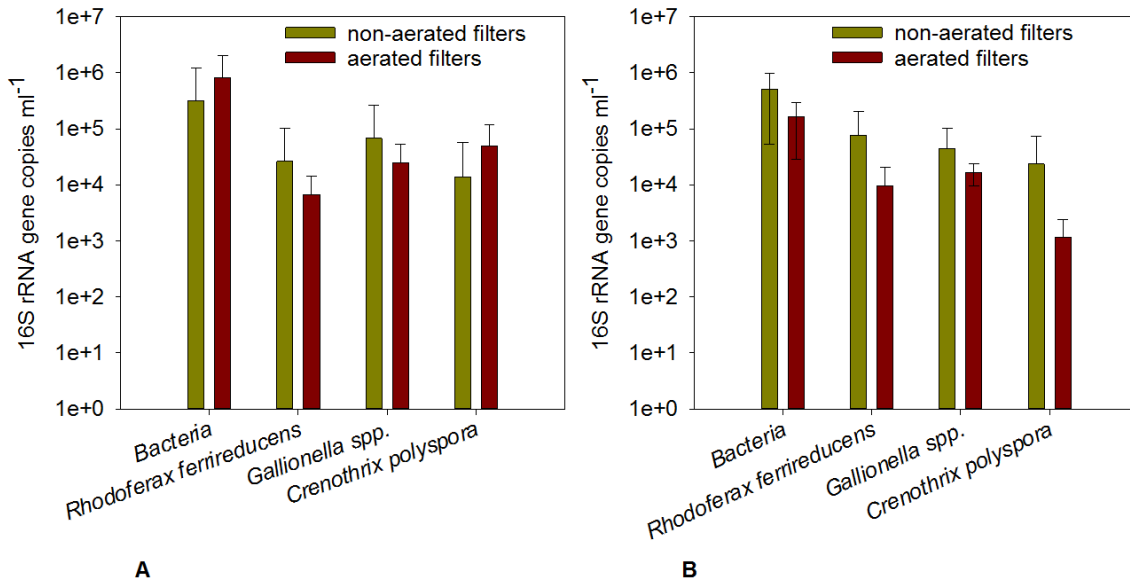


Figure 46. Plot of 16S rRNA gene copies from water samples taken from several water wells at the opencast mines: (A) Hambach and (B) Garzweiler. Gene copies of *Bacteria*, *Rhodoferrax ferrireducens*, *Gallionella* spp. and *Crenothrix polyspora* were detected. Error bars represent the standard error.

Furthermore, the bacterial 16S rRNA gene abundance in the iron deposits on several dewatering well components were analysed; all targeted groups in these samples could be detected by means of 454-pyrosequencing analysis (Figure 45). The samples analysed derived from pumps, filters and risers (Figure 47). The highest gene copy abundance was found in samples from the inlets (R_E) and the flap trap (R_RK) of pumps. *Gallionella*-related gene copies were highly abundant in samples taken from the pipes (R_HD), as well as those obtained from the inlet of the pump (R_E), with an average of 1×10^{10} copies g⁻¹ moist mass. *Crenothrix polyspora* gene copies were most abundant at the inlet of the pump (R_E), as also shown by the results of 454-pyrosequencing.

Geothrix fermentans 16S rRNA genes, as iron-reducing bacteria, were abundant in all samples due to the available amount of iron(III) found in all of the water wells; *Geothrix*-related sequences could also be detected by means of clone library construction and by 454-pyrosequencing. *Rhodoferrax ferrireducens* gene copies ranged from 1×10^5 to 1×10^{10} per g⁻¹ moist mass, depending on ochrous sample (Figure 47).

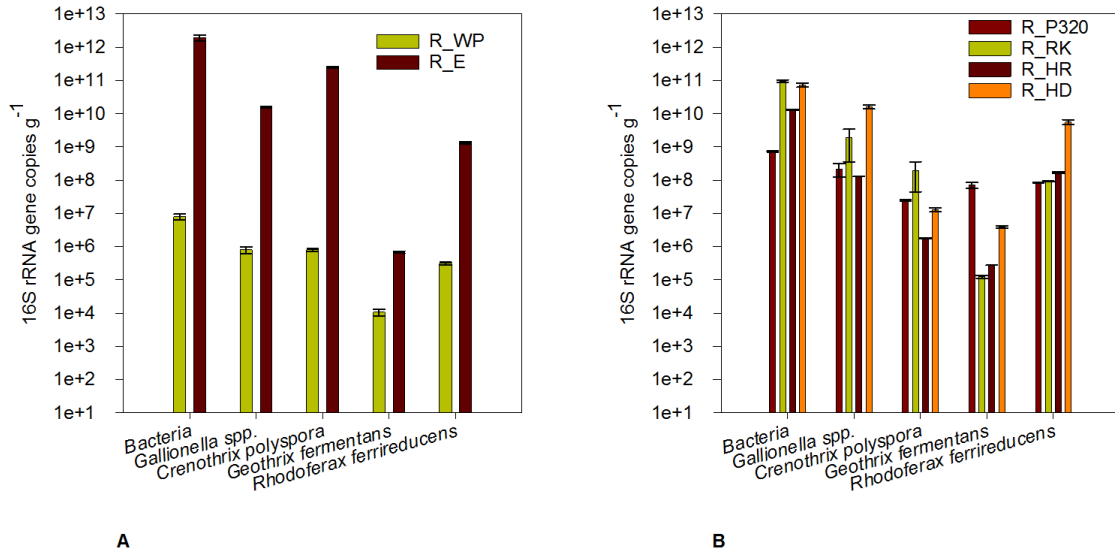


Figure 47. Plot of 16S rRNA gene copies of the ochrous samples derived from various components of the opencast mines' dewatering wells. (A) Garzweiler R_WP (WR2377, pump intake), R_E (WR2378, inlet filter) and (B) Hambach R_HD (HR45, riser), R_HR (HR1402, riser), R_P320 (H1424, pump), R_RK (HS1362, flap trap of pump). Gene copies of *Bacteria*, *Rhodoferrax ferrireducens*, *Gallionella* spp., *Geothrix fermentans* and *Crenothrix polyspora* were detected. Error bars represent the standard error.

Additionally, RDA was employed to explain the variance in gene copy data between these two groups (i.e., the bacterial populations of wells equipped with aerated and those of wells with non-aerated filter screens) caused by the environmental factors at Garzweiler and Hambach (Figure 48); these results show that the statistical test applied identified no significant differences between the groups from both sampling sites. However, the model accounted a fairly large portion of the variance ($r^2=25\%$) by determining the redox potential of the Garzweiler samples. However, this potential only serves as evidence of the factors that contribute to the differences in bacterial abundance between aerated and non-aerated filter screens ($p\text{-value}_{Eh} = 0.092$). Furthermore, the variance of the Hambach samples can mainly be explained (44 %) by the iron(III) concentration ($p\text{-value}_{Fe^{3+}} = 0.062$).

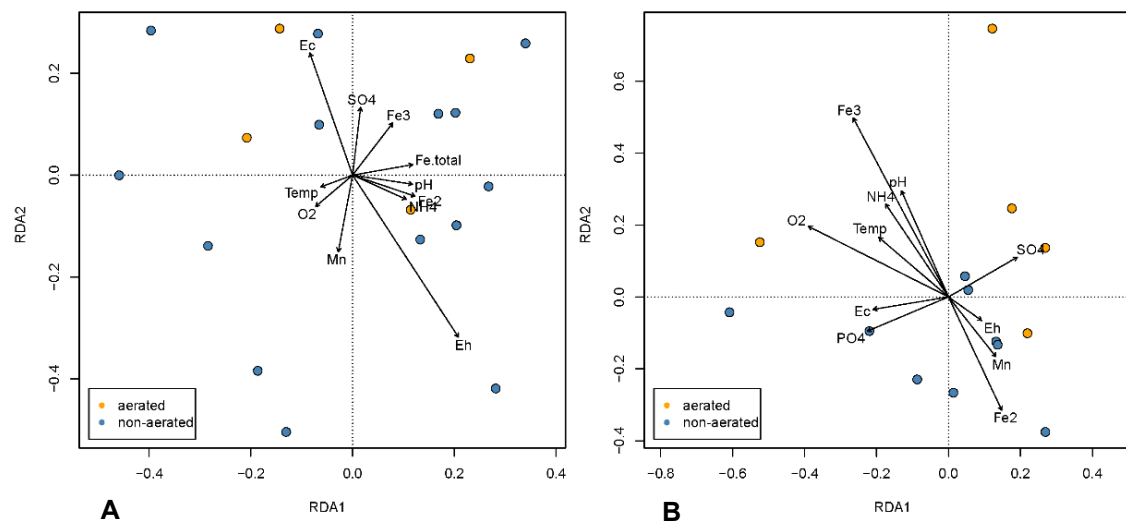


Figure 48. Graphical representation of RDA. (A) Samples derived from the Garzweiler and (B) Hambach opencast mines. The RDA model depicts the influence of environmental factors on the two microbial groups. The lengths and direction of the arrows indicate importance and correlation of environmental variables to the bacterial community.

3.4 Regeneration effects on the bacterial population of a lab-scale reactor with natural ochrous formation

The aim was to determine whether chemical and hydromechanical regeneration procedures affect the structure, diversity, composition and quantity of bacterial populations in a lab-scale reactor (Chapter 2.7.4). In total, the bacterial populations of two test series (TS I and TS II), with a total of seven columns including 26 samples were investigated. All test series, columns, parameters and regeneration types are summarized in Table A 5.

3.4.1 Hydrochemistry of groundwater from Dresden

The chemical values from of groundwater were provided by the HTW Dresden; all parameters were only determined once. The parameters investigated and results are shown in Table A 6. The oxygen concentration was below 0.05 mg l^{-1} , and the groundwater had a pH value of 6.8. Iron(II) had a concentration of 2.7 mg l^{-1} , and the electrical conductivity was 1.906 S cm^{-1} . Manganese(II) had a concentration of 0.3 mg l^{-1} , in contrast to the high sulphate content of 564 mg l^{-1} . The DOC value was below 3.5 mg l^{-1} . All columns were flushed with groundwater from groundwater station I.

3.4.2 Denaturing gradient gel electrophoresis profiling of the bacterial communities of biofilm samples within a lab-scale reactor

In order, to compare the bacterial genetic diversity of the large number of samples derived from the lab-scale reactor, DGGE profiling of the 16S rRNA gene was used.

The bacterial populations derived from the samples used in test series I showed two distinct clusters of approximately 40 % similarity (Figure 49). Within cluster one, patterns in the bacterial population from samples taken at a depth of 5 cm formed a former cluster with 78 % similarity. Another cluster, consisting of samples taken from S1 and S4 at depths of 15 to 20 cm, showed a similarity of 70 %; the bacterial populations of both columns were affected by the regeneration procedures, whereas S6, which served as the outgroup column, showed a different bacterial community. At a depth of 45 cm, the bacterial fingerprints of all

of the columns revealed a greater number of bands and clustered together with the groundwater sample fingerprint (70 % similarity).

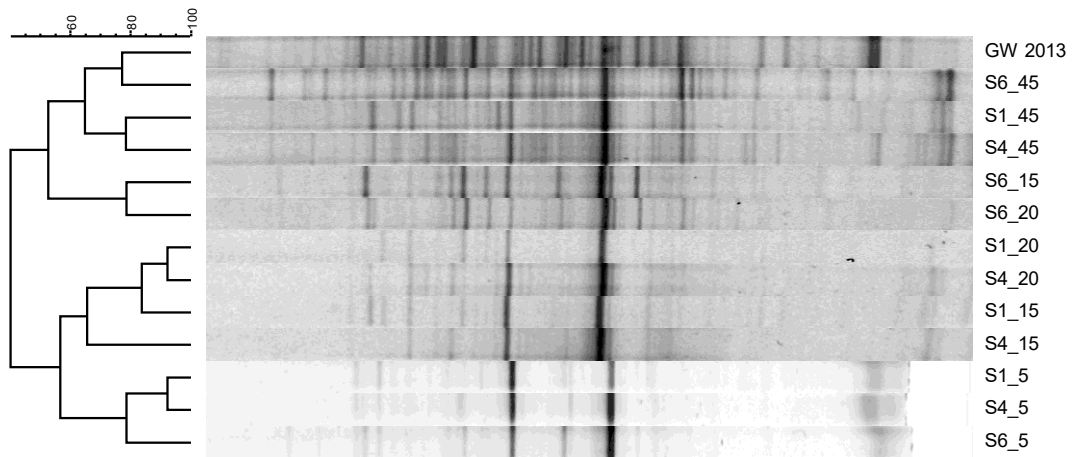


Figure 49. Dendrogram constructed with bacterial fingerprints of the biofilm and groundwater samples derived from TS I. The dendrogram is based on the Dice coefficient and UPGMA cluster analysis. The scale bar indicates the similarity of community profiles [%]: the numbers _5, _15, _20 and _45 stand for the depth [cm] at which each sample was taken.

The bacterial populations derived from the samples used in test series II revealed two distinct clusters of approximately 70 % similarity, while the groundwater sample represented an outgroup sample (Figure 50). Within the first cluster, three bacterial fingerprints belonged to S5 (78 % similarity) and one fingerprint to S8; the filter sand of both columns was pretreated using AIXTRACTOR® 2.0 in order to dissolve the iron (Chapter 2.7.4). Within the second cluster, two further clusters, consisting of fingerprints from columns S2, S4 and S5 were calculated with a similarity of 72 % to each other; the filter sand of columns two and four was not pretreated. No clear clustering of bacterial fingerprints was found in either the pretreated or non-pretreated material groups.

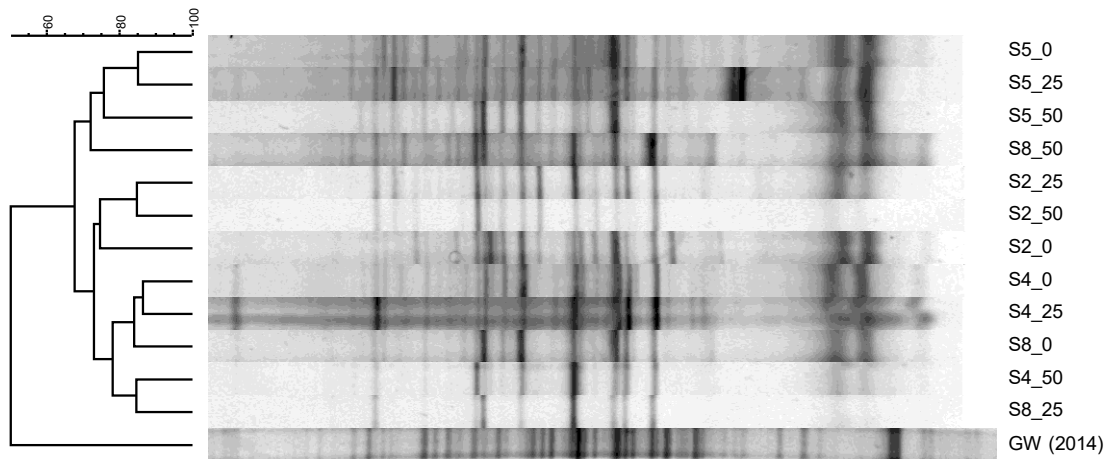


Figure 50. Dendrogram constructed with bacterial fingerprints of biofilm and groundwater samples derived from TS II; This dendrogram is based on the Dice coefficient and UPGMA cluster analysis. The scale bar indicates the similarity of community profiles [%]: The numbers _0, _25 and _50 stand for the depth (cm) at which each sample was taken.

In order to graphically illustrate the structure of the bacterial communities from both test series, P-L evenness curves were constructed based on the DGGE profiles (Figure 51). The P-L curves of test series I ranged from 40 to 65 %, while the P-L of test series II only ranged from 40 to 48 %; therefore, both communities can be described as being balanced, with medium *Fo*. No influence from the various regeneration procedures on the bacterial community structure could be seen by this evaluation method, as shown by the similar values of the P-L curves.

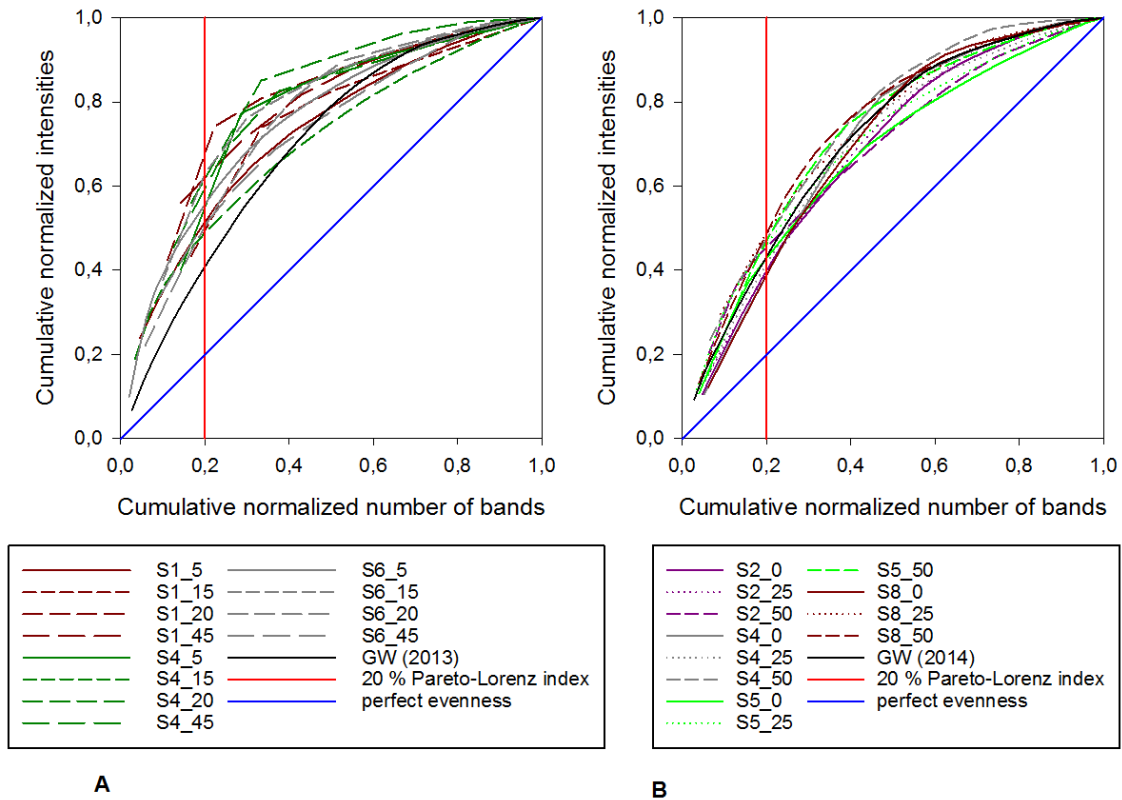


Figure 51. Comparison of the P-L distribution curves based on the DGGE profiles of the biofilm samples derived from the columns of the two test series: (A) TS I and (B) TS II.

Additionally, the range-weighted richness of the bacterial populations at different depths of all columns and of the groundwater samples was calculated by correlating the distribution (number) of bands in one fingerprint in association with the denaturing gradient (Figure 52). The *Rr* values of samples (TS I) from the lower sections (5-20 cm) of the columns were particularly low when compared to those found at the higher sections (45 cm), where the richness increased. The highest bacterial richness calculated was that of column S6, which served as the control column and did not undergo any kind of regeneration procedure.

In total, the lowest richness was calculated for column S1; S1 was immediately regenerated after storage by means of chemical and mechanical regeneration. In contrast to the *Rr* values of TS I, the *Rr* values calculated for test series II showed different results. The values for columns S2 and S4, which were not pretreated, ranged from 95 to 110, while the highest values were found in the lower sections of the columns. Richness was higher in column S4, which was not regenerated. Column S5 showed the highest richness values, though the material was

pretreated and regenerated twice. However, the bacterial richness of the groundwater samples remained stable between 2013 and 2014.

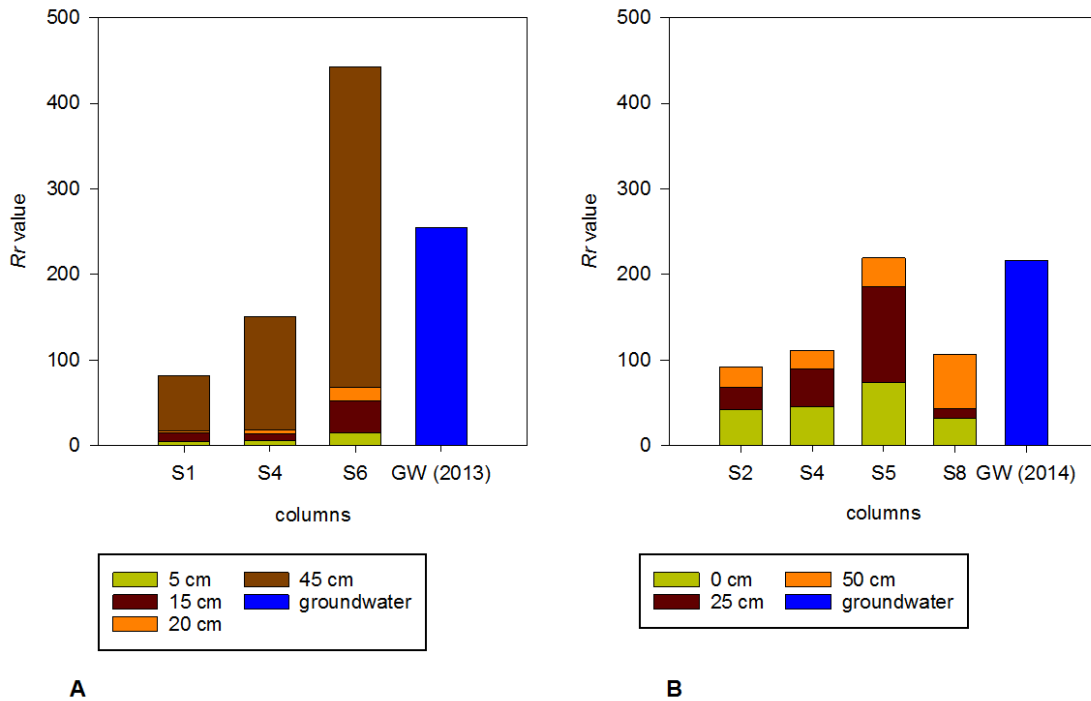


Figure 52. Plots of R_r values based on the DGGE profiles of samples taken from the lab-scale reactor. (A) Test series I and (B) test series II.

3.4.3 Bacterial population analysis within a lab-scale reactor by 16S rRNA gene clone libraries

In order, to gain deeper insight into the bacterial population composition, two samples were used for clone library construction: The groundwater with which the columns were flushed and a biofilm sample derived from a non-regenerated column. At the phylum level, the bacterial populations inhabiting the groundwater and the bacteria found in the biofilm samples differed, despite the presence of *Proteobacteria* in both (21 to 25 %). Sequences associated with the phyla *Firmicutes* (2 %), *Nitrospirae* (4 %) and *Ignavibacteria* (2 %) were present in the groundwater, while sequences associated with *Acidobacteria* (43 %), *Actinobacteria* (2 %) and *Bacteroidetes* (2 %) were represented the biofilm community (Figure 53 A).

Furthermore, the top 10 OTUs at the family and genus levels were calculated. Both samples showed variations in the OTU composition (Figure 53 B); the water sample was mainly associated with a group of uncl. *Deltaproteobacteria* (21 %) and *Cellvibrio* (9 %). Sequences derived from biofilm sample of column S4 showed similarities to the iron-reducing family *Holophagaceae* (41 %) and the genus *Geobacter* (11 %).

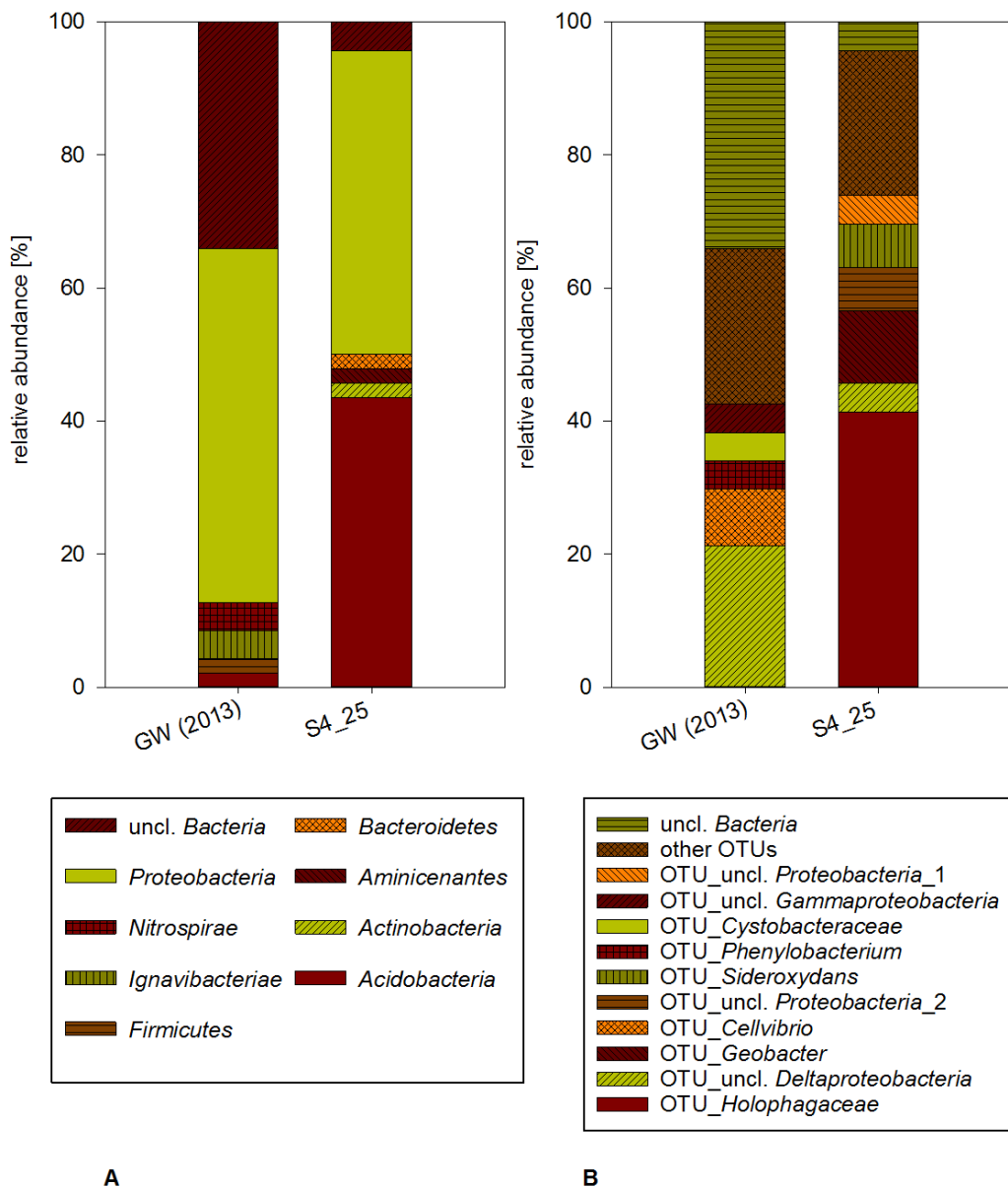


Figure 53. Plots of 16S rRNA clone libraries (A) at the phylum level and (B) the top 10 OTUs from the groundwater and biofilm samples.

3.4.4 Quantification of 16S rRNA gene copies from biofilm samples taken from columns of a lab scale reactor

Bacterial gene copies of the 16S rRNA gene of the total genomic DNA derived from various biofilm samples were quantified. In addition, the gene copies of the groundwater samples were determined.

The quantitation reports produced by the qPCR runs always had a certain reaction efficiency of between 80 to 95 %, as well as a required r^2 value of >0.99 . The melt curve analysis performed at the end of each run showed overlapping peaks at a consistent temperature, depending on fragment size, and a second, lower peak in the negative control, which was due to the remaining primers in the reaction.

Test series I

The gene copies were calculated for three columns at four different depths and were correlated with the decreases in hydraulic conductivity (k_f -values), which served as an indicator of clogging within the columns (Figure 54); the highest decrease of k_f was found in S6 (control column with no regeneration), whereas the lowest decrease was achieved in column S4 (two times regeneration).

The maximum gene copies (approximately 5×10^9 gene copies g^{-1}) targeting *Bacteria* were found at 5 cm depth for all three columns, independent of regeneration procedures; the number of gene copies calculated from biofilms taken at the 20 cm depth remained stable for all three columns. The highest abundances of gene copies targeting specific groups of bacteria were calculated for iron-oxidising *Gallionella* spp. and were found in S6 at all depths, except at the end of the column (Figure 54 C).

Furthermore, the Bacterial gene copy numbers of the groundwater sample were higher compared to the other specific bacterial groups. The lowest decrease in the k_f -value was found in S4, which was regenerated twice; no gene copies of *Gallionella* spp. could be detected at the 20 to 45 cm depths. No gene copies targeting *Crenothrix polyspora* could be found in S4, whereas 10^4 to 10^5 copies g^{-1} were calculated for S1 and S6 (Figure 54 D). *Rhodoferrax*-related gene copies were detected in all columns as well as at all depths, with the exception of S1 at

a depth of 45 cm (Figure 54 B). Iron-reducing gene copies targeting *Geothrix fermentans* were only found at 5 cm depths; no *Geothrix* gene copies were detected in the groundwater sample (Figure 54 E).

In summary, no correlation could be found between the total number of bacterial gene copies and the decrease in the k_f -values. However, there was evidence for a correlation between the highest decrease in the k_f -value and the highest number of distributed gene copies targeting the iron-oxidiser of *Gallionella* and methane-oxidiser *Crenothrix*.

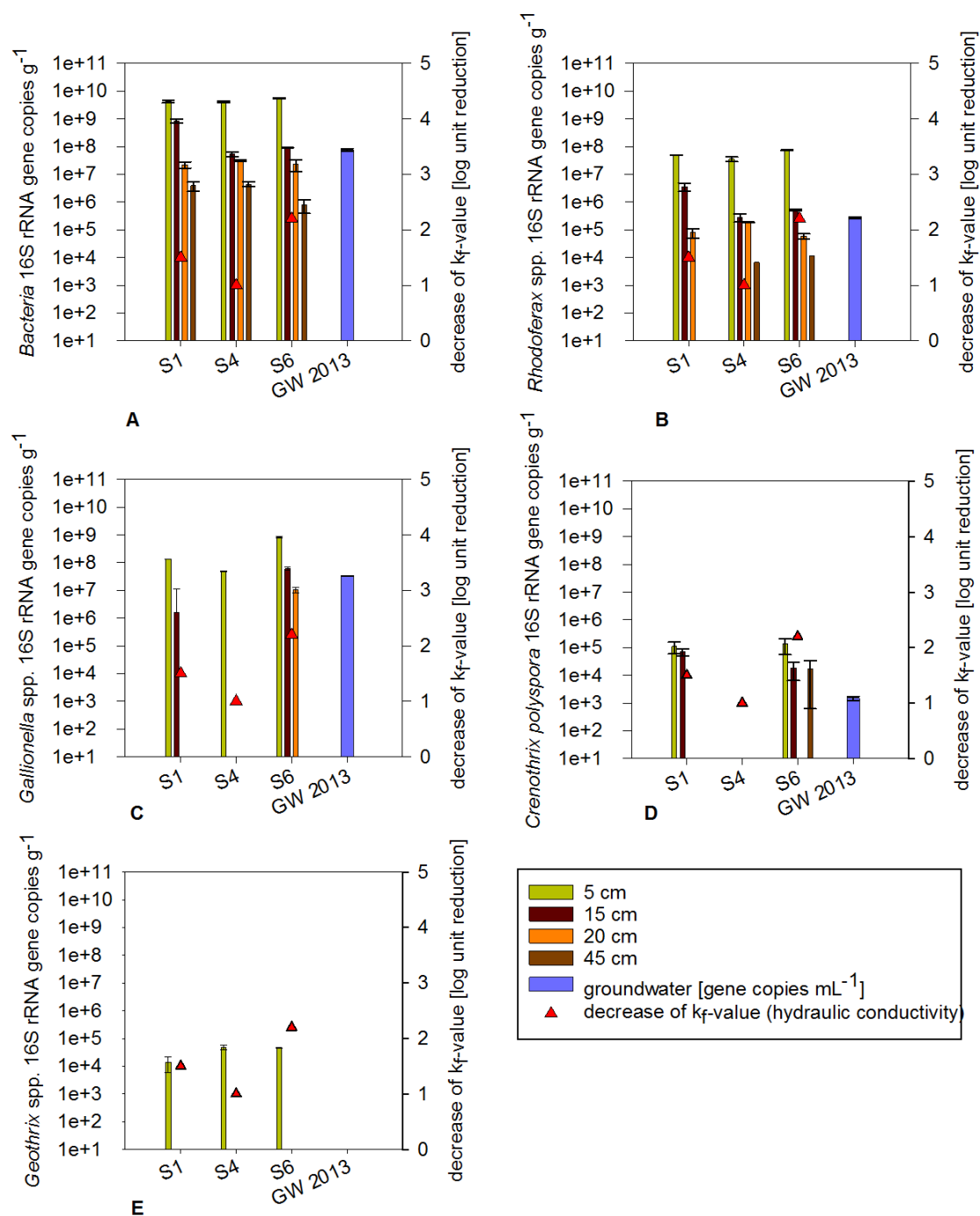


Figure 54. Plots of 16S rRNA gene copies from the biofilm and water samples taken from several columns from test series I correlated to hydraulic conductivity. Gene copies targeting of (A) *Bacteria*, (B) *Rhodoferrax ferrireducens*, (C) *Gallionella* spp., (D) *Crenothrix polyspora* and (E) *Geothrix fermentans*. Error bars represent the standard error.

Test series II

The number of gene copies were calculated for four columns at three different depths and were correlated with the decrease in hydraulic conductivity (k_f -values), which served as an indicator of clogging within the columns (Figure 55); the highest decrease in k_f was achieved in S2 (filter sand with no pretreatment and one time regeneration), whereas the lowest decrease was detected in column S5 (material pretreated and regenerated twice).

The highest gene copy numbers (10^4 to 10^{10}) of all of the targeting bacterial groups were always found at a depth of 0 to 2 cm depth, with the exception of column S5, which showed the highest gene copies (10^4 to 10^9) at the 25 and 50 cm depths (Figure 55 A-E). Gene copies of all qPCR primer assays, except those of *Gallionella* spp. within columns S2 and S4, always ranged in the same region per g^{-1} ; the filter sand within both columns was not pretreated with AIXTRACTOR 2.0®, but, in contrast to S4, S2 was regenerated. No gene copies targeting *Gallionella* were found at the 50 cm depth within S2 (Figure 55 C).

Columns S5 and S8 differed in the regeneration procedures that they underwent; S5 was regenerated twice, whereas S8 served as the control column. However, the filter-sand in both columns was pretreated. The gene copies of both columns S5 and S8 showed major variations, in particular with regard to gene copies targeting *Gallionella*, *Crenothrix* and *Geothrix* (Figure 55 C-D). Furthermore, in the groundwater sample, gene copy numbers targeting *Bacteria* ($10^4 g^{-1}$) and *Rhodoferrax ferrireducens* ($10^1 g^{-1}$) could only be detected.

Similarly to the findings of test series I, no correlation could be identified between the total number of bacteria and the decrease in hydraulic conductivity caused by the application of the various regeneration procedures. However, *Crenothrix ployspora* related gene copies were not detected within S5 and showed no decrease of the k_f -value; *Gallionella* spp. was only found at a depth of 50 cm.

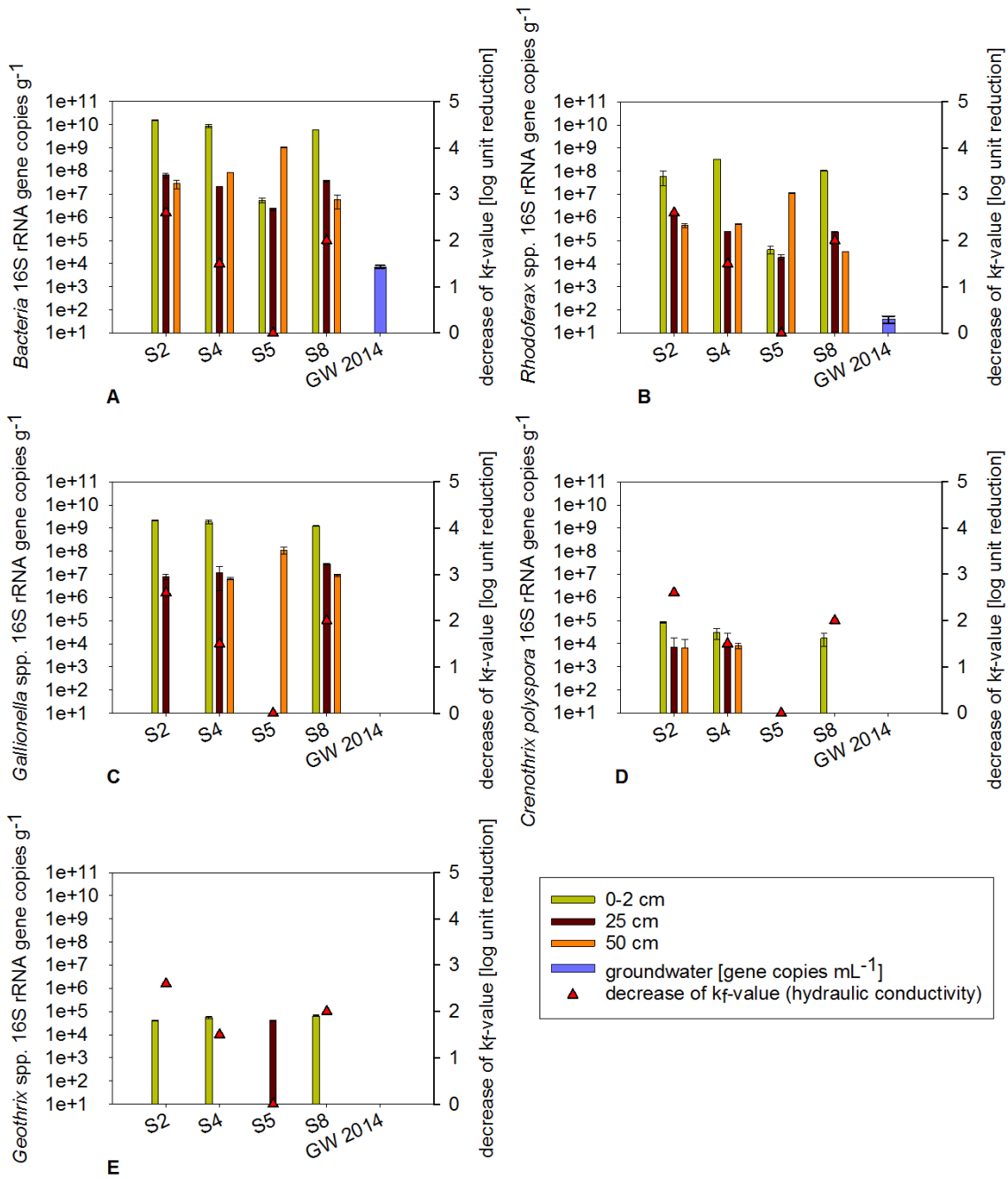


Figure 55. Plots of 16S rRNA gene copies from the biofilm and water samples taken from several columns from test series II correlated to hydraulic conductivity. Gene copies targeting of (A) *Bacteria*, (B) *Rhodoferrax ferrireducens*, (C) *Gallionella* spp., (D) *Crenothrix polyspora* and (E) *Geothrix fermentans*. Error bars represent the standard error.

In addition, the iron content was measured at different depths and was correlated to the qPCR results (Figure 56). The highest iron content (15 mg g^{-1}) was found within columns S2, S4 and S8 at a depth of 0 to 2 cm, correlating with the high abundances of *Bacteria* ($\sim 10^{10}$), *Rhodoferrax* ($\sim 10^8$) and *Gallionella* ($\sim 10^9$) gene

copies g^{-1} , whereas S5 only had a content of 9 mg g^{-1} . (Figure 56 A). The iron content at the 25 cm depth within all of the columns varied from 1 mg g^{-1} (S5) to 12 mg g^{-1} (S4). All of the columns showed high abundances of *Gallionella* gene copies g^{-1} , with the exception of S5 (Figure 56 B). At a depth of 50 cm, the highest abundances of gene copies, except those related to *Crenothrix* and *Geothrix*, were found for S5. However, S5 contained the lowest amount of iron (1 mg g^{-1}) compared to the iron content of the remaining columns (S2, S4, S8) and ranged from 4 to 10 mg g^{-1} (Figure 56 C).

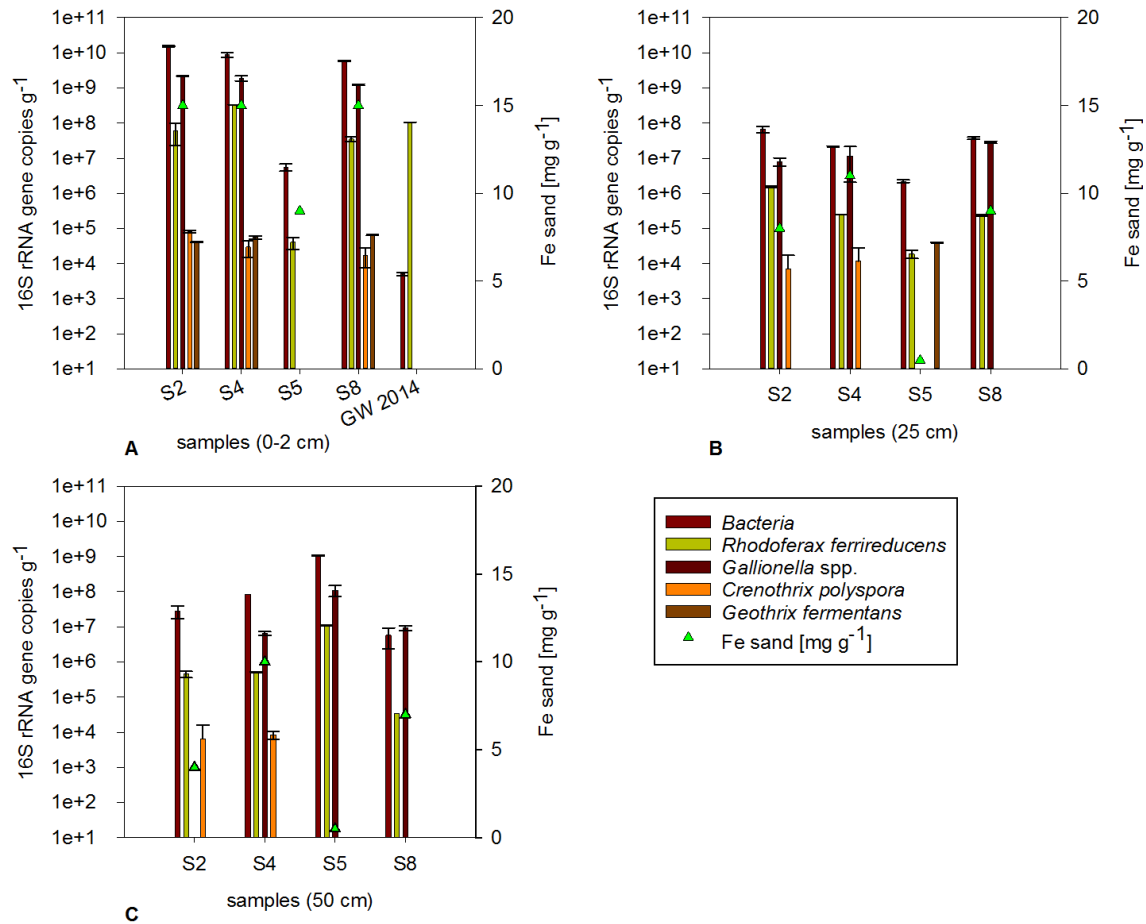


Figure 56. Plots of 16S rRNA gene copies from the biofilm samples taken from several columns from test series II at various depths correlated to the Fe sand content. Gene copies targeting of (A) *Bacteria*, (B) *Rhodoferrax ferrireducens*, (C) *Gallionella* spp., (D) *Crenothrix polyspora* and (E) *Geothrix fermentans*. Error bars represent the standard error.

3.5 Isolation of iron-depositing bacteria from the biofilm samples of technical groundwater systems

In addition to culture-independent biomolecular methods, aerobic isolation and cultivation of iron-depositing bacteria were carried out (Chapter 2.5); bacteria from various biofilm samples taken from technical groundwater systems were isolated on LSM2 and H₂O media (Chapter 2.6). In total, 33 strains, grouped into 13 OTUs (according to 97 % similarity), were isolated (Table 30). Within the 33 isolates, the phylum *Actinobacteria* (~45 %) represented the major group, followed by *Proteobacteria* (~36 %), *Firmicutes* (~15 %) and *Bacteroidetes* (~3 %).

The 16S rRNA sequences which were affiliated to the phyla *Actinobacteria* including the genera *Tetrasphaera*, *Terrabacter*, *Kineosporia*, *Micromonospora*, *Brevibacterium* and *Nocardioides*. The genera within the phyla *Proteobacteria* belonged to *Rhodomicrobium*, *Pedomicrobium*, *Caulobacter* and *Rheinheimera*. The phyla *Firmicutes* and *Bacteroidetes* were only affiliated to one genera (*Bacillus* and *Flavobacterium*) each. Considering the 16S rRNA gene sequence similarity of 99 % proposed by Stackebrand and Ebers (2006), 19 out of 33 strains belonged to the species level. Sequences of the strains which belonged to *Rhodomicrobium* only had a similarity of 93 % and should be named as uncl. *Rhizobiales* due to the fact that the sequence is only 91 % similar to the family *Hyphomicrobiaceae*; however, the sequence is 100 % similar to *Rhizobiales* (order level). The strains were isolated from the pump check valve of a dewatering well at the Hambach opencast mine.

The iron and manganese deposition activity of all isolates was verified by dissolving the colonies with oxalic acid (10 %) as previously described by Schmidt et al., (2014); however, phylogenetic analysis revealed that most of the isolated strains could not be affiliated to known iron-depositing bacteria.

In order to unravel the bacterial iron-depositing ability, whole-genome sequencing was performed for several strains. The draft genome sequence of S_A_1 has already been published by Schröder et al. (2016); in addition, the draft genome sequence of R_RK_3, isolated from biofilm deposits of dewatering wells, was published by Braun et al. (2017).

Table 30. Phylogenetic affiliation of bacterial cultures isolated from various technical groundwater systems.

Strain number	Next relative (NCBI database)	Accession-number	Max. identity	Media	Point of origin	Classification			
						Phyla	Class	Family	OTU
R_RK_10	<i>Rhodomicrobium vanniellii</i>	NR_117027.1	93 %	H ₂ O	Hambach opencast mine HS1326 (check valve)	<i>Proteobacteria</i>	<i>Alphaproteobacteria</i>	<i>Hyphomicrobiaceae</i>	1
R_RK_3	<i>Rhodomicrobium vanniellii</i>	NR_117027.1	93 %	H ₂ O	Hambach opencast mine HS1326 (check valve)	<i>Proteobacteria</i>	<i>Alphaproteobacteria</i>	<i>Hyphomicrobiaceae</i>	1
R_RK_1	<i>Rhodomicrobium vanniellii</i>	NR_117027.1	93 %	H ₂ O	Hambach opencast mine HS1326 (check valve)	<i>Proteobacteria</i>	<i>Alphaproteobacteria</i>	<i>Hyphomicrobiaceae</i>	1
R_RK_2	<i>Rhodomicrobium vanniellii</i>	NR_117027.1	93 %	H ₂ O	Hambach opencast mine HS1326 (check valve)	<i>Proteobacteria</i>	<i>Alphaproteobacteria</i>	<i>Hyphomicrobiaceae</i>	1
RU_RCW_9	<i>Pedomicrobium americanum</i>	NR_104908.1	99 %	H ₂ O	Komsomolsk (pure water container)	<i>Proteobacteria</i>	<i>Alphaproteobacteria</i>	<i>Hyphomicrobiaceae</i>	2
RU_RCW_12	<i>Pedomicrobium americanum</i>	NR_104908.1	99 %	H ₂ O	Komsomolsk (pure water container)	<i>Proteobacteria</i>	<i>Alphaproteobacteria</i>	<i>Hyphomicrobiaceae</i>	2
RU_1132_2	<i>Pedomicrobium americanum</i>	NR_104908.1	99 %	LSM2	Komsomolsk (pure water container)	<i>Proteobacteria</i>	<i>Alphaproteobacteria</i>	<i>Hyphomicrobiaceae</i>	2
RU_1132_1	<i>Pedomicrobium americanum</i>	NR_104908.1	99 %	LSM2	Komsomolsk (pure water container)	<i>Proteobacteria</i>	<i>Alphaproteobacteria</i>	<i>Hyphomicrobiaceae</i>	2
RU_RCW_13	<i>Pedomicrobium americanum</i>	NR_104908.1	99 %	LSM2	Komsomolsk (pure water container)	<i>Proteobacteria</i>	<i>Alphaproteobacteria</i>	<i>Hyphomicrobiaceae</i>	2

Strain number	Next relative (NCBI database)	Accession-number	Max. identity	Media	Point of origin	Classification			
						Phyla	Class	Family	OTU
RU_RCW_14	<i>Caulobacter henricii</i>	NR_025319.1	99 %	H ₂ O	Komsomolsk (pure water container)	<i>Proteobacteria</i>	<i>Alphaproteobacteria</i>	<i>Caulobacteraceae</i>	3
S_A_1	<i>Rheinheimera chironomi</i>	NR_044581.1	98 %	LSM2	BWB, Stolpe Borgsdorf (Sludge basin)	<i>Proteobacteria</i>	<i>Gammaproteobacteria</i>	<i>Chromatiaceae</i>	4
S_A_7	<i>Rheinheimera chironomi</i>	NR_043699.1	99 %	LSM2	BWB, Stolpe Borgsdorf (Sludge basin)	<i>Proteobacteria</i>	<i>Gammaproteobacteria</i>	<i>Chromatiaceae</i>	4
D_FH_1	<i>Bacillus subterraneus</i>	NR_104749.1	99 %	LSM2	reactor with ochrous formation (filter sand)	<i>Firmicutes</i>	<i>Bacilli</i>	<i>Bacillaceae</i>	5
S_BO_2	<i>Bacillus thio-parans</i>	NR_043762.1	99 %	LSM2	BWB, Stolpe Borgsdorf (Sludge basin)	<i>Firmicutes</i>	<i>Bacilli</i>	<i>Bacillaceae</i>	5
RU_1134_1	<i>Bacillus subterraneus</i>	NR_104749.1	99 %	LSM2	Khabarovsk 1 st section (measuring point 1134)	<i>Firmicutes</i>	<i>Bacilli</i>	<i>Bacillaceae</i>	5
RU_1134_2	<i>Bacillus subterraneus</i>	NR_104749.1	99 %	LSM2	Khabarovsk 1 st section (measuring point 1134)	<i>Firmicutes</i>	<i>Bacilli</i>	<i>Bacillaceae</i>	5
RU_RCW_4	<i>Bacillus subterraneus</i>	NR_104749.1	99 %	LSM2	Khabarovsk 1 st section (measuring point 1134)	<i>Firmicutes</i>	<i>Bacilli</i>	<i>Bacillaceae</i>	5
R_HD_1	<i>Tetrasphaera duodecadis</i>	NR_040880.1	98 %	LSM2	Garzweiler opencast mine HR45 (riser)	<i>Actinobacteria</i>	<i>Actinobacteria</i>	<i>Intrasporangiaceae</i>	6
R_BR_6	<i>Terrabacter tumescens</i>	NR_044984.2	99 %	H ₂ O	Garzweiler opencast mine WE2378 (Refractory tube)	<i>Actinobacteria</i>	<i>Actinobacteria</i>	<i>Intrasporangiaceae</i>	7
R_WP_1	<i>Kineosporia mikuniensis</i>	NR_041678.1	96 %	H ₂ O	Garzweiler opencast mine WR2377 (pump intake)	<i>Actinobacteria</i>	<i>Actinobacteria</i>	<i>Kineosporiaceae</i>	8

Results

Strain number	Next relative (NCBI database)	Accession-number	Max. identity	Media	Point of origin	Classification			
						Phyla	Class	Family	OTU
R_H_3	<i>Kineosporia rhizophila</i>	NR_117176.1	96 %	H ₂ O	Hambach opencast mine HS1376 (320 m depth)	<i>Actinobacteria</i>	<i>Actinobacteria</i>	<i>Kineosporiaceae</i>	8
R_WP_4	<i>Kineosporia aurantiaca</i>	NR_041718.1	97 %	H ₂ O	Garzweiler opencast mine WR2377 (pump intake)	<i>Actinobacteria</i>	<i>Actinobacteria</i>	<i>Kineosporiaceae</i>	8
R_HR_3	<i>Micromonospora maritima</i>	NR_109311.1	99 %	H ₂ O	Garweiler opencast mine HR1402 (riser)	<i>Actinobacteria</i>	<i>Actinobacteria</i>	<i>Micromonosporaceae</i>	9
R_HR_4	<i>Micromonospora maritima</i>	NR_109311.1	100 %	H ₂ O	Garweiler opencast mine HR1402 (riser)	<i>Actinobacteria</i>	<i>Actinobacteria</i>	<i>Micromonosporaceae</i>	9
R_HR_2	<i>Micromonospora maritima</i>	NR_109311.1	99 %	H ₂ O	Garweiler opencast mine HR1402 (riser)	<i>Actinobacteria</i>	<i>Actinobacteria</i>	<i>Micromonosporaceae</i>	9
R_HR_8	<i>Micromonospora maritima</i>	NR_109311.1	100 %	H ₂ O	Garweiler opencast mine HR1402 (riser)	<i>Actinobacteria</i>	<i>Actinobacteria</i>	<i>Micromonosporaceae</i>	9
R_WR_2	<i>Brevibacterium casei</i>	NR_041996.1	99 %	H ₂ O	Garzweiler opencast mine WR2377 (riser)	<i>Actinobacteria</i>	<i>Actinobacteria</i>	<i>Brevibacteriaceae</i>	10
S_BE_1	<i>Nocardioides terrigena</i>	NR_044185.1	99 %	H ₂ O	BWB, Stolpe Borgsdorf (aeration tank)	<i>Actinobacteria</i>	<i>Actinobacteria</i>	<i>Nocardioideaceae</i>	11
R_WRS_2	<i>Nocardioides mesophilus</i>	NR_116027.1	98 %	H ₂ O	Garzweiler opencast mine WR2377 (flap trap of pump)	<i>Actinobacteria</i>	<i>Actinobacteria</i>	<i>Nocardioideaceae</i>	12
R_WP_1	<i>Nocardioides mesophilus</i>	NR_116027.1	98 %	H ₂ O	Garzweiler opencast mine WR2377 (flap trap of pump)	<i>Actinobacteria</i>	<i>Actinobacteria</i>	<i>Nocardioideaceae</i>	12

Results

Strain number	Next relative (NCBI database)	Accession-number	Max. identity	Media	Point of origin	Classification			
						Phyla	Class	Family	OTU
R_WR_1	<i>Nocardioides mesophilus</i>	NR_116027.1	98 %	LSM2	Garzweiler opencast mine WR2377 (riser)	<i>Actinobacteria</i>	<i>Actinobacteria</i>	<i>Nocardioideaceae</i>	12
R_WRS_1	<i>Nocardioides mesophilus</i>	NR_116027.1	97 %	H ₂ O	Garzweiler opencast mine WR2377 (flap trap of pump)	<i>Actinobacteria</i>	<i>Actinobacteria</i>	<i>Nocardioideaceae</i>	12
R_H_2	<i>Flavobacterium chungangense</i>	NR_044581.1	98 %	H ₂ O	Hambach open castmine HS1376 (320 m depth)	<i>Bacteroidetes</i>	<i>Flavobacteria</i>	<i>Flavobacteriaceae</i>	13

4 Discussion

4.1 Comparison of the bacterial population compositions of ochrous biofilms and groundwater samples obtained from technical groundwater-fed systems

In this study, the bacterial compositions of water and ochrous samples from various groundwater-fed systems were compared. Those sampling systems were all characterised by a vulnerability to iron-clogging due to the availability of oxygen and ferruginous source waters.

4.1.1 Comparison of the bacterial population composition of ochrous biofilms from clogged and non-clogged drinking water wells

The drinking water wells were located at various well galleries in Berlin, Germany (Figure 1). Ochrous biofilms were obtained from the suction strainers of several drinking water well pumps, which were grouped into two categories: clogged and non-clogged wells. The bacterial populations of these biofilms were investigated according to their dominant bacterial groups (OTUs) using 16S rRNA gene clone libraries and qPCR. In addition, their structure and richness were analysed by DGGE. Moreover, the chemical parameters of the drinking water samples were correlated to the qPCR results in order to investigate potential correlations between hydrochemical characteristics and specific bacterial sub populations (Chapter 3.1).

The clogged wells were characterised by voluminous, amorphous and soft iron precipitates, while the non-clogged wells contained thin biofilms. The deposits around the pumps affected the specific well yields and the functioning of equipment such as pumps and pipes; over time, iron-deposits may transform into more crystalline and harder structures, making regeneration procedures more complex and expensive (Tuhela et al., 1997). However, in this study, soft and 'young' (max. 6 years) iron-deposits were investigated. The incrustations mostly contained iron(III)-oxid, with a range content of 52.6 to 70.72 %.

The hydrochemical results of groundwater samples suggested only minor differences between the groundwater in the clogged and non-clogged wells. The sulphate concentrations were very high (up to 309 mg l⁻¹) in both well groups. Bacterial sulphate reduction is an important process in an anoxic environment such as this aquifer. The reduced sulphide precipitates with iron(III) and manganese(IV) (van Beek, 1989), and along with bacterial biomass, it may contribute to clogging in wells. However, in this study, the highest sulphate concentration in a water sample was measured in a non-clogged well. None of the hydrochemical parameters measured significantly differed between clogged and non-clogged wells, and this fact, that no difference was found, was also reflected by the bacterial population structure analysed via DGGE. In the DGGE analysis, no correlation between the microbial patterns of clogged and non-clogged wells was found (Figure 8). In addition, according to the DGGE profiles, the richness of the bacterial community of both wells groups were high, but higher in non-clogged wells compared to clogged wells.

The 16S rRNA gene clone libraries of both groups (clogged and non-clogged wells) were primarily associated with the iron-reducing groups, such as *Geobacter* spp., *Geothrix* spp. and *Pseudomonas* spp.; no common iron-oxidising bacteria were found by clone library construction. However, Weber et al. (2006) demonstrated that *Geobacter metallireducens*, a typical iron reducer, is capable of nitrate-dependent iron(II) oxidation and could therefore contribute to iron-clogging. Two different OTUs (based on 97 % similarity) of the genus *Geobacter* were found in the clogged drinking water wells, while OTU_*Geobacter*_4 was not detected in the non-clogged wells. In addition, some *Geobacter* can couple nitrate reduction to ammonium with iron(II) oxidation in the presence of acetate (Coby et al., 2011). That means, that without a typical iron-oxidiser, drinking water wells might be particularly susceptible to iron-clogging, due to anoxic iron(II) oxidation. Melton et al. (2014) proposed that small environmental fluctuations may shift the balance between iron oxidation or reduction processes. Inhabiting a fluctuating environment like a groundwater well, the different bacterial groups need to be metabolically flexible, if they want to survive the social pressure within their communities. Elliott et al. (2014) proposed that iron-reducing bacteria and heterotrophic bacteria form a collaboration that expands the iron-oxidising bacteria niche, and they identified the importance of

cooperation that the iron-oxidising bacteria require iron-reducing bacteria, rather than a simple Fe(II) media salt, to provide an accessible Fe(II) source under the appropriate environmental conditions. In turn, this structural partnership, which includes cooperation with aerobic bacteria, generates the anoxic microenvironment needed to support iron metabolism.

Pseudomonas was the second most abundant OTU detected in this study, and they are naturally found in drinking water (Allen et al., 2004). Some species of *Pseudomonas* are capable of oxidising iron (Straub et al., 1996) and manganese (Cerrato et al., 2010). *Pseudomonas*-associated sequences were more abundant in clogged wells than in non-clogged wells and may have contributed to iron-clogging and biofilm formation. Within the non-clogged wells, a low abundance was detected, potentially indicating the beginning of an iron-precipitating biofilm. Despite the presence of bacteria involved in iron-cycling, common soil bacteria were found (e.g., *Curvibacter* and *Brevundimonas*); their relation to the iron cycle is still unclear.

The 16S rRNA gene copy numbers g^{-1} of all of the investigated bacterial groups (*Bacteria*, *R. ferrireducens*, *Gallionella* spp., *G. fermentans* and *C. polyspora*) were higher in clogged wells than in non-clogged wells (Figure 12). That might be explained by the massive depositions around the pumps suction strainers of the clogged wells, which offers a diverse habitat for metabolic different groups as well as a large surface to colonise. The only exception, which showed less gene copy numbers in clogged wells was the assay that targeted the iron-reducing species *Geothrix fermentans*. That species was more abundant in non-clogged wells, as confirmed by qPCR and 16S rRNA clone library analysis. The *G. fermentans* strain was first isolated from a hydrocarbon aquifer, and it is known as an iron(III)-reducing bacterium (Coates et al., 1999). The release of iron(II) due to microbial reduction increases dissolved metal concentrations in aquifers and could result when used by iron-oxidising bacteria, in corrosion or clogged pipes (Lovley, 2011, 2004), but iron(III) reduction is also an important process coupled to the degradation of various contaminants in groundwater and aquifers polluted by hydrocarbons (e.g., petroleum and toxic heavy metal contaminants (Mehta, 2013).

Wang et al. (2014) suggested that high abundances of *Gallionella* in groundwater promote well clogging. As also shown in this study, the specific quantity of

Gallionella-related gene copies revealed that this group was highly abundant in clogged wells, which stands in contrast to the clone library results, where no typical iron-oxidiser was detected. Limitations of both methods are explained in chapter 4.2.

Fleming et al. (2014) and Wang et al. (2014) have stated that *Gallionella*-related bacteria are most likely related to a low DOC content and may stimulate the formation of iron oxides during the early stage of clogging. The RDA analysed the variance in the gene copy data between the clogged and non-clogged wells by correlating them to environmental factors; only DOC demonstrated the ability to affect the variance in bacterial abundances between the clogged and non-clogged wells ($p\text{-value}_{\text{DOC}} = 0.05$). Due to the p -value, the DOC can only be seen as indication to affect the bacterial abundances. As already described, a groundwater well offers a fast and complex environment with constantly changing environmental conditions, which makes it difficult to define uniform parameters. The lack of a clear correlation between the bacterial community and the abiotic variables is common within groundwater studies, and was also observed by Zhou et al. (2012) and Tánácsics et al. (2013). This finding is due to the fact that groundwater ecosystems offer vast and complex habitats for diverse bacterial communities. However, more frequent sampling is needed to verify the significance of these findings and to fully analyse them.

In order to quantify the number of methanotrophic bacteria, the *Crenothrix polyspora* gene copies were quantified; the *Crenothrix* assay displayed the largest deviation between clogged ($1.3 \times 10^8 \text{ g}^{-1}$) and non-clogged ($3.2 \times 10^6 \text{ g}^{-1}$) wells. *Crenothrix* is a filamentous methane oxidiser and represents a global problem organism in regard to drinking water production and supply (Stoecker et al., 2006). Methane, as a parameter that may reflect the microbial activity in groundwater (Lovley and Chapelle, 1995), was not analysed at this sampling site. However, Stoecker et al. (2006) have proposed that *C. polyspora* is a biological indicator for methane in drinking water wells. Kato et al. (2013) suggested that there could be a tight cycling of primary production by iron-oxidising and methanotrophic bacteria and organic degradation by iron reducers and other organisms.

In summary, the bacterial composition of the clogged and non-clogged wells were comparable, as clone library construction did not identify any differences between

them. Clone libraries were only constructed for a minor number of samples, which might not be sufficient to detect differences in the composition of clogged and non-clogged wells. In contrast to the clone library results, the qPCR results highlighted differences in the gene copy numbers targeting *Bacteria*, *Gallionella* spp. and *Crenothrix polyspora*, all of which were more abundant in clogged wells. In addition, on the basis of hydrochemical characteristics of the groundwater samples, it was not possible to determine whether a well was clogged or not. Medihala et al. (2011) revealed that biofilms continue to grow as pumping continues. The pumping times of the wells included in this study were found to be independent of the formation of clogging, with no correlation found between the two variables. In addition, iron-bacteria may be introduced to other wells via the re-use of contaminated tools during well servicing or drilling. Li et al. (2016) demonstrated that biofilters inoculated with iron- and manganese-oxidising bacteria and a biofilm-forming bacterium improved and enhanced iron(II) and manganese(II) oxidation. However, this phenomenon seems impossible to control in well servicing. Menz (2016) claimed well ageing depends also on sedimentological heterogeneities, the well operation scheme (switching), and well interactions within the well field.

4.1.2 Bacterial population compositions of a groundwater catchment system in Russia with a decreased specific well yield

The bacterial community composition of water and biofilm samples from a groundwater catchment system equipped with an in situ iron- and manganese removal system was investigated in terms of detecting the dominant bacterial groups (OTUs) using 16S rRNA gene amplicon pyrosequencing and qPCR, as wells as their structure and richness were analysed by means of DGGE.

The sampling site is located near the Amur River (Figure 2). This in-situ system was characterised by the infiltration of aerated water derived from aeration tanks and was then injected to the groundwater by means of water wells creating a subsurface oxidation zone around the wells (Chapter 2.7.2). Consequently, at the end of the infiltration phase and at the beginning of the abstraction phase the water had a high oxygen concentration, whereas at the end of the abstraction

phase (unaffected groundwater), almost no oxygen was available. No oxygen concentration were measured in the anoxic groundwater of the 2nd, 3rd and 4th sections, none of which were in operation during sampling. In contrast to the operating wells of the 1st section, which specific well yields drastically declined since starting operation of the wells (Table A 2).

The aim of the sampling campaigns (Chapter 2.7.2) was to analyse the potential effects of subsurface iron and manganese removal systems on the bacterial population responsible for the clogging problems in the wells.

The results of the biomolecular analysis in SC I clearly demonstrated that the well operation modes (infiltration and abstraction phases) had altered the composition of the bacterial community or rather the bacterial composition developed might be a consequence of the well operation scheme. Despite that, biofilm flocs were detected in the aeration tank of the 1st section featuring high levels of the OTUs *Flavobacterium* (up to 40 %) and *Pseudomonas* (up to 45 %), which have been long recognised as biofilm inhabitants and producers by microbiological and biomolecular methods (LeChevallier et al., 1987; Stewart et al., 2012). Biofilm development in particular can supply organic growth substrates for bacterial regrowth, and in some cases, it promotes the proliferation of opportunistic pathogens (van der Wielen and van der Kooij, 2013). Some *Pseudomonas* species can be opportunistic pathogens, and in particular, *P. aeruginosa* is not found in sufficiently protected groundwater (Szewzyk et al., 2000).

The water from the aeration tank entered as oxygenated infiltration water the groundwater well. The simultaneous entering of the bacterial population of the aeration tank may explain the decreasing well performance, or rather, the clogging of the wells, as confirmed by the detection of the OTUs *Flavobacterium* (up to 30 %) and *Pseudomonas* (up to 70 %) in the biofilm samples derived from well 1105 (SC III). When the water will be extracted, the well microbiome than can act as a seed bank, dispersing cells to subsequent drinking water supply systems all the way to the tap (Karwautz, 2015). If pathogenic bacteria inhabit the supply system and find favourable conditions to grow, this arrangement poses a risk to humans. On the other hand, due to the limitations of the method (Chapter 4.2), the species level of both OTUs is unknown and it is uncertain whether they are actually pathogenic or instead common and harmless soil

species. However, a neutral pH and the introduction of oxygen to a well can promote biofilm formation if DOC is also available.

The overall DOC concentration indicates an oligotrophic system. The growth of heterotrophic bacteria with a DOC content of 0.05 mg l^{-1} cannot be completely avoided (Röske and Uhlmann, 2005). Fonte et al. (2013) determined that different DOC sources had a positive effect on the bacterial biomass production. The sampling area often suffered under flooding events, resulting in decreased water quality (Kulakov et al., 2011), which can in turn lead to short-circuiting between the surface water and the groundwater, increasing the groundwater DOC and permitting bacterial infiltration.

A more important parameter to determine the proliferation of microbial cells is the assimilable organic carbon (AOC), as it is part of the DOC that is most readily consumed by microorganisms. As Hijnen and Van der Kooij (1992) have already described, the influence of AOC of the infiltration water is an important parameter that helps to determine the biological clogging and regrowth potential; it should take a value of less than $10 \mu\text{g L}^{-1}$ AOC to prevent biological regrowth (Van Der Kooij, 2000). However, a specific carbon fraction like AOC was not measured at this sampling site. Limited amounts of oxygen and nutrients within a water system may reduce the growth of rapidly developing organisms; nevertheless, it is not possible to reduce the oxygen introduction rate in an in-situ subsurface removal system, as it is part of the treatment system. Here, the only option to reduce microbial growth may be the restriction of nutrients.

Wells that were not in operation during sampling (2nd, 3rd and 4th sections) demonstrated a less diverse bacterial community as compared to the operating wells. The alpha diversity calculated from pyrosequencing results of operating wells and aeration tank samples was higher than in non-operating wells. The bacterial population of non-operational wells reflected the natural groundwater population in this area. After the wells became operational, the bacterial community changed its composition, which was also confirmed by the larger number of DGGE bands in contrast to the lower number of bands in the samples from the 2nd, 3rd and 4th sections. The injection of aerated waters can promote the growth of facultative anaerobic organisms, as oxygen served as a preferred electron acceptor. Facultative anaerobic, initially inhabiting the aquifer in relative low numbers, may have increased in abundance due to oxygen introduction and

entered the wells during subsequent water abstraction. As a result of infiltration of oxygen-containing water, aerobic degradation of a wider range of organic matter could be reflected in a higher diversity.

In SC II, different abstraction times (the beginning, 3rd, 4th, 5th and end phases) of well 1101 were analysed in order to investigate the dynamics of the bacterial populations during well management. Based on the percentage of Pearson correlation similarity of samples derived from several abstraction phases, the calculated rate of change was found to be particularly high, at approximately 85 %. Due to the abstraction of groundwater and the resulting environmental changes, various bacterial species became dominant or left actively or passively the community during the abstraction process, resulting in a broad range of dynamics. As also reported by Medihala et al. (2011) microbial numbers, metabolic activities and community composition changed in a water well system as a result of water pumping. The population at the beginning of the abstraction phase reflected a mixture of the bacterial community from the injected water, the planktonic groundwater population and the detached biofilm bacteria. Whereas, the population at the end of abstraction phase consisted of a mixture of the injected water and groundwater (Figure 26). The presence of injected water during the end of the abstraction was indicated by the detection of the OTUs *Pseudomonas* and *Rhodoferrax*, which have also been found in aeration tank samples. Sequences associated with *Oxalobacteraceae* represented the bacterial composition of non-operational wells and have been detected at the end of the abstraction phase indicating the groundwater population.

The abundance of *actinobacterial* group ACK-M1 sequences increased in accordance with the abstraction volume. Recent studies have demonstrated that the ACK-M1 cluster is a typical freshwater group and not commonly found in groundwater ecosystems. It has been detected in several different lakes in Europe's north and middle regions (Lindström et al., 2005). Lin et al. (2012) even suggested that the emergence and disappearance of the ACK-M1 cluster was correlated with river water intrusion to the aquifer. In addition, Kulakov et al. (2011) estimated that bank filtration would reach the nearest wells (1st and 2nd sections) after two years of operation (in this study samples were taken after five years of operation), implying that the groundwater wells and presumably the 1st section wells were influenced by Amur River water. In addition, the ACK-M1

group served as an indicator for the 1st well section ($p < 0.005$) but was not found in other sections, which have not yet been started operation. The influence of surface water from the Amur River might have affected the availability of nutrients and the introduction of bacteria to the sampling area. When bank filtration happens too quickly due to flooding events resulting in short circuits between the surface and subsurface water, the water quality might decline enormously. Recently, Li et al. (2015) detected ACK-M1 and *Methylothera* in association with seasonal algal bloom in a eutrophic lake, which is typical for surface water but not for groundwater indicating again the influence of Amur River water to groundwater of the 1st well section. Both OTUs were detected in samples from the 1st section but not in outgroup samples, which represents the natural groundwater population in that area.

Methylothera, a facultative methylotrophic and obligate aerobic organism, uses one-carbon (C1) compounds in addition to a limited range of multicarbon compounds. It served as an OTU indicating the beginning of the aerobic abstraction phase ($p > 0.005$), but it was also found at the end of the abstraction phase, albeit in a lower abundance due to the reduced oxygen concentration. This widespread genus has been previously detected in polluted soils and contaminated water (Baek et al., 2012; Paul et al., 2015). Therefore, it can be taken as a further indication that the groundwater within the water catchment system had been reached by water from the Amur River, which is contaminated with aromatic and polyaromatic substances (Kulakov et al., 2011). The pyrosequencing results from the aeration tank samples did not yield any *Methylothera* species.

Furthermore, the sampling site was characterised by the formation of a subsurface oxidation zone around the wells, which served to remove iron(II) from the groundwater. The oxidation process transforms the dissolved iron(II) into less soluble iron(III) hydroxide, which is stored in the aquifer's pore space, a location that provides adsorption sites. This massive deposition of iron oxides may favour the iron reduction potential of the psychrotolerant, facultative anaerobic bacterium *Rhodospirillum rubrum*, first described by Finneran et al. (2003). Microbial reductions of iron and manganese oxides are of environmental significance in an oligotrophic environment like groundwater, due to their interactions in the carbon cycle and their relevance in metal metabolism. *R.*

ferrireducens was found by 454-pyrosequencing in particularly high abundances in the 1st well section and the aeration tank samples. In addition, qPCR also revealed high gene abundances in the water samples derived from 1st well cluster, as well as in all of the biofilm samples. Recent studies by Benedek et al. (2016) and Inaba et al. (2017) demonstrated the strong contribution of *R. ferrireducens* to biofilm development, which would explain the high abundance in the biofilm samples from the aeration tank and the inner pipes of the wells. Additionally to its promotion of biofilm development, *R. ferrireducens* is also known for anaerobic hydrocarbon degradation and was commonly isolated from hydrocarbon-contaminated environments. It has been described as key organism involved in the breakdown of aromatic hydrocarbons in subsurface, hypoxic environments (Aburto et al., 2009; Zaa et al., 2010; Táncsics et al., 2013). Its high abundance within the abstracted water indicated the arrival of the contaminated Amur water at the 1st section wells.

The pyrosequencing results revealed that *Gallionella* was an indicator OTU for the 2nd well section, as demonstrated by its high abundance in the 2nd section wells and its scarcity in the 1st section wells. In contrast to the pyrosequencing results, *Gallionella* spp. 16S rRNA gene copies were abundant in those water samples obtained from the 1st and 2nd sections, as well as in the biofilm samples from the aeration tank. Neutrophilic iron-oxidisers, such as *Gallionella*, are commonly found in groundwater and are indigenous to that setting (Yang et al., 2014). The iron(II) concentration was very high in the wells from the 2nd cluster, reaching levels as high as 26.6 mg l⁻¹. At the same time, oxygen was not detected, and the DOC concentration was rather low. This is supported by the findings of Fleming et al. (2014) and Wang et al. (2014); they claimed that *Gallionella*-related bacteria are most likely related to a low DOC content and stimulate the formation of iron oxides at the early stage of clogging. However, neither Wang et al. (2014) nor this study found any relation between the DOC content and the abundance of *Gallionella* spp. at all. The independence between the *Gallionella* spp. abundance and the DOC content may not be surprisingly due to the autotrophic metabolism of these bacterial group. Furthermore, both studies by Fleming et al. (2014) and Wang et al. (2014) suggested that high abundances of *Gallionella* spp. in groundwater indicate a higher risk for well clogging. Wells from the 2nd section of the water catchment system revealed the highest abundance of

Gallionella OTUs, and well clogging in that cluster may occur more quickly after operations begin, as the injection of aerated water favours the growth of the microaerophilic *Gallionella*, as reported by de Vet et al. (2012).

Crenothrix polyspora gene copies were predominantly found in the biofilm samples from the aeration tank but were also observed in lower numbers in all water samples, with the exception of the EF samples from the 1st section. *Crenothrix polyspora* is a filamentous methane-oxidiser (Stoecker et al., 2006). Methane, a parameter that may reflect the microbial activity of methanogenic bacteria in groundwater (Lovley and Chapelle, 1995), was measured at specific control points within the 1st and 2nd well sections in low concentrations. Therefore, the growth and activity of *C. polyspora* as methanotrophic bacteria may have been related to traces of methane in groundwater. In addition, a recent study by Demir (2016) suggested that the activity of *C. polyspora*, in addition to that of other bacterial species, was the main iron- and manganese-oxidation mechanism in the early stages of slow sand filters' operation, implying its role in this subsurface iron cycle. Furthermore, Edlund et al. (2016) conducted microbial investigations during infiltration experiments and found that oxygen inputs into an anaerobic shallow groundwater system increased metabolic activity and the growth of the inherent microbial population. They also detected an increase in the abundance of biofilm sequences associated with aerobic methane-oxidising bacteria, such as *Crenothrix*. This study demonstrated that the infiltration of oxygen-containing water resulted in the aerobic degradation of a wider range of organic substances, as reflected in the higher number of 16S rRNA gene copies in samples from the beginning of the abstraction phase rather than from the end. The large number of *C. polyspora* gene copies in the aeration tank samples and at the beginning of the abstraction phase further supported that finding.

In summary, the analysis of the bacterial population clearly displayed that the well management activities had altered the bacterial community. Constructing a well changes the subsurface environment in a manner that increases the activity of natural groundwater bacteria and also introduces new ones. Well pumping characteristics, aquifer properties and water quality are among the factors that influence the potential for biofouling problems. The groundwater samples from the non-operating wells had less diverse bacterial populations than did the operating wells. The drastic decrease of the specific well yield may be attributable

to several factors. On the one hand, the aeration tank had favourable conditions for microbial activity, as confirmed by the biofilm formation. Due to the infiltration management, the biofilm population was spread and inoculated to the 1st section wells, as indicated by the detection of bacteria in the aeration tank. Another reason might be that the Amur River influences the groundwater. In consequence, the groundwater is affected by flooding events, which decrease its quality considerably if circuits are created between the surface water and the groundwater. A specific indicator bacteria analysis confirmed those hypotheses. The OTUs ACK-M1 and *Methylothermobacter* were almost exclusively found in operating wells, but in literature there are described as typical inhabitants of surface water and commonly are not found in groundwater. Therefore, their abundances can be taken as an indication that the groundwater within the water catchment system had been reached by water from the Amur River.

4.1.3 Comparison of the bacterial population between wells equipped with aerated and non-aerated filter screens in opencast mining areas

The bacterial population in the water samples obtained from wells with aerated and non-aerated filter screens at two opencast mines were compared in terms of their dominant bacterial groups (OTUs) by using 454-pyrosequencing, 16S rRNA gene clone library construction and qPCR (Chapter 3.3). Moreover, the structure and richness of these populations were analysed by means of DGGE. In addition to the water samples, several biofilm samples from well equipment were analysed. In contrast to the drinking water supply, well operations in opencast mines aim to dewater all intersected aquifers above the coal seams in the opencast area (Henkel et al., 2012). In particular, the wells equipped with aerated filter screens were vulnerable to clogging due to the formation of iron oxide incrustations in the gravel pack and well screen (personal notification RWE Power AG). Maintaining a water level that ensures that the filter screens are constantly subjacent to the water results in slower well aging and less iron-clogging (personal notification RWE Power AG).

Among the wells at the Garzweiler opencast mine, major differences in hydrochemical values were identified between those wells equipped with aerated

and those with non-aerated filters. In particular, dissolved oxygen, iron(II), iron(III) and sulphate concentrations were higher in aerated dewatering wells, as was the redox potential. Due to the low operating water level in the well, oxygen inside the well tube can reach the reduced groundwater and lead to 'aerated' filter screens (Henkel et al., 2012). The aeration of the filter screens can result in the more rapid iron-clogging of those screens, an outcome that tends to be followed by a decrease in the abstraction volume. In contrast to the wells at the Garzweiler site, those wells at Hambach displayed minor differences in their oxygen and iron(III) concentrations and redox potentials, but the values were also higher in water samples from wells equipped with aerated filter screens. Clogging effects generally occur if reduced groundwater enriched with dissolved iron(II) and manganese(II) ions is brought in contact with oxygen from the ambient air in the tube well. Iron-oxidising bacteria can profit during pumping from the combined presence of low oxygen concentrations in the air flowing into the well via the upper well screen and high iron(II) concentrations in anoxic groundwater flowing upwards from the lower well screen section. Under such conditions, anoxic groundwater becomes oxidised resulting in a change of the groundwater composition and microbial ecology (Larroque and Franceschi, 2011).

Among the wells at Hambach, the bacterial 16S rRNA gene copies were higher in non-aerated wells. The exception was the *Crenothrix*-related genes, which were 0.5 log phases higher in the aerated wells. A methane analysis of well water revealed a profound concentration of methane among wells in Hambach (up to 3.0 mg l⁻¹, data not shown). The influence of *Crenothrix polyspora* activity, which plays a role in methane metabolism and is a main mechanism involved in iron and manganese oxidation, was discussed previously (Chapter 4.1.2). All biofilm samples obtained from well dewatering equipment revealed high levels of *Gallionella*-, *Crenothrix*-, *Geothrix*- and *Rhodoferrax*-related gene copies (up to 10¹⁰ copies g⁻¹). Furthermore, most of the variance (44 %) within the Hambach samples was explained by the iron(III) concentration ($p\text{-value}_{\text{Fe}^{3+}} = 0.062$); the significance of iron(III) in explaining the variance of bacterial quantities needs to be tested using a larger number of samples. Iron(III) deposits develop when the de-oxygenated water reaches a source of oxygen. Iron-oxidising bacteria use that oxygen to convert the soluble ferrous iron into an insoluble reddish precipitate of ferric iron. There is a possible correlation between the abundance of iron-

oxidising bacteria and the iron(III) content, but chemical oxidation might be also possible due to the high oxygen concentration in aerated wells. In fully oxygenated water, at circum-neutral pH, the abiotic oxidation of iron(II) occurs very rapidly (Emerson et al., 2010).

Among the wells at Garzweiler, major differences were detected between aerated and non-aerated filter screens in terms of the abundance of the bacterial 16S rRNA gene; in particular, the *Crenothrix*-associated 16S rRNA gene copies were found to be present in higher levels in the non-aerated wells. An RDA analysis exhibited that the redox potential of the Garzweiler samples was the factor with the greatest ability to explain the differences in bacterial abundance levels between the aerated (positive redox potential) and non-aerated (negative redox potential) filter screens ($p\text{-value}_{\text{EH}} = 0.092$), but this potential only served as evidence. However, Menz (2016) found that to achieve a sustainable well operation, in combination with other factors, wells should be located in an confined aquifer with a high redox potential (150 mV). Anyway, Menz (2016) did not analyse the influence of the microbiological population. Nevertheless, a high redox potential resulted in an oxygen-rich environment (e.g., aerated filter screens), thus contradicting a statement by RWE Power AG that wells equipped with aerated filter screens are more vulnerable to iron-clogging. However, there is no positive relation between the gene copy numbers of specific bacteria and well clogging; according to RWE Power AG, aerated filters result in more rapid and extensive iron-clogging, leading to a decrease of the specific well yield.

All of the biofilm samples collected from the various dewatering wells were further subjected to a bacterial community analysis via clone library construction and 454-pyrosequencing to gain deeper insights into the bacterial community composition. Clone library construction revealed *Novosphingobium*, which are known for their aromatic degradation, the iron-reducing *Geothrix* and the methanotrophic *Methylococcaceae* as the most dominant OTUs in the Garzweiler samples. The genus *Novosphingobium* was also found by Pan et al. (2017) in an increased number after iron-reducing bioaugmentation in sediments, indicating a connection between this genus and the iron cycle. In addition, methanotrophic *Methylococcaceae* were found to play an important role in waterworks sand filters at concentration levels as low as 0.05 mg l⁻¹ methane in groundwater (Albers et al., 2015). An analysis of the top ten OTUs, as estimated by pyrosequencing the

biofilm samples at the Garzweiler site, revealed that *Crenothrix* and *Methylobacter* were the most dominant OTUs, again approving the role of methane-oxidising bacteria in iron-containing biofilms. Quaiser et al. (2014) provided strong hints that iron and methane oxidation occur simultaneously in microbial mats and that both groups of microorganisms are major players involved in the functioning of this ecosystem.

The strictly anaerobic group *Anaeromyxobacter* served as the core OTU in the biofilm samples taken at Hambach, as estimated by clone library construction and 454-pyrosequencing. *Anaeromyxobacter* may possibly degrade the organic compounds in the iron deposits as it was found by Hori et al. (2010) that *Anaeromyxobacter* spp. is an actively iron-reducing bacteria in rice paddy soil with crystalline goethite as an electron acceptor. Furthermore, the methanotrophic genera *Methylococcus* and *Methylobacter* were the most abundant OTUs in the biofilms obtained from the Hambach site, as Kato et al. (2013) suggested that there could be a tight cycling of primary production (by iron-oxidising and methanotrophic bacteria), organic degradation (by iron reducers and other organisms) and methanogenesis. The results of the microbial composition associated with pipe deposits in dewatering wells provided a difference to the findings of Wang et al. (2014) findings; those authors found that pipe deposits mostly contained *Gallionella*, which may initiate the formation of iron oxides and lead to greater bacterial diversity, along with the accumulation of deposits. However, this study showed at both sites (Hambach and Garzweiler), *Gallionella* were detected by 454-pyrosequencing but was not the dominating group.

In summary, methane seems to be an important factor with an influence on microbial activity, as suggested by the findings on *C. polyspora* and several other methanotrophic OTUs. The methane concentration should be considered as a key factor with an effect on microbial iron-clogging at this site. Further investigations should examine the correlation between the methane concentration, specific methanotrophic microbial activity and iron-clogging. However, no relation between the gene copy numbers of specific bacteria and well clogging was found; aerated filters, which, according to RWE Power AG, are vulnerable to iron-clogging, did not necessarily contain more gene copies in the water samples. A possible reason might be that high gene copy numbers did not

imply high microbial activity due to the fact that free DNA of already destroyed cells can be amplified, too. In addition, only four bacterial groups, which are involved in the iron cycle, were analysed in this study by qPCR but they might not be the cause of iron-clogging in this environment.

4.1.4 Regeneration influence on the bacterial population of an iron clogged lab-scale reactor

The bacterial population of an iron clogged lab-scale reactor affected by different regeneration procedures were determined and analysed according to its dominant bacterial groups using 16S rRNA gene clone libraries and qPCR. Furthermore, its structure and richness were analysed by DGGE. In addition, the qPCR results were correlated to the decrease in hydraulic conductivity (k_f value), which served as indicator for iron-clogging; two test series (TS I and TS II) were conducted (Chapter 3.4).

The Dresdner groundwater had favourable conditions for iron-clogging, namely, a very low oxygen concentration, a neutral pH, iron(II) availability, a high sulphate content and a DOC concentration of 3.5 mg l⁻¹. However, the hydrochemical parameters were only measured once, and it is not clear whether those values remain stable during groundwater extraction.

Test series I consisted of three columns: S1 and S4 were regenerated once and twice, respectively, whereas S6 served as the control column. The R_r values of the bacterial population, as calculated by DGGE bands, were particularly high in S6, which did not undergo regeneration, while S1 and S4 were associated with low R_r values indicating a decrease in the bacterial diversity due to regeneration procedures. Further differences between the samples derived from the columns according to the influence on regeneration procedure were detected by qPCR analysis; *Gallionella* spp. and *Crenothrix polyspora* 16S rRNA gene copies were higher in S6 and correlated to the largest decrease in k_f values. In contrast, in S1 and S4, this decline was less as were the *Gallionella* and *Crenothrix* abundance. The single regeneration in S1 resulted in a weaker decrease of the k_f value and less abundance of *Gallionella* and *Crenothrix* gene copies, and the two times regeneration led to an even lower decrease and abundance level. From these findings, it was deduced that the regeneration procedure resulted in a higher k_f

value and a less number of specific bacterial gene copies of *Gallionella* and *Crenothrix* than in the S6 bacterial population, which did not undergo regeneration. This indicated that *C. polyspora* and *Gallionella* spp. growth were responsible for the biofilm formation and the decrease in the k_f values in S6 (no regeneration). Numerous studies have made clear that there might be a relationship between the number of polysaccharides and a decrease in hydraulic conductivity (Rinck-Pfeiffer et al., 2000; Pavelic et al., 2011; Page et al., 2014). Page et al. (2014) found that the dominant cause of clogging was biological, as a result of biofilm production. Anyway, in this present study, samples could only be analysed according to their microbial populations at the end of each test series and therefore biofilm development could not be investigated. However, the complete bacterial population composition need to be analysed, and samples needs to be taken over time.

Furthermore, TS II consisted of four columns: S5 and S8 had been pretreated with AIXTRACTOR 2.0®, a pH-neutral water well rehabilitation agent with an iron-dissolving component (sodium dithionite). S5 was regenerated once, whereas S8 served as a control column. In only one study AIXTRACTOR 2.0® was used for well cleaning, but that analysis did not investigate the effect on the microbial community (Lerm et al., 2011); however, they found that the microbial population in the well fluids mainly contained iron-oxidising *Gallionella* and sulphur-oxidising *Thiothrix*. Two further columns (S2 and S4) did not undergo any pretreatment; S2 was regenerated once, and S4 served as a control column. In contrast to the richness results of TS I, column S5 (TS II) revealed the highest richness values, although the material was pretreated and regenerated twice. However, the lowest decrease in the k_f value was found for S5. The results of TS I could be confirmed by the results of TS II as S5 revealed the lowest distribution of *Gallionella*, which could only be detected at a depth of 50 cm. In addition, *Crenothrix* gene copies could also not be detected in S5.

Furthermore, the highest iron content was found in 0 to 2 cm, a depth were also the largest number of gene copies was found, resulting in high levels of bacterial activity, though gene copies were detected at the entire length of the column but in a less number. These findings were similar to the results presented by Pavelic et al. (2011); biomass levels were higher near the inlet of the column where the substrate and electron acceptor availability were highest, but bacteria were found

in the entire column. In addition, Pavelic et al. (2011) suggested that biomass production is strongly dependent on water quality. However, the microbial data only provided a representative 'snapshot' of the conditions at the end of the experiment.

In summary, this study indicated that *Crenothrix* and *Gallionella* due to their high gene copy numbers caused biofilm formation in the columns resulting in a decrease of the k_f values. The only column (S5) that contained pretreated filter sand and which was regenerated twice showed no decrease in the k_f value. At the same time only few bacterial gene copies were detected confirming the hypothesis that high *Crenothrix* and *Gallionella* gene copies accompanied with biofilm formation and low k_f values.

4.1.5 Comparison of the bacterial populations of the investigated technical systems

The bacterial populations of the biofilm and groundwater samples obtained from four different technical groundwater-fed systems were investigated and compared with several biomolecular methods. These analyses focused on the populations' dominant OTUs, composition, genetic diversity and ecological function.

These sampling systems were all characterised by a vulnerability to iron-clogging, due to the presence of (at least) a minimum oxygen concentration in the groundwater and ferruginous source waters. Each of the four sampling sites is characterised by altered hydrochemical, geological and technical conditions resulting in a different composition and availability of nutrients. The substrate availability determines the possible development of bacteria. Bacteria are found wherever water is available, but which physiological groups dominate depends on the substrate. The water catchment site in Russia is characterised not only by the continuous extraction of groundwater as shown for the drinking water wells in Berlin, but also by the infiltration of oxygen-rich water into the wells. As a result, all sites have very different characteristics and the bacterial composition cannot easily be compared, since each site already has a high bacterial diversity. From this point of view, the comparison of the bacterial composition from all four sites must be considered.

Data derived from biomolecular methods like DGGE lack of a universal means of interpreting the raw fingerprint itself, thus making it challenging to compare results across sites (Marzorati et al., 2008). However, Marzorati et al. (2008) provide values, each representing a score allowing researchers to describe and compare microbial community structures and the diversity of different sampling sites.

The range-weighted richness of all sampling sites was calculated. The results ranged from highly diverse (*Rr* of 395) for a biofilm obtained from a clogged drinking water well in Berlin to an adverse environment affected by regeneration showing a very low value of <3 in column S1_20 cm. The biofilm samples from the Berlin drinking water wells were all highly diverse (>80), which according to Marzorati et al. (2008) implies a very habitable environment with a broad carrying capacity and a high level of microbial diversity. The pumps belonging to the drinking water wells had hydrochemical values favourable to microbial life and a complex biofilm offering a complex habitat. Some studies demonstrated that the substratum is the most important factor in biofilm development (e.g., Donlan, 2002; Terlizzi and Faimali, 2010). The biofilms, which developed on the pump inlet were highly diverse due to the variety of nutritional and physical potentialities. In contrast, the biofilms that developed in the filter-sand of the lab-scale reactor were regenerated, and at most, only a few species resisted the regeneration procedure. As additional parameter, the functional organisation of the environment based on DGGE was calculated. The *Fo* calculated for S2_20 was high (PL 70 %), which means that a specialised community with a small number of species was dominant and the remaining species are present in low numbers, has been developed. This community can be sensitive to external changes, like regeneration procedures.

The overall *Rr* values for all sampling sites revealed a high level of bacterial richness (mean *Rr* values of >30 are typical of highly habitable environments), suggesting that all sampling sites are very habitable environments able to host a range of microorganisms and support genetic variability (Marzorati et al., 2008). Groundwater ecosystems offer vast and complex habitats; in addition, the abstraction of the groundwater will result in the development of diverse microhabitats for various bacterial communities. These circumstances made it very difficult to find indicator organisms, which are predominantly involved in the iron-oxidising process, for this kind of habitat. It is much more of a structural

partnership between many different organisms. Some of these organisms may be actively involved, while others take a more passive role and generate the necessary microenvironments. Higher levels of species richness may increase the ecosystem's functionality and stability (Bell et al., 2005). An *Rr* analysis of groundwater in Spain by Purswani et al. (2011) and a soil study by Pereira e Silva et al. (2011) showed comparably high richness values.

In addition to the range-weighted richness values, *Fo* values were calculated for all sampling sites. This functional organisation depends on the types of microorganisms that are most fitting for the environment, and for this reason, such species tend to become dominant within the microbial community structure (Marzorati et al., 2008). The more that the PL curve deviates from the 45° line (the theoretical perfect evenness line), the greater the shift in the evenness and potential functionality of the studied community. The 25 %, 45 % and 80 % curves refer to those communities with a low, medium and high *Fo* value but a high, medium and low level of evenness, respectively (Marzorati et al., 2008). In this present study, the overall *Fo* values ranged from 35 % for some samples obtained from opencast mining sites to 70 % at Berlin drinking water wells sites and the lab-scale reactor. A *Fo* value of 35 % meant that only a small number of species were dominant (indicated by lighter bands). Such results suggested a community with high evenness but a weak functional organisation due to the permanent disturbance of the system by the abstraction process; such a community may result from a lack of selective pressure, and such conditions were represented in this study by the biofilms samples obtained from dewatering well components. It is possible that a significant amount of soil and water bacteria inhabited the biofilms. In contrast to these findings, the microbial populations of some of the drinking water wells represented more specialised communities with a high level of functional organisation. However, most sampling sites reflected a balanced community with a medium *Fo* score, resulting in a moderate level of evenness within the community. An elevated concentration of some species and the availability of many others can help a community to deal with changing environmental conditions and to preserve its functionality (Marzorati et al., 2008). These findings, in combination with the *Rr* values approved that a bacterial population inhabiting a technical or man-made groundwater-fed system can

adapt to changing environmental conditions. Therefore, it is difficult to find satisfactory solutions for mitigating bacterial iron-clogging.

Furthermore, the bacterial composition of all sampling sites was analysed by clone library construction and 454-pyrosequencing. All sites had highly comparable distributions of the relative abundance of phyla, which mainly consisted of *Proteobacteria*. However, they differed in terms of the class. Sequences with high homology to the class of *Deltaproteobacteria* were predominantly abundant in those samples obtained from the lab-scale reactor and the drinking water wells in Berlin. Clone library construction of wells located within the Russian water catchment revealed sequences associated with *Betaproteobacteria*, while sequences from the opencast mine dewatering wells were associated with *Alphaproteobacteria*; in contrast, 454-pyrosequencing revealed that the predominant class was *Gammaproteobacteria*. Romaní et al. (2013) and Karwautz (2015) found that the bacterial diversity of aquatic biofilms is typically dominated by *Alpha*-, *Beta*- and *Gammaproteobacteria*; The presence of *Alpha*- or *Betaproteobacteria* might depend on the habitat type and the environmental conditions (Romaní et al., 2014). Wang et al. (2014) investigated the microbial community structure of clogging materials in dewatering wells and found *Betaproteobacteria* to be the predominant class. Moreover, several unidentified candidate phyla (e.g., TM7 and ZB2) were found in wells from the water catchment site in Russia and in the dewatering wells at the opencast mining sites, confirming their general presence in groundwater and groundwater-associated biofilm samples. In addition to culture-independent biomolecular methods, the aerobic isolation of iron-depositing bacteria revealed that half of the strains belonged to the phylum *Actinobacteria*, which represented the major group. Depending on the media, specific easily cultivable groups are isolated, and data may possibly did not represent the real bacterial community composition within in the habitat.

Furthermore, the bacterial populations were investigated according to their dominant bacterial groups (OTUs). Navarro-Noya et al. (2013) defined phylotypes, which were present in all water samples investigated as core OTUs. However, in this present study, phylotypes that were observed within the top 10 OTUs (genus level) were defined as core OTUs. The data did not reveal any core OTUs for all sampling sites. However, phylogenetically different but

physiologically similar top 10 core groups for almost each site were found, e.g., *Rhodoferrax* and *Geobacter* as iron-reducing bacteria. The coexistence of many species with a similar metabolism makes it more likely that some will back up a given function, while others will fail, due to the presence of multiple species for each functional group (Yachi and Loreau, 1999; Wittebolle et al., 2009).

Geobacter spp. was a top 10 core OTU in the ochrous samples obtained from drinking water wells in Berlin; the role of *Geobacter metallireducens* as a type of iron-reducing and nitrate-depending, iron-oxidising bacteria was discussed in chapter 4.1.1. There might be a big potential of iron-clogging in the drinking water wells due to anoxic iron(II) oxidation. The iron-reducing *Rhodoferrax* spp. and iron-oxidising *Gallionella* spp. served as the top 10 core OTUs in the samples from the wells located in the Russian water catchment area and in the ochrous samples obtained from opencast mining well components. In addition, *Geothrix* was a further core OTU in the ochrous samples derived from the opencast mining wells; in contrast to Karwautz (2015), who detected *Gallionella* as a core OTU in all investigated biofilms of drinking water wells. No top 10 core OTUs were identified for the samples obtained from the lab-scale reactor, due to the fact that only one groundwater sample and one biofilm sample were analysed. All core OTUs, with the exception of *Geobacter* spp., were also targeted and quantified by means of qPCR. Instead of *Geobacter* spp. another iron reducer was detected; *Geothrix* spp., as strictly anaerobic bacteria, was only detected in the biofilm samples due to the anaerobic areas in the lower part of the biofilm and was never found in the water samples.

The aerobic isolation of the iron-depositing bacteria from the ochrous samples highlighted the presence of other phylogenetical groups, like *Kineosporia*, *Pedomicrobium* and *Bacillus*. As demonstrated by Li et al. (2016), *Bacillus* spp. promoted iron- and manganese-oxidising bacteria in biofilters. In addition, several isolates that only revealed a maximal identity of 93 % with their phylogenetic neighbour demonstrated strong iron depositions on agar plates. The next relative was *Rhodomicrobium vannielii*, which is known for its phototrophically ferrous iron oxidation (Heising and Schink, 1998). Phylogenetic analysis revealed that most of the isolated strains were unaffiliated with known iron-depositing bacteria; however, it is still unknown whether the bacteria deposit the iron or whether they actively oxidised iron(II). A gene involved in iron oxidation serving as genetic

marker for the detection of neutrophilic iron-oxidising bacteria has not yet been described. However, Kato et al. (2015) discussed several possible genes (*act* and *cyc2*) as genetic marker; *cyc2* encodes a protein that has been shown to oxidise iron in acidophilic iron-oxidising bacteria but it was also found in bacteria with other metabolism, though it is possible that these other organism oxidise iron(II). The *act* genes are monophyletic and present in all neutrophilic iron oxidising-bacteria, but their role in iron oxidation is not clear yet.

4.2 Limitations of biomolecular techniques and sampling

The majority of bacteria are not yet cultivable. Therefore, culture-independent methods are of major importance for gaining insight into the bacterial population within oligotrophic habitats like groundwater systems. These culture-independent techniques can overcome the strong limitations concerning cultivation efficiency, although they do have drawbacks. Specifically, with such methods, bacteria can only be studied using DNA- or RNA-based approaches, while their 'behaviour' can only be analysed by characterising them in pure cultures, which can be useful for future applications. In addition, isolates allowed bacterial identifications to the species level, in contrast to the other procedures that rarely produced identifications below the genera.

Furthermore, the aqueous geochemical measurements in this study were often provided by others (project partners). Most of the analyses were done according to DIN standards. However, it is not clear how consistent and reliable these measurements and therefore the resulting data were.

Sampling is always a critical point. In particular, biofilm particles, including cells, are actively and passively shed from pipes and fixtures, resulting in changes in the bacterial concentration. Strong fluctuations across phylogenetic groups over time indicated the high heterogeneity of the communities in the well itself. However, Ranjard et al. (2003) found that samples of <1 g soil sample were convenient for obtaining reproducible fingerprints.

Subsequently, when investigating the microbial community in groundwater using DNA extraction, the challenge is to sample a sufficient volume of water to obtain enough extracted DNA from the biomass to avoid reagent contamination biases.

Otherwise, contamination in extraction kits might significantly influence the results of a microbiome study containing a low microbial biomass (Salter et al., 2014). Purswani et al. (2011) compared three microbial DNA extraction protocols for groundwater samples and found that the FastDNA SPIN Kit for Soil from MP Biomedical (similar to Soil DNA Purification Kit from Roboklon) yielded the lowest diversity but the best reproducibility. In addition, Vishnivetskaya et al., (2014) used several commercial DNA extraction kits for microbial community analysis in permafrost samples and verified, that the FastDNA SPIN Kit for Soil provided the highest gDNA yields and 16S rRNA gene concentrations.

Furthermore, a limitation that should always be considered is PCR artefacts, such as the preferential amplification of certain sequences (biases) due to small differences in conserved regions or inhibitory compounds. In addition, the formation of chimeric sequences during PCR approaches can give inaccurate information about the diversity of microbial communities in environmental samples (Fogel et al., 1999; Hongoh et al., 2003). It should also be kept in mind that the universality of commonly used universal primer sets is not absolute (Ben-Dov et al., 2006) and the diversity of an environment might be underestimated.

In terms of the DGGE method, the number and intensity of bands in a gel do not necessarily generate an accurate picture of the microbial community structure. Such results arise, since one bacterial species may produce more than one band because of multiple, heterogeneous rRNA operons, which may have copy numbers within the genomes in the range from 1 to 14 (Head et al., 1998). However, this is not only a problem concerning DGGE analysis. Also considering the use of clone libraries, 454-pyrosequencing and qPCR analysis would produce results containing a higher number of several bacteria due to multiple, heterogeneous rRNA operons. Considering heterogeneous rRNA operons means that one can never confidently extrapolate from the sequence composition in a clone library to a quantitative population composition in an environmental sample (Head et al., 1998). In addition, partial 16S rRNA gene sequences do not always allow researchers to differentiate among species, and a single band may represent more than one species. Yeung et al. (2011) used different primer sets for DGGE analysis, and produced *Rr* values ranging from medium to high richness levels, depending on the primer set in question. This suggests that the

choice of primer might yield a discrepancies in results, such as over- or underestimations. Janse et al. (2004) found that artefactual 'double bands', which lead to an overestimation of diversity, can be minimised by implementing a final PCR elongation step of up to 30 min; in this study, it was made use of that approach.

To compare the findings produced via the clone libraries and 454-pyrosequencing, six samples from ochrous-encrusted dewatering well components were analysed with both methods (Chapter 3.3.3 and 3.3.4). At the phylum level, the results were similar. Phylum-level sequences that were detected by means of clone library construction were also identified using pyrosequencing. Additionally, pyrosequencing identified 11 further phyla as a result of the higher sequence output afforded by that method relative to clone library construction. Former studies relying on the 16S rDNA clone library approach only present limited numbers of clones, which are insufficient for covering the complexity of the bacterial community (Kröber et al., 2009). In addition, that method is a time-consuming and expensive approach (DeSantis et al., 2007).

However, using 454-pyrosequencing means that the phylogenetic assignment of hundreds of thousands of metagenomics sequences to taxonomic groups requires an ambitious bioinformatics effort; these classifications are based on a comparison of metagenomics sequences across databases, and therefore, the contents of such databases have an influence on the results. In addition, 454-pyrosequencing analyses always results in a group of unknown *Bacteria*. That outcome is a result of the artefactual sequences and the limitations imposed by the short read lengths (Roh et al., 2010).

In contrast to the results at the phyla level, at the genus level were key differences between the two methods. Sequences for which both methods detected coinciding top 10 OTUs only belonged to the genera *Flavobacterium*, *Novospingobium*, *Anaeromyxobacter* and *Geothrix*. Nevertheless, 454-pyrosequencing currently only produces short read lengths, which are not always sufficient to accurately characterise microbial communities (Wommack et al., 2008). In this present study, amplification of the variable V1-V3 regions of the 16S rRNA gene were done using 454-pyrosequencing; however, Yang et al. (2016) investigated the sensitivity of hypervariable regions in 16S rRNA gene for

phylogenetic analysis and suggested that V4-V6 might be the optimal sub-regions. In contrast, the longer amplicon sizes of 16S rDNA clone libraries usually allow for more precise assignments of 16S rDNA clones. However, the 454-pyrosequencing platform was shut down by Roche in 2013 and replaced by newer sequencing technologies, such as Illumina® MiSeq and HiSeq applications.

Furthermore, considering the limitations of qPCR, group-specific primer for analysing natural bacterial communities could be biased by the fact that the accuracy of their specificity depends on the available cultured isolates and the known sequences in the database. However, it can also be prone to overestimation, because gene copy numbers are not always adaptable to cell numbers. The target gene copy number per microbial genome is sometimes unknown, and the number of genome copies per microbial cell can vary across growth phases (Ludwig and Schleifer, 2000). The specificity of the primer used in this study were checked against the Silva ribosomal RNA gene database (www.arb-silva.de/search/testprime/). The primer pair targeting *R. ferrireducens* amplified several uncultured bacteria (clone sequences), as well as the recently described *Rhodoferrax saidenbachensis* ED16. This strain was isolated from sediment within a drinking water reservoir in Germany by Kaden et al. (2014).

The primer pair targeting *Geothrix fermentans* 16S rRNA gene seemed to be very specific as no additional matches were found. Moreover, no uncultured bacterial or clone sequences matched the primer assay.

Furthermore, the *Gallionella* spp. primer produced fewer additional matches with several *Gallionella* spp. enrichment cultures, as well as with uncultured soil bacteria. The primer targeting the 16S rRNA gene of *Crenothrix polyspora* matched both *C. polyspora* and a range of uncultured bacteria. Those results demonstrated that overestimation caused by the unspecific amplification of otherwise unknown bacterial cultures is likely and should always be considered by interpreting qPCR results.

All biomolecular approaches were DNA-based (using the 16S rRNA gene), and such methods do not necessarily indicate bacterial activity; studies of the 16S rRNA gene only reveals the diversity of a bacterial community and do not distinguish between DNA from active and inactive bacteria.

However, despite these methodical drawbacks, all sampling sites were evaluated with the same DNA extraction kit, primer sets and population analysis methods. As a result, the samples from all sites in this study were at least comparable with each other, considering the limitations of each method. All parameters and results calculated via these biomolecular techniques must be interpreted as indications rather than as absolute measurements.

5 Conclusions and Outlook

In order, to answer the research questions:

- I) Which bacteria are involved in causing iron-clogging in water wells?
- II) Can these bacteria be used as an indicator of iron-clogging in water wells?
- III) What do these bacteria prefer in terms of environmental conditions?

Various ochrous and groundwater samples obtained from four technical groundwater-fed systems were subjected to different biomolecular analyses. The results revealed an enormous bacterial diversity in the water and biofilm samples. Each site, and sometimes even each well, harboured its own bacterial community; as a result, the bacterial composition cannot easily be compared. However, this study is the first that compared the microbial population of several technical groundwater-fed systems, which are vulnerable to iron-clogging. Here, the bacterial population compositions and functions were correlated to hydrochemical data.

Nevertheless, the results suggest that it is impossible to define a single group of bacteria that is responsible for iron related clogging processes in wells. This limitation is due to the fact that many bacterial metabolism strategies have not yet been explored, and in some cases, it remains unclear whether a bacterial species is an iron-oxidising or iron-reducing bacterial strain, or whether it can utilise both metabolic strategies depending on the surrounding environmental conditions. Iron-clogging within water wells primarily seems originate from interactions among iron-bacteria, their bacterial partners (common soil and groundwater bacteria), the well operation scheme (usage routines and production intensities), local hydrological and hydrochemical conditions and chemical anthropogenic contaminants.

Each sampling site investigated had its own specific conditions, which made it impossible to detect a shared core OTU. Bacteria are found wherever water is available, but which physiological groups dominate depends on the habitat and environmental conditions. However, several bacterial groups were found at high frequencies at most of the sampling sites, indicating an influence on the iron-

clogging processes. The OTUs *Geobacter*, *Rhodoferrax*, *Gallionella* and *Geothrix* were frequently detected; all of these are involved in iron oxidation and reduction, and their biofilm formation potential became apparent. In addition, site-dependent characteristics, such as the level of methane availability in groundwater, caused high abundances of methano- and methylotrophic bacterial groups, such as *Crenothrix* and *Methylobacter*. These groups are common sources of problems in the water supply. The coexistence of some species with similar metabolisms resulted in a greater guarantee that some would back up a given function, allowing the bacterial community to deal with changing environmental conditions (e.g., regeneration procedures by peroxide solution). In addition to the influence of methane on the microbial community composition, the groundwater DOC concentration and the redox potential, which is affected by the availability of oxygen, were found to play a major role. A higher number of samples and frequent sampling are required to verify the significance of DOC and the redox potential; a more important parameter to determine the proliferation of microbial cells might be the assimilable organic carbon (AOC) as it is part of the DOC that is most readily consumed by microorganisms. Assessing the relationships between these data and the community composition (based on the 16S rRNA gene) for clearly separated well groups (iron-clogged and non-clogged) would be one means of successfully analysing these issues.

The abstraction of groundwater leads to a mixing of groundwater from different redox states and can result in the co-occurrence of dissolved oxygen and iron. The specific hydrogeological conditions and well operation scheme determine how oxic and anoxic groundwater mix. Furthermore, bacterial biofilms inhabited by various bacterial groups in combination with extracellular polymeric substances resulting in thick layers that keep disinfectants from penetrating beyond the surface cells. In addition, mineral iron dissolved in water can absorb a significant amount of disinfectant before it reaches the bacterial cells.

Well operators should determine and employ the optimum well operation scheme for each well (stagnation should be avoided). Moreover, the hydrogeological and hydrochemical conditions and bacterial compositions need to be analysed. Collecting operational data and conducting visual inspections by camera survey can support such analyses. All water well tools that operators plan to utilise again should be pressure-washed and disinfected after use to avoid contamination.

A combination of 16S rRNA gene amplicon sequencing, metagenomics and metatranscriptomics could provide a new opportunity for identifying how microbial community compositions, dynamics, interactions and functionalities influence the iron-clogging process in water wells. These techniques, considered in combination with hydrogeological and hydrochemical conditions and the well operation scheme, can advance our understanding.

Appendix

Table A 1. Ochrous samples from pump intakes of BWB water wells and chemical analysis of associated water samples.

Water well	Abbreviation	Clogging grade	Date of sampling	DOC [mg l ⁻¹]	temperature [°C]	E° [mV]	Ec [µS cm ⁻¹]	Fe ²⁺ [mg l ⁻¹]	Fe total [mg l ⁻¹]	NO ₃ [mg l ⁻¹]	pH	Mn [mg l ⁻¹]	NH ₄ [mg l ⁻¹]	PO ₄ [mg l ⁻¹]	SO ₄ [mg l ⁻¹]	O ₂ [mg l ⁻¹]	comment
STOborg17-/1990V	B_STo17	+	03.08.2012	4.7	11.2	20	541	0.99	0.99	<0.2	7.6	0.23	0.66	0.49	68	0,2	a; d
TEGwest01-/1985V	B_TEGw01	+	10.08.2012	5	12.7	14	793	0.8	0.83	<0.05	7.4	0.51	0.93	1,04	117	0,7	a; d
TEGwest04-/1976V	B_TEGw04	-	13.08.2012	4.6	11.1	103	800	1.57	1.6	<0.05	7.5	0.43	3	1,56	128	0,3	a; b
TEGwest05-/1985V	B_TEGw05	-	13.08.2012	4.7	11.2	n.d.	795	1.05	1.1	<0.05	7.5	0.65	1.2	1,4	117	n.d.	a
STOborg10-/1990V	B_STo10	+	15.08.2012	6.6	14.1	20	763	0.9	0.91	<0.05	7.4	0.21	0.26	0,27	73	0,4	a
FRIf---07-/1981V	B_FRIf07	-	20.09.2012	5.8	11.3	n.d.	743	1.45	1.5	<0.05	7.5	0.36	0.28	0,55	168	n.d.	c
FRIf---12-/1981V	B_FRIf12	-	15.10.2012	4.7	8.3	n.d.	782	1.38	1.4	<0.05	7.5	0.37	0.41	0,83	180	n.d.	a
KAUsued02-/1995V	B_Kausued2	+	16.10.2012	2.1	10.5	-71.7	771	1.56	1.7	0.12	7.3	0.3	0.29	0,25	101	0,16	a ;d
FRIf---06-/1981V	B_FRIf06	-	25.10.2012	5.1	9.8	n.d.	745	0.54	0.55	1.3	7.5	0.58	0.42	0,43	180	n.d.	c
FRIf---10-/1981V	B_FRIf10	-	26.10.2012	4.4	9.8	n.d.	743	1.23	1.4	0.15	7.5	0.38	0.34	0,52	176	n.d.	c
STOborg11-/1990V	B_STo11	+	29.11.2012	6	8.7	-89.54	572	1.1	1.1	<0.05	7.4	0.19	0.39	0,37	60	0,01	a
STOborg07-/1990V	B_STo07	-	12.12.2012	6.4	14.1	n.d.	522	1.02	1.1	0.06	7.3	0.26	0.37	0,3	38	n.d.	c
TEGwest20-/1985V	B_TEGw20	-	16.01.2013	5.30	n.d.	n.d.	815	0.86	0.86	n.d.	7.4	0.42	0.46	0,27	108	n.d.	c
TEGwest21-/1985V	B_TEGw21	+	17.01.2013	4.30	11.3	-52.77	763	n.d.	0.82	0.75	7.4	0.30	0.50	0,20	126	0,11	a; d
TEGost-05/1986V	B_TEGo05	+	21.01.2013	4.10	11.3	-94.88	874	1.31	1.40	n.d.	7.4	0.58	1.9	0,66	135	0,04	a; d
FRIf---24-/1981V	B_FRIf24	-	23.01.2013	1.7	n.d.	n.d.	891	1.11	1.2	1.2	7.5	0.28	0.27	0,20	71	n.d.	c
FRIf---25-/1981V	B_FRIf25	+	25.01.2013	4.1	10.9	0	831	1.24	1.50	n.d.	7.5	0.52	0.48	0,34	150	0,23	a; d
TEGost-06-/1986V	B_TEGo06	+	14.02.2013	3.9	11.8	-98.79	975	1.57	1.70	n.d.	7.4	0.48	1.4	0,63	137	0	a; d
TEGwest24-/1975V	B_TEGw24	+	20.02.2013	3.9	9.5	-67.94	927	1.57	1.80	1.81	7.3	0.37	0.45	0,14	202	0,18	a; b; d
TEGwest19-/1985V	B_TEGw19	-	21.02.2013	4.90	n.d.	n.d.	784	0.71	0.71	1.77	7.3	0.28	0.45	0,20	126	n.d.	a ;b ;d
FRle---04-/1994V	B_FRle04	-	30.04.2013	3.6	11.3	n.d.	778	1	1	0.1	7.6	0.39	0.89	0,85	179	n.d.	a
FRIf---28-/1994V	B_FRIf28	-	21.05.2013	4	n.d.	n.d.	766	0.98	1	<0.05	7.6	0.49	0.26	0,30	166	n.d.	c
FRIf---14-/1981V	B_FRIf14	-	22.05.2013	4.2	n.d.	n.d.	753	1.04	1.2	<0.05	7.4	0.5	0.47	0,82	196	n.d.	c
TEGwest25-/1985V	B_TEGw25	-	23.05.2013	2.4	n.d.	n.d.	1032	2.22	2.3	<0.05	7.3	0.49	1.2	0,49	309	n.d.	c
TEGwest22-/1985V	B_TEGw22	+	23.05.2013	3.7	11.7	-58.65	769	0.96	1.2	<0.05	7.4	0.44	0.34	0,82	133	0,13	a; b
TEGwest07-/1985V	B_TEGw07	+	19.06.2013	5.3	11.5	-87.54	815	0.86	0.86	n.d.	7.4	0.42	0.46	n.d.	108	0,06	a

n.d.: not determined; "+": pumps with ochrous biofilm; "-": pumps without ochrous biofilm; a: sample used for microbial analysis; b: clone library construction of 16S rRNA gene; c: only used for chemical analysis; d: XRF and LOI

analysis; STo: Stolpe waterworks; FRIf and FRle: Friedrichshagen waterworks; TEGw and TEGo: Tegel waterworks; KAUsued: Kaulsdorf waterwork;

Table A 2. Overview of well characteristics from water wells with subsurface iron and manganese removal.

Water well/ component	Abbreviation	Date of sampling	Sampling campaign	Well infrastructure					
				Abstraction phase	Abstraction volume before sampling [m ³]	Operation time [months]	Filter depth [m]	Well-cluster	Reduction of specific well yield [%]
1101	RU_1101H_AF	21.01.2013	SC I/ SC II	begin	6	9	31	1 st	42.7
1101	RU_1101_F	21.01.2013	SC II	3 rd abstraction phase	1368	9	31	1 st	42.7
1101	RU_1101_G	21.01.2013	SC II	4 th abstraction phase	2056	9	31	1 st	42.7
1101	RU_1101_E	22.01.2013	SC II	5 th abstraction phase	2750	9	31	1 st	42.7
1101	RU_1101D_EF	22.01.2013	SC I/ SC II	end	3394	9	31	1 st	42.7
1104	RU_1104C_AF	22.01.2013	SC I	begin	6	9	30	1 st	42.1
1106	RU_1106A_AF	22.01.2013	SC I	begin	8	73	31	1 st	62.5
1107	RU_1107B_AF	21.01.2013	SC I	begin	23	12	34	1 st	49.3
1108	RU_1108E_AF	21.01.2013	SC I	begin	14,4	61	35	1 st	40.4
1109	RU_1109B_AF	21.01.2013	SC I	begin	6	12	31	1 st	50.2
1110	RU_1110C_AF	22.01.2013	SC I	begin	3	3	32	1 st	75.7
1110	RU_1110D_AF	24.01.2013	SC I	begin	6	3	32	1 st	75.7
1111	RU_1111D_AF	21.01.2013	SC I	begin	6	9	32	1 st	42.7
1112	RU_1112D_AF	22.01.2013	SC I	begin	12	9	33	1 st	46.4
1103	RU_1103E_EF	23.01.2013	SC I	end	4270	12	35	1 st	47.9
1104	RU_1104D_EF	23.01.2013	SC I	end	4286	9	30	1 st	42.1
1105	RU_1105A_EF	24.01.2013	SC I	end	3257	73	30	1 st	63.6
1105	RU_1105F_EF	24.01.2013	SC I	end	4192	73	30	1 st	63.6
1107	RU_1107A_EF	22.01.2013	SC I	end	4209	12	30	1 st	49.3
1108	RU_1108D_EF	22.01.2013	SC I	end	4193	61	30	1 st	40.4
1109	RU_1109A_EF	23.01.2013	SC I	end	4300	12	30	1 st	50.2
1111	RU_1111C_EF	22.01.2013	SC I	end	3996	9	30	1 st	42.7
1112	RU_1112C_EF	23.01.2013	SC I	end	4212	9	30	1 st	46.4
1212	RU_1212_AG	21.03.2013	SC I	pumping test	-	0	30	2 nd	0

Appendix

Water well/ component	Abbreviation	Date of sampling	Sampling campaign	Well infrastructure					
				Abstraction phase	Abstraction volume before sampling [m ³]	Operation time [months]	Filter depth [m]	Well-cluster	Reduction of specific well yield [%]
1211	RU_1211_AG	23.03.2013	SC I	pumping test	-	0	30	2 nd	0
1210	RU_1210_AG	25.03.2013	SC I	pumping test	-	0	30	2 nd	0
1203	RU_1203_AG	10.04.2013	SC I	pumping test	-	0	30	2 nd	0
1204	RU_1204_AG	11.04.2013	SC I	pumping test	-	0	30	2 nd	0
1205	RU_1205_AG	13.04.2013	SC I	pumping test	-	0	30	2 nd	0
1206	RU_1206_AG	16.04.2013	SC I	pumping test	-	0	30	2 nd	0
1307	RU_1307_AG	03.06.2013	SC I	pumping test	-	0	30	3 rd	0
1306	RU_1306_AG	04.06.2013	SC I	pumping test	-	0	30	3 rd	0
1303	RU_1303_AG	10.06.2013	SC I	pumping test	-	0	30	3 rd	0
1402	RU_1402_AG	12.06.2013	SC I	pumping test	-	0	32	4 th	0
Aeration tank	RU_001	23.02.2013	SC I	biofilm sample of the wall	-	73	-	1 st	-
Aeration tank	RU_KH	22.03.2012	SC I	biofilm sample of the wall	-	73	-	1 st	-
Aeration tank	RU_ZuDEK	17.12.2012	SC I	water sample of aeration tank	-	73	-	1 st	-
Aeration tank	RU_FLB_2	14.06.2013	SC I	biofilm sample of the wall	-	73	-	1 st	-
Aeration tank	RU_FLB_1	17.05.2013	SC I	water sample of aeration tank	-	73	-	1 st	-
1105	RU_1105_H	17.05.2013	SC III	manganese biofilm of infiltration pipe	-	77	73	1 st	53.8
1105	RU_1105_I	17.05.2013	SC III	biofilm sample before regeneration	-	77	73	1 st	53.8
1105	RU_1105_1	06.06.2013	SC III	end of abstraction phase after regeneration	n.d.	77	73	1 st	53.8

n.d.: not determined

Table A 3. Ochrous and water samples from water wells with subsurface iron and manganese removal system and chemical analysis of associated water samples.

Water well/ component	Abbreviation	Date of sampling	T [°C]	pH	O ₂ [mg L ⁻¹]	Ec [μS cm ⁻¹]	E° [mV]	Fe ²⁺ [mg l ⁻¹]	Mn ²⁺ [mg l ⁻¹]	NO ₃ ⁻ [mg l ⁻¹]	Fe ³⁺ [mg l ⁻¹]	NO ₂ [mg l ⁻¹]	NH ₄ ⁺ [mg l ⁻¹]	DOC [mg l ⁻¹]
1101	RU_1101H_AF	21.01.2013	6	7.54	11.93	132.4	defect	<0.04	<0.1	5.4	<0.1	<0.005	<0.02	4.3
1101	RU_1101_F	21.01.2013	6.3	6.81	0.26	130.4	342.8	<0.04	<0.1	5	<0.1	<0.005	<0.02	4.3
1101	RU_1101_G	21.01.2013	6.2	6.34	0.14	154.8	defect	<0.04	0.2	5.2	<0.1	<0.005	<0.02	4.3
1101	RU_1101_E	22.01.2013	6.2	6.41	0.14	151.4	380	<0.04	0.3	4.9	<0.1	<0.005	<0.02	4.3
1101	RU_1101D_EF	22.01.2013	6.1	6.44	0.08	161.8	defect	<0.04	0.3	5	<0.1	<0.005	<0.02	4.3
1104	RU_1104C_AF	22.01.2013	6.3	7.5	12.36	145.6	defect	<0.04	<0.1	5.2	<0.1	<0.005	<0.02	n.d.
1106	RU_1106A_AF	22.01.2013	6.4	7.62	12.46	139.5	defect	<0.04	<0.1	5	<0.1	<0.005	<0.02	0.7
1107	RU_1107B_AF	21.01.2013	6.4	7.55	12.19	137.9	defect	<0.04	<0.1	4.6	<0.1	<0.005	<0.02	2.7
1108	RU_1108E_AF	21.01.2013	6.1	7.5	12.9	136.8	defect	<0.04	<0.1	3	<0.1	<0.005	<0.02	1.3
1109	RU_1109B_AF	21.01.2013	6.4	7.69	12.4	134.9	defect	<0.04	<0.1	5	<0.1	<0.005	<0.02	1.5
1110	RU_1110C_AF	22.01.2013	6.3	7.55	11.46	138.3	defect	<0.04	<0.1	3.9	<0.1	<0.005	<0.02	3.3
1110	RU_1110D_AF	24.01.2013	6.3	7.59	12.5	141.5	defect	<0.04	<0.1	4.9	<0.1	<0.005	<0.02	3.3
1111	RU_1111D_AF	21.01.2013	6.2	7.62	11.84	134.6	defect	<0.04	<0.1	5.4	<0.1	<0.005	<0.02	n.d.
1112	RU_1112D_AF	22.01.2013	6.2	7.45	12.62	143.8	defect	<0.04	<0.1	5	<0.1	<0.005	<0.02	n.d.
1103	RU_1103E_EF	23.01.2013	5.8	6.35	0.04	156.9	defect	<0.04	<0.1	4	<0.1	<0.005	<0.02	n.d.
1104	RU_1104D_EF	23.01.2013	5.8	6.29	0.06	158.8	defect	<0.04	<0.1	4	<0.1	<0.005	<0.02	n.d.
1105	RU_1105A_EF	24.01.2013	5.8	6.27	0.06	140.1	defect	<0.04	<0.1	3.7	<0.1	<0.005	<0.02	1.5
1105	RU_1105F_EF	24.01.2013	5.7	6.35	0.09	147.9	defect	<0.04	<0.1	4.5	<0.1	<0.005	<0.02	1.5
1107	RU_1107A_EF	22.01.2013	6	6.43	0.49	181.7	defect	<0.04	<0.1	5	<0.1	<0.005	<0.02	2.7
1108	RU_1108D_EF	22.01.2013	6.1	6.49	0.18	167.4	defect	<0.04	<0.1	4.8	<0.1	<0.005	<0.02	1.3
1109	RU_1109A_EF	23.01.2013	6.2	6.4	0.05	160.2	defect	<0.04	<0.1	4.2	<0.1	<0.005	<0.02	1.5
1111	RU_1111C_EF	22.01.2013	5.6	6.35	0.05	169.2	defect	<0.04	<0.1	5	<0.1	<0.005	<0.02	n.d.
1112	RU_1112C_EF	23.01.2013	6.2	6.43	1.7	179	defect	<0.04	<0.1	4.8	<0.1	<0.005	<0.02	n.d.
1212	RU_1212_AG	21.03.2013	n.d.	n.d.	n.d.	n.d.	n.d.	24	1.4	1.82	n.d.	<0.2	0.8	1.4
1211	RU_1211_AG	23.03.2013	n.d.	n.d.	n.d.	n.d.	n.d.	23.8	1.4	0.22	n.d.	<0.2	0.5	1.9
1210	RU_1210_AG	25.03.2013	n.d.	n.d.	n.d.	n.d.	n.d.	23.9	1.3	0.92	n.d.	<0.2	0.5	0.2
1203	RU_1203_AG	10.04.2013	n.d.	n.d.	n.d.	n.d.	n.d.	26.1	1.4	<0.2	n.d.	<0.2	0.4	0.2
1204	RU_1204_AG	11.04.2013	n.d.	n.d.	n.d.	n.d.	n.d.	24.5	1.3	0.45	n.d.	<0.2	0.6	1.9
1205	RU_1205_AG	13.04.2013	n.d.	n.d.	n.d.	n.d.	n.d.	25.7	1.2	<0.2	n.d.	<0.2	0.8	1.0
1206	RU_1206_AG	16.04.2013	n.d.	n.d.	n.d.	n.d.	n.d.	26.6	1.1	1.92	n.d.	<0.2	0.6	1.0
1307	RU_1307_AG	03.06.2013	6.5	5.72	0	229	-79.8	25.11	0.8	5.7	25.11	<0.005	1	n.d.

Appendix

Water well/ component	Abbreviation	Date of sampling	T [°C]	pH	O ₂ [mg L ⁻¹]	Ec [µS cm ⁻¹]	E° [mV]	Fe ²⁺ [mg l ⁻¹]	Mn ²⁺ [mg l ⁻¹]	NO ₃ ⁻ [mg l ⁻¹]	Fe ³⁺ [mg l ⁻¹]	NO ₂ [mg l ⁻¹]	NH ₄ ⁺ [mg l ⁻¹]	DOC [mg l ⁻¹]
1306	RU_1306_AG	04.06.2013	6.3	5.72	0	211	-37.3	31.94	0.8	6	31.93	<0.005	1	1.4
1303	RU_1303_AG	10.06.2013	6.5	5.45	0	n.d.	n.d.	26.66	0.7	5	26.66	<0.005	1.1	1.3
1402	RU_1402_AG	12.06.2013	6.1	5.91	0.05	157.3	20.8	11.8	0.6	6.2	11.18	<0.005	0.5	n.d.
Aeration tank	RU_001	23.02.2013	n.d.	7	n.d.	n.d.	n.d.	n.d.	n.d.	n.d.	n.d.	n.d.	n.d.	n.d.
Aeration tank	RU_KH	22.03.2012	n.d.	7	n.d.	12	n.d.	n.d.	0.5	n.d.	<0.1	n.d.	n.d.	n.d.
Aeration tank	RU_ZuDEK	17.12.2012	6.6	6.1	n.d.	127.4	434.2	<0.01	n.d.	<0.1	n.d.	n.d.	n.d.	n.d.
Aeration tank	RU_FLB_2	14.06.2013	n.d.	n.d.	n.d.	n.d.	n.d.	n.d.	n.d.	n.d.	n.d.	n.d.	n.d.	n.d.
Aeration tank	RU_FLB_1	17.05.2013	6.1	6.61	n.d.	127.4	434.2	<0.01	<0.02	<1.0	<0.1	<0.02	<0.05	n.d.
1105	RU_1105_H	17.05.2013	n.d.	n.d.	n.d.	n.d.	n.d.	n.d.	n.d.	n.d.	n.d.	n.d.	n.d.	n.d.
1105	RU_1105_I	17.05.2013	n.d.	n.d.	n.d.	n.d.	n.d.	n.d.	n.d.	n.d.	n.d.	n.d.	n.d.	n.d.
1105	RU_1105_1	06.06.2013	n.d.	n.d.	n.d.	n.d.	n.d.	n.d.	n.d.	n.d.	n.d.	n.d.	n.d.	2.6

n.d.: not determined

Table A 4. Ochrous and water samples from two opencast mines and chemical analysis of associated water samples.

Water well	Abbreviation	Specification	Filter	Date of sampling	T °C	pH	Ec [μS cm ⁻¹]	E° [mV]	Fe ²⁺ [mg l ⁻¹]	Fe ³⁺ [mg l ⁻¹]	Fe _{total} [mg l ⁻¹]	NO ₃ [mg l ⁻¹]	Mn [mg l ⁻¹]	NH ₄ [mg l ⁻¹]	PO ₄ [mg l ⁻¹]	O ₂ [mg l ⁻¹]	SO ₄ ²⁻ [mg l ⁻¹]	comment
WR2377	R_WP	pump intake (biofilm)	a	11.04.2011	13.5	6.8	570	110	0.15		0.86	0.9	0.14	0.2	0.07	1	39	b;c
HR45	R_HD	riser (biofilm)	a	11.04.2011	14.4	6.35	840	16	n.d.	n.d.	175	0.5	0.47	0.51	1.57	4.4	295	b;c
HR1402	R_HR	riser (biofilm)	n	11.04.2011	n.d.	n.d.	n.d.	n.d.	n.d.	n.d.	n.d.	n.d.	n.d.	n.d.	n.d.	n.d.	n.d.	b;c
H1424	R_P320	pump (320 m)	a	18.06.2012	n.d.	n.d.	n.d.	n.d.	n.d.	n.d.	n.d.	n.d.	n.d.	n.d.	n.d.	n.d.	n.d.	b;c
WR2378	R_E	Pump intake	a	29.09.2011	13.5	7.5	600	139	0.1	n.d.	0.75	0.5	0.13	0.2	0.07	2.7	45	b;c
HS1362	R_RK	flap trap of pump (biofilm)	a	29.09.2011	n.d.	n.d.	n.d.	n.d.	n.d.	n.d.	n.d.	n.d.	n.d.	n.d.	n.d.	n.d.	n.d.	b;c
WR2509	WR2509	water	n	15.05.2014	14.4	6.6	440	6	0.97	0.41	1.38	< 0.5	0.11	0.35	0.28	0.8	3	
WR2512	WR2512	water	n	15.05.2014	14.4	6.6	420	13	1.05	0.43	1.48	< 0.5	0.11	0.35	0.28	1.4	< 2	
WR2514	WR2514	water	n	15.05.2014	14.4	6.6	410	-12	1.73	0.17	1.9	< 0.5	0.11	0.37	0.31	0.8	< 2	
WR2517	WR2517	water	n	15.05.2014	14.4	6.55	400	-2	1.68	0.13	1.81	< 0.5	0.11	0.38	0.35	0.6	< 2	
WR2378	WR2378	water	a	24.05.2014	12.9	6.6	700	139	7.9	3.5	11.4	< 0.5	0.28	0.23	< 0.05	1	133	
WR2496	WR2496	water	a	15.05.2014	11.8	6.85	670	4	1.36	0.66	2.02	< 0.5	0.16	< 0.2	0.14	3.2	102	
WR2510	WR2510	water	n	15.05.2014	11.8	7	560	-60	2.14	0.95	3.09	< 0.5	0.17	< 0.2	0.23	0.7	36	
WR2511	WR2511	water	n	15.05.2014	11.6	7	540	-56	2.04	0.18	2.22	< 0.5	0.17	< 0.2	0.2	0.7	35	
WR2513	WR2513	water	n	15.05.2014	11.7	6.9	540	-58	2.14	0.17	2.31	< 0.5	0.2	< 0.2	0.21	0.8	25	
WR2515	WR2515	water	n	15.05.2014	11.6	7	500	-67	1.93	0.14	2.07	< 0.5	0.16	< 0.2	0.19	0.3	21	
WR2516	WR2516	water	n	15.05.2014	11.8	7	570	-59	2.4	0	2.4	< 0.5	0.19	< 0.2	0.19	0.4	14	
W5827	W5827	water	n	15.05.2014	12.7	6.75	630	-35	1.66	0.11	1.77	< 0.5	0.14	0.23	0.2	0.2	38	
W6618	W6618	water	n	06.01.2014	12.7	6.8	580	17	1.92	0.13	2.05	< 0.5	0.19	< 0.2	0.27	0.1	18	
W5603	W5603	water	a	15.05.2014	11.2	7	730	11	1.36	2.52	1.16	<0.5	0.1	0.2	0.15	0.21	93	
WR2498	WR2498	water	a	15.05.2014	12.4	7.02	669	107	1.4	2.86	4.26	<0.5	0.09	0.2	0.07	1.71	34	
W5655	W5655	water	n	15.05.2014	12.6	6.75	540	11	1.7	2.55	4.25	<0.5	0.13	0.29	0.1	0.41	10	
W5656	W5656	water	n	15.05.2014	12.4	6.75	590	7	1.56	0.26	1.82	<0.5	0.12	0.24	0.24	1.79	20	
W6619	W6619	water	n	15.05.2014	12.3	6.78	585	-32	1.99	0.11	2.1	<0.5	0.21	0.2	0.26	0.12	17	
HR1498	HR1498	water	n	24.02.2014	15.7	6.9	450	-75	2.9	0	2.9	< 0.5	0.28	< 0.2	0.22	0.3	26	
HR1499	HR1499	water	n	24.02.2014	17.5	6.8	530	-79	2.69	0	2.39	< 0.5	0.28	0.46	0.67	0.3	20	
HR1500	HR1500	water	n	24.05.2014	16.4	6.9	450	30	2.66	0	2.66	< 0.5	0.35	0.33	0.28	0.5	28	

Appendix

Water well	Abbreviation	Specification	Filter	Date of sampling	T °C	pH	Ec [μS cm ⁻¹]	E° [mV]	Fe ²⁺ [mg l ⁻¹]	Fe ³⁺ [mg l ⁻¹]	Fe _{total} [mg l ⁻¹]	NO ₃ [mg l ⁻¹]	Mn [mg l ⁻¹]	NH ₄ [mg l ⁻¹]	PO ₄ [mg l ⁻¹]	O ₂ [mg l ⁻¹]	SO ₄ ²⁻ [mg l ⁻¹]	comment
H1308	H1308	water	a	24.05.2014	17.3	6.9	490	124	1.69	0.52	2.21	< 0.5	0.12	0.56	0.63	0.4	23	
H1310	H1310	water	a	24.05.2014	17.6	6.8	470	46	0.84	0.39	1.23	< 0.5	0.11	0.56	0.62	0.5	10	
H1316	H1316	water	n	24.05.2014	17.9	6.7	520	-36	1.64	0	1.64	< 0.5	0.12	0.63	1.16	0.2	5	
H1317	H1317	water	n	24.05.2014	18.3	6.7	500	-38	1.8	0	1.8	< 0.5	0.11	0.6	1.21	0.3	5	
H1429	H1429	water	n	06.05.2014	15.5	6.8	540	n.d.	0.11	0.02	0.13	1	n.d.	n.d.	n.d.	0.3	33	
H1431	H1431	water	n	16.04.2014	17.6	6.7	470	n.d.	1.5	0.07	1.57	< 0.5	n.d.	n.d.	n.d.	1	5	
H1309	H1309	water	a	16.05.2014	17	6.71	506	-60	1.61	0.2	1.81	< 0.5	0.14	0.49	1.13	0.71	5	
H1313	H1313	water	a	16.05.2014	16.1	6.6	480	-48	1.73	0	1.73	< 0.5	0.13	0.47	1.17	0.68	7	
H1415	H1415	water	a	16.05.2014	15.9	6.85	485	-30	1.47	1.06	2.53	< 0.5	0.25	0.33	0.4	3.41	22	
H1301	H1301	water	n	16.05.2014	16.4	6.85	490	-62	1.91	0	1.91	< 0.5	0.17	0.4	0.88	0.61	11	
H1307	H1307	water	n	16.05.2014	17.1	7.05	590	-58	1.79	0	1.79	< 0.5	0.07	0.56	1.54	0.11	5	
H2054	H2054	water	n	16.05.2014	16.9	6.6	525	-57	2.09	0.05	2.14	< 0.5	0.26	0.42	0.64	0	27	
H2055	H2055	water	n	16.05.2014	17.4	6.55	525	-45	2.13	0.02	2.15		0.22	0.47	08.1	0	18	

n.d.: not determined; a: aerated filter; n: non-aerated filter; b: clone library construction of 16S rRNA gene; c: 454-pyrosequencing of 16S rRNA gene; W and WR: wells of the opencast mine Garzweiler; H and HR wells of the opencast mine Hambach

Table A 5. Ochrous and water samples from different columns with ochrous formation and chemical analysis of associated water samples.

Test series	Column	Sample	Date of sampling	Running time before regeneration	Running time after regeneration	specification	regeneration	Ec [$\mu\text{S cm}^{-1}$]	O ₂ [mg l ⁻¹]	pH	T °C	k _r -value [m s ⁻¹]	decrease of k _r -value [log reduction]	Fe sand [mg g ⁻¹]	comment
TS I	column 1		28.06.2013	47	100	storage for 120 days during 21 °C, column was closed	1x chemical and mechanical regeneration by 3 cycles	1500	<0.05	6.9	18	2x10 ⁻⁰⁴	1.5	n.d.	
		S1_5													
		S1_20													
		S1_45													
TS I	column 6	S1_15	28.06.2013	169		-	no regeneration (negative control)	1500	<0.05	6.9	18	8x10 ⁻⁰⁵	2.2	n.d.	
		S6_5													
		S6_15													
		S6_20													
TS I	column 4	S6_45	28.06.2013	41	74/23	storage for 91 days during 21 °C, column was closed	2x chemical and mechanical regeneration by 5 and 3 cycles each	1500	<0.05	6.9	18	9x10 ⁻⁰⁴	1	n.d.	
		S4_5													
		S4_15													
		S4_20													
TS II	column 2	S4_45	21.05.2014	57	47	material not pretreated	1x chemical and hydromechanical regeneration	1500	<0.05	6.9	18	9x10 ⁻⁰⁶	2.6		
		S2_0													15
		S2_25													8
		S2_50													4
TS II	column 4		21.05.2014	39		material not pretreated	no regeneration (negative control)	1500	<0.05	6.9	18	8x10 ⁻⁰⁵	1.5		
		S4_0													15

Appendix

Test series	Column	Sample	Date of sampling	Running time before regeneration	Running time after regeneration	specification	regeneration	Ec [$\mu\text{S cm}^{-1}$]	O ₂ [mg l ⁻¹]	pH	T °C	k _r -value [m s ⁻¹]	decrease of k _r -value [log reduction]	Fe sand [mg g ⁻¹]	comment
TS II	column 5	S4_25	21.05.2014	46	49	filter sand pretreated by AIXTRACTOR 2.0	2x chemical and hydromechanical regeneration	1500	<0.05	6.9	18	9x10 ⁻⁰⁴	0	11	b
		S4_50												10	
		S5_0												9	
		S5_25												0,5	
TS II	column 8	S5_50	21.05.2014	39		filter sand pretreated by AIXTRACTOR 2.0	no regeneration (negative control)	1500	<0.05	6.9	18	3x10 ⁻⁰⁵	2	0,5	
		S8_0												15	
		S8_25												9	
		S8_50												7	
TS I	ground-water	GW 2013	10.07.2013				measuring point 1	1.906	<0.05	6.8					b
TS II	ground-water	GW 2014	29.07.2014				measuring point 1	1.906	<0.05	6.8					

b: clone library construction of 16S rRNA gene

Table A 6. Chemical parameters of groundwater from Dresden (HTW Dresden; 2012)

Parameter	Value
Ca ²⁺ [mg l ⁻¹]	356
Mg ²⁺ [mg l ⁻¹]	39.8
Na ⁺ [mg l ⁻¹]	50.2
Fe ²⁺ [mg l ⁻¹]	2.7
Mn ²⁺ [mg l ⁻¹]	0.34
NH ₄ ⁺ [mg l ⁻¹]	0.13
K ⁺ [mg l ⁻¹]	4.6
Cl ⁻ [mg l ⁻¹]	83.1
SO ₄ ²⁻ [mg l ⁻¹]	564
NO ₃ ⁻ [mg l ⁻¹]	6.4
HCO ₃ ⁻ [mmol l ⁻¹]	9.5
DOC [mg l ⁻¹]	3.4
O ₂ [mg l ⁻¹]	<0.05
pH	6.8
Ec [μS cm ⁻¹]	1.906

References

- Aburto, A., Fahy, A., Coulon, F., Lethbridge, G., Timmis, K.N., Ball, A.S., McGenity, T.J., 2009. Mixed aerobic and anaerobic microbial communities in benzene-contaminated groundwater. *J. Appl. Microbiol.* 106, 317–328. doi:10.1111/j.1365-2672.2008.04005.x
- Albers, C.N., Ellegaard-Jensen, L., Harder, C.B., Rosendahl, S., Knudsen, B.E., Ekelund, F., Aamand, J., 2015. Groundwater chemistry determines the prokaryotic community structure of waterworks sand filters. *Environ. Sci. Technol.* 49, 839–846. doi:10.1021/es5046452
- Allen, M.J., Edberg, S.C., Reasoner, D.J., 2004. Heterotrophic plate count bacteria - What is their significance in drinking water? *Int. J. Food Microbiol.* 92, 265–274. doi:10.1016/j.ijfoodmicro.2003.08.017
- Altschul, S.F., Gish, W., Miller, W., Myers, E.W., Lipman, D.J., 1990. Basic Local Alignment Search Tool. *J. Mol. Biol.* 215, 403–410.
- Amann, R.L., Binder, B.J., Olson, R.J., Chisholm, S.W., Devereux, R., Stahl, D.A., 1990. oligonucleotide probes with flow cytometry for analyzing mixed microbial populations . Combination of 16S rRNA-Targeted Oligonucleotide Probes with Flow Cytometry for Analyzing Mixed Microbial Populations. *Appl. Environ. Microbiol.* 56, 1919–1925. doi:10.1111/j.1469-8137.2004.01066.x
- Baek, K., McKeever, R., Rieber, K., Sheppard, D., Park, C., Ergas, S.J., Nüsslein, K., 2012. Molecular approach to evaluate biostimulation of 1,2-dibromoethane in contaminated groundwater. *Bioresour. Technol.* 123, 207–213. doi:10.1016/j.biortech.2012.05.119
- Bell, T., Newman, J.A., Silverman, B.W., Turner, S.L., Lilley, A.K., 2005. The contribution of species richness and composition to bacterial services. *Nature* 436, 1157–1160. doi:10.1038/nature03891

- Ben-Dov, E., Shapiro, O.H., Siboni, N., Kushmaro, A., 2006. Advantage of using inosine at the 3' termini of 16S rRNA gene universal primers for the study of microbial diversity. *Appl. Environ. Microbiol.* 72, 6902–6906. doi:10.1128/AEM.00849-06
- Benedek, T., Táncsics, A., Szabó, I., Farkas, M., Szoboszlai, S., Fábíán, K., Maróti, G., Kriszt, B., 2016. Polyphasic analysis of an *Azoarcus*-*Leptothrix*-dominated bacterial biofilm developed on stainless steel surface in a gasoline-contaminated hypoxic groundwater. *Environ. Sci. Pollut. Res.* 23, 9019–9035. doi:10.1007/s11356-016-6128-0
- Braun, B., Künzel, S., Schröder, J., Szewzyk, U., 2017. Draft genome sequence of strain R_RK_3, an iron-depositing isolate of the genus *Rhodomicrobium*, isolated from a dewatering well of an opencast mine. *Genome Announc.* 5. doi:10.1128/genomeA.00864-17
- Braun, B., Schröder, J., Knecht, H., Szewzyk, U., 2016. Unraveling the microbial community of a cold groundwater catchment system. *Water Res.* 107. doi:10.1016/j.watres.2016.10.040
- Bustos Medina, D.A., van den Berg, G.A., van Breukelen, B.M., Juhasz-Holterman, M., Stuyfzand, P.J., 2013. Iron-hydroxide clogging of public supply wells receiving artificial recharge: near-well and in-well hydrological and hydrochemical observations. *Hydrogeol. J.* 21, 1393–1412. doi:10.1007/s10040-013-1005-0
- Campbell, M.D., Gray, G.R., 1975. Mobility of Well-Drilling Additives in the Ground-Water System, in: *Environmental Aspects of Chemical Use in Well-Drilling Operations*. Houston, Texas, p. 261.
- Cerrato, J.M., Falkinham, J.O., Dietrich, A.M., Knocke, W.R., McKinney, C.W., Pruden, A., 2010. Manganese-oxidizing and -reducing microorganisms isolated from biofilms in chlorinated drinking water systems. *Water Res.* 44, 3935–45. doi:10.1016/j.watres.2010.04.037
- Coates, J.D., Achenbach, L.A., 2001. *The Biogeochemistry of Aquifer Systems, Manual of Environmental Microbiology*.

- Coates, J.D., Ellis, D.J., Gaw, C. V, Lovley, D.R., 1999. *Geothrix fermentans* gen. nov., sp. nov., a novel Fe(III)-reducing bacterium from a hydrocarbon-contaminated aquifer. *Int. J. Syst. Bacteriol.* 49, 1615–1622. doi:10.1099/00207713-49-4-1615
- Coby, A.J., Picardal, F., Shelobolina, E., Xu, H., Roden, E.E., 2011. Repeated anaerobic microbial redox cycling of iron. *Appl. Environ. Microbiol.* 77, 6036–6042. doi:10.1128/AEM.00276-11
- Cohn, F., 1853. Überlebende Organismen im Trinkwasser. *Jahresber Schles Ges Vaterl Kult.* 31.
- Cullimore, D.R., McCann, A.E., 1977. The identification, cultivation and control of iron bacteria in ground water. *London Acad. Press. Inc* 219–61.
- de Vet, W.W.J.M., Dinkla, I.J.T., Abbas, B.A., Rietveld, L.C., van Loosdrecht, M.C.M., 2012. *Gallionella* spp. in trickling filtration of subsurface aerated and natural groundwater. *Biotechnol. Bioeng.* 109, 904–912. doi:10.1002/bit.24378
- Demir, N.M., 2016. Experimental study of factors that affect iron and manganese removal in slow sand filters and identification of responsible microbial species. *Polish J. Environ. Stud.* 25, 1453–1465. doi:10.15244/pjoes/62679
- Dericks, B., 2015. Integration, persistence and control of hygienically relevant bacteria in iron oxide incrustations in wells. *Universität Duisburg-Essen.*
- DeSantis, T.Z., Brodie, E.L., Moberg, J.P., Zubieta, I.X., Piceno, Y.M., Andersen, G.L., 2007. High-density universal 16S rRNA microarray analysis reveals broader diversity than typical clone library when sampling the environment. *Microb. Ecol.* 53, 371–383. doi:10.1007/s00248-006-9134-9
- Donlan, R.M., 2002. Biofilms: microbial life on surfaces. *Emerg. Infect. Dis.* 8, 881–890. doi:10.3201/eid0809.020063

- Dowd, S.E., Callaway, T.R., Wolcott, R.D., Sun, Y., McKeehan, T., Hagevoort, R.G., Edrington, T.S., 2008. Evaluation of the bacterial diversity in the feces of cattle using 16S rDNA bacterial tag-encoded FLX amplicon pyrosequencing (bTEFAP). *BMC Microbiol.* 8, 125. doi:10.1186/1471-2180-8-125
- Edlund, J., Eriksson, L., Johansson, L., Chukharkina, A., Johansson, J., Hallbeck, B., Pedersen, K., 2016. Microbial Investigations During Infiltration Experiment (INEX) Phase 2. Posiva Work. report, 2016-38.
- Elliott, A.V.C., Plach, J.M., Droppo, I.G., Warren, L.A., 2014. Collaborative microbial Fe-redox cycling by pelagic floc bacteria across wide ranging oxygenated aquatic systems. *Chem. Geol.* 366, 90–102. doi:10.1016/j.chemgeo.2013.11.017
- Emerson, D., Fleming, E.J., McBeth, J.M., 2010. Iron-oxidizing bacteria: an environmental and genomic perspective. *Annu. Rev. Microbiol.* 64, 561–83. doi:10.1146/annurev.micro.112408.134208
- Finneran, K.T., Johnsen, C. V., Lovley, D.R., 2003. *Rhodoferrax ferrireducens* sp. nov., a psychrotolerant, facultatively anaerobic bacterium that oxidizes acetate with the reduction of Fe(III). *Int. J. Syst. Evol. Microbiol.* 53, 669–673. doi:10.1099/ijs.0.02298-0
- Finneran, K.T., Johnsen, C. V, Lovley, D.R., 2003. *Rhodoferrax ferrireducens* sp. nov., a psychrotolerant, facultatively anaerobic bacterium that oxidizes acetate with the reduction of Fe (III) Printed in Great Britain 669–673. doi:10.1099/ijs.0.02298-0
- Fleming, E.J., Cetinić, I., Chan, C.S., Whitney King, D., Emerson, D., 2014. Ecological succession among iron-oxidizing bacteria. *ISME J.* 8, 804–15. doi:10.1038/ismej.2013.197
- Fogel, G.B., Collins, C.R., Li, J., Brunk, C.F., 1999. Prokaryotic genome size and SSU rDNA copy number: Estimation of microbial relative abundance from a mixed population. *Microb. Ecol.* 38, 93–113. doi:10.1007/s002489900162

- Fonte, E.S., Amado, A.M., Meirelles-Pereira, F., Esteves, F.A., Rosado, A.S., Farjalla, V.F., 2013. The Combination of Different Carbon Sources Enhances Bacterial Growth Efficiency in Aquatic Ecosystems. *Microb. Ecol.* 66, 871–878. doi:10.1007/s00248-013-0277-1
- Fuchs, G., Schlegel, H.-G., 2007. *Allgemeine Mikrobiologie*, 8. ed, Thieme Verlag, 8. Auflage. doi:10.1016/0014-5793(81)80456-5
- Gino, E., Starosvetsky, J., Kurzbaum, E., Armon, R., 2010. Combined Chemical-Biological Treatment for Prevention/Rehabilitation of Clogged Wells by an Iron-Oxidizing Bacterium. *Environ. Sci. Technol.* 44, 3123–3129.
- Golladay, S.W., Sinsabaugh, R.L., 1991. Biofilm development on leaf and wood surfaces in a boreal river. *Freshw. Biol.* 25, 437–450. doi:10.1111/j.1365-2427.1991.tb01387.x
- Griseck, T., Ahrens, J., Kuehne, M., Bartak, R., Herlitzius, J., Ghodeif, K., Wahaab, R.A., 2013. Coupling Riverbank Filtration and Subsurface Iron Removal. *Proc. Int. Symp. Manag. Aquifer Recharg.* 1–12. doi:10.13140/RG.2.1.3402.5689
- Hallbeck, L., Pedersen, K., 1991. Autotrophic and mixotrophic growth of *Gallionella ferruginea*. *J. Gen. Microbiol.* 137, 2657–2661. doi:10.1099/00221287-137-11-2657
- Head, I., Saunders, J., RW, P., 1998. Microbial evolution, diversity, and ecology: a decade of ribosomal RNA analysis of uncultivated microorganisms. *Microb. Ecol.* 35, 1–21.
- Heising, S., Schink, B., 1998. Phototrophic oxidation of ferrous iron by a *Rhodospirillum rubrum* strain. *Microbiology* 144, 2263–2269. doi:10.1099/00221287-144-8-2263
- Henkel, S., Weidner, C., Roger, S., Schüttrumpf, H., Rude, T.R., Klauder, W., Vinzelberg, G., 2012. Untersuchung der Verockerungsneigung von Vertikalfilterbrunnen im Modellversuch: Ein Beitrag zum Prozessverständnis der chemischen Verockerung in der Tagebauentwässerung. *Grundwasser* 17, 157–169. doi:10.1007/s00767-012-0198-9

- Hijnen, W.A.M., Van der Kooij, D., 1992. The effect of low concentrations of assimilable organic carbon (AOC) in water on biological clogging of sand beds. *Water Res.* 26, 963–972. doi:10.1016/0043-1354(92)90203-G
- Hongoh, Y., Yuzawa, H., Ohkuma, M., Kudo, T., 2003. Evaluation of primers and PCR conditions for the analysis of 16S rRNA genes from a natural environment. *FEMS Microbiol. Lett.* 221, 299–304. doi:10.1016/S0378-1097(03)00218-0
- Hori, T., Müller, A., Igarashi, Y., Conrad, R., Friedrich, M.W., 2010. Identification of iron-reducing microorganisms in anoxic rice paddy soil by ¹³C-acetate probing. *ISME J.* 4, 267–278. doi:10.1038/ismej.2009.100
- Houben, G.J., 2003. Iron oxide incrustations in wells. Part 2: Chemical dissolution and modeling. *Appl. Geochemistry* 18, 941–954. doi:10.1016/S0883-2927(02)00185-3
- Hutchinson, M., Ridgway, J.W., 1977. Microbiological aspects of drinking water supplies. *Aquat. Microbiol.* 179–218.
- Imhoff, J.F., Hiraishi, A., Suling, J., 2005. Anoxygenic Phototrophic Purple Bacteria, in: *Bergey's Manual® of Systematic Bacteriology of Systematic Bacteriology*. Springer US, pp. 119–132. doi:10.1007/0-387-28021-9_15
- Inaba, T., Hori, T., Aizawa, H., Ogata, A., Habe, H., 2017. Architecture, component, and microbiome of biofilm involved in the fouling of membrane bioreactors. *npj Biofilms Microbiomes* 3, 5. doi:10.1038/s41522-016-0010-1
- Janse, I., Bok, J., Zwart, G., 2004. A simple remedy against artifactual double bands in denaturing gradient gel electrophoresis. *J. Microbiol. Methods* 57, 279–281.
- Kaden, R., Spröer, C., Beyer, D., Krolla-Sidenstein, P., 2014. *Rhodoferrax saidenbachensis* sp. nov., a psychrotolerant, very slowly growing bacterium within the family Comamonadaceae, proposal of appropriate taxonomic position of *Albidiferrax ferrireducens* strain T118T in the genus *Rhodoferrax* and emended description of. *Int. J. Syst. Evol. Microbiol.* 64, 1186–1193. doi:10.1099/ijs.0.054031-0

- Karwautz, C., 2015. Microbial Biofilms in Groundwater Ecosystems. Technische Universität München.
- Kato, S., Chan, C., Itoh, T., Ohkuma, M., 2013. Functional gene analysis of freshwater iron-rich flocs at circumneutral pH and isolation of a stalk-forming microaerophilic iron-oxidizing bacterium. *Appl. Environ. Microbiol.* 79, 5283–5290. doi:10.1128/AEM.03840-12
- Kato, S., Ohkuma, M., Powell, D.H., Krepski, S.T., Oshima, K., Hattori, M., Shapiro, N., Woyke, T., Chan, C.S., 2015. Comparative genomic insights into ecophysiology of neutrophilic, microaerophilic iron oxidizing bacteria. *Front. Microbiol.* 6, 1–16. doi:10.3389/fmicb.2015.01265
- Knecht, H., Neulinger, S.C., Heinsen, F.A., Knecht, C., Schilhabel, A., Schmitz, R.A., Zimmermann, A., dos Santos, V.M., Ferrer, M., Rosenstiel, P.C., Schreiber, S., Friedrichs, A.K., Ott, S.J., 2014. Effects of β -lactam antibiotics and fluoroquinolones on human gut microbiota in relation to *Clostridium difficile* associated diarrhea. *PLoS One* 9, e89417. doi:10.1371/journal.pone.0089417
- Kröber, M., Bekel, T., Diaz, N.N., Goesmann, A., Jaenicke, S., Krause, L., Miller, D., Runte, K.J., Viehöver, P., Pühler, A., Schlüter, A., 2009. Phylogenetic characterization of a biogas plant microbial community integrating clone library 16S-rDNA sequences and metagenome sequence data obtained by 454-pyrosequencing. *J. Biotechnol.* 142, 38–49. doi:10.1016/j.jbiotec.2009.02.010
- Kulakov, V. V., Fisher, N.K., Kondratyeva, L.M., Grischek, T., 2011. Riverbank filtration as an alternative to surface water abstraction for safe water supply to the city of Khabarovsk, Russia, in: *Riverbank Filtration for Water Security in Desert Countries*. Springer, Dordrecht, pp. 281–298. doi:10.1007/978-94-007-0026-0
- Lane, J., Pace, B., Olsen, G.J., Stahl, D.A., Sogin, M.L., Pace, N.R., Lane, D.J., Stahl, D.A., Sogin, M.L., 1985. Rapid determination of 16S ribosomal RNA sequences for phylogenetic analyses. *Proc. Natl. Acad. Sci.* 82, 6955–6959.

- Larroque, F., Franceschi, M., 2011. Impact of chemical clogging on de-watering well productivity: Numerical assessment. *Environ. Earth Sci.* 64, 119–131. doi:10.1007/s12665-010-0823-9
- Le-Clech, P., Chen, V., Fane, T.A.G., 2006. Fouling in membrane bioreactors used in wastewater treatment. *J. Memb. Sci.* 284, 17–53. doi:10.1016/j.memsci.2006.08.019
- LeChevallier, M.W., Babcock, T.M., Lee, R.G., 1987. Examination and Characterization of Distribution-System Biofilms. *Appl. Environ. Microbiol.* 53, 2714–2724.
- Lerm, S., Alawi, M., Miethling-Graff, R., Wolfgramm, M., Rauppach, K., Seibt, A., Würdemann, H., 2011. Influence of microbial processes on the operation of a cold store in a shallow aquifer: Impact on well injectivity and filter lifetime. *Grundwasser* 16, 93–104. doi:10.1007/s00767-011-0165-x
- Li, C., Wang, S., Du, X., Cheng, X., Fu, M., Hou, N., Li, D., 2016. Immobilization of iron- and manganese-oxidizing bacteria with a biofilm-forming bacterium for the effective removal of iron and manganese from groundwater. *Bioresour. Technol.* 220, 76–84. doi:10.1016/j.biortech.2016.08.020
- Li, J., Zhang, J., Liu, L., Fan, Y., Li, L., Yang, Y., Lu, Z., Zhang, X., 2015. Annual periodicity in planktonic bacterial and archaeal community composition of eutrophic Lake Taihu. *Sci. Rep.* 5, 15488. doi:10.1038/srep15488
- Lin, X., McKinley, J., Resch, C.T., Kaluzny, R., Lauber, C.L., Fredrickson, J., Knight, R., Konopka, A., 2012. Spatial and temporal dynamics of the microbial community in the Hanford unconfined aquifer. *ISME J.* 6, 1665–76. doi:10.1038/ismej.2012.26
- Lindström, E.S., Agterveld, M.P.K., Zwart, G., Kamst-Van Agterveld, M.P., Zwart, G., 2005. Distribution of Typical Freshwater Bacterial Groups Is Associated with pH , Temperature , and Lake Water Retention Time Distribution of Typical Freshwater Bacterial Groups Is Associated with pH , Temperature , and Lake Water Retention Time. *Appl. Environ. Microbiol.* 71, 8201–8206. doi:10.1128/AEM.71.12.8201

- Lovley, D.R., 2011. Powering microbes with electricity: Direct electron transfer from electrodes to microbes. *Environ. Microbiol. Rep.* 3, 27–35. doi:10.1111/j.1758-2229.2010.00211.x
- Lovley, D.R., 2004. Potential role of dissimilatory iron reduction in the early evolution of microbial respiration. *Cell. Orig. Life Extrem. Habitats Astrobiol.* 6, 299–313.
- Lovley, D.R., Chapelle, F.H., 1995. Deep Subsurface Microbial Processes. *Rev. Geophys.* 33, 365–381.
- Lovley, D.R., Holmes, D.E., Nevin, K.P., 2004. Dissimilatory Fe(III) and Mn(IV) reduction. *Adv Microb Physiol* 49, 221 –286.
- Lu, C., Zhao, T., Shi, X., Cao, S., 2016. Ecological restoration by afforestation may increase groundwater depth and create potentially large ecological and water opportunity costs in arid and semiarid China. *J. Clean. Prod.* 1–10. doi:10.1016/j.jclepro.2016.03.046
- Lu, S., Chourey, K., Reiche, M., Nietzsche, S., Shah, M.B., Neu, T.R., Hettich, R.L., Küsel, K., 2013. Insights into the structure and metabolic function of microbes that shape pelagic iron-rich aggregates (“iron snow”). *Appl. Environ. Microbiol.* 79, 4272–81. doi:10.1128/AEM.00467-13
- Ludwig, W., Schleifer, K.-H., 2000. How Quantitative is Quantitative PCR with Respect to Cell Counts? *Syst. Appl. Microbiol.* 23, 556–562.
- Madsen, E.L., Ghiorse, W.C., 1993. Groundwater microbiology: subsurface ecosystem processes. *Aquat. Microbiol. An Ecol. Approach.* 167–213.
- Marchesi, J.R., Sato, T., Weightman, A.J., Martin, A., Fry, J.C., Hiom, S.J., Wade, W.G., Martin, T. a, 1998. Design and Evaluation of Useful Bacterium-Specific PCR Primers That Amplify Genes Coding for Bacterial 16S rRNA Design and Evaluation of Useful Bacterium-Specific PCR Primers That Amplify Genes Coding for Bacterial 16S rRNA. *Appl. Environ. Microbiol.* 64, 795–799.
- Marzorati, M., Wittebolle, L., Boon, N., Daffonchio, D., Verstraete, W., 2008. How to get more out of molecular fingerprints: Practical tools for microbial ecology. *Environ. Microbiol.* 10, 1571–1581. doi:10.1111/j.1462-2920.2008.01572.x

- Medihala, P.G., Lawrence, J.R., Swerhone, G.D.W., Korber, D.R., 2011. Effect of pumping on the spatio-temporal distribution of microbial communities in a water well field. *Water Res.* 46, 1286–1300. doi:10.1016/j.watres.2011.12.036
- Mehta, M.G., 2013. Metal reduction by *Geothrix fermentans*. University of Minnesota.
- Melton, E.D., Swanner, E.D., Behrens, S., Schmidt, C., Kappler, A., 2014. The interplay of microbially mediated and abiotic reactions in the biogeochemical Fe cycle. *Nat. Rev. Microbiol.* 12, 797–809. doi:10.1038/nrmicro3347
- Mendonça, M.B. de, Ehrlich, M., Cammarota, M.C., 2003. Conditioning factors of iron ochre biofilm formation on geotextile filters. *Can. Geotech. J.* 40, 1225–1234. doi:10.1139/t03-064
- Menz, C., 2016. Oxygen Delivering Processes in Groundwater and Their Relevance for Iron - Related Well Clogging Processes – A Case Study On The Quaternary Aquifers of Berlin. Freie Universität Berlin.
- Mulder, E.G., 1964. Iron Bacteria, particularly those of the *Sphaerotilus-Leptothrix* Group, and Industrial Problems. *J. Appl. Bacteriol.* 27.1, 151–173.
- Mulder, E.G., van Veen, W.L., 1963. Investigations on the *Sphaerotilus-Leptothrix* group. *Antonie Van Leeuwenhoek* 29, 121–153. doi:10.1007/BF02046045
- Muyzer, G., de Waal, E.C., Uitterlinden, A.G., 1993. Profiling of complex microbial populations by denaturing gradient gel electrophoresis analysis of polymerase chain reaction-amplified genes coding for 16S rRNA. *Appl. Environ. Microbiol.* 59, 695.
- Navarro-Noya, Y.E., Suárez-Arriaga, M.C., Rojas-Valdes, A., Montoya-Ciriaco, N.M., Gómez-Acata, S., Fernández-Luqueño, F., Dendooven, L., 2013. Pyrosequencing analysis of the bacterial community in drinking water wells. *Microb. Ecol.* 66, 19–29. doi:10.1007/s00248-013-0222-3

- Neubauer, S.C., Emerson, D., Megonigal, J.P., 2002. Life at the energetic edge: kinetics of circumneutral iron oxidation by lithotrophic iron-oxidizing bacteria isolated from the wetland-plant rhizosphere. *Appl. Environ. Microbiol.* 68, 3988.
- Page, D., Vanderzalm, J., Miotliński, K., Barry, K., Dillon, P., Lawrie, K., Brodie, R.S., 2016. Determining treatment requirements for turbid river water to avoid clogging of aquifer storage and recovery wells in siliceous alluvium. *Water Res.* 101, 640–641. doi:10.1016/j.watres.2016.06.020
- Paul, D., Kazy, S.K., Gupta, A.K., Pal, T., Sar, P., 2015. Diversity, metabolic properties and arsenic mobilization potential of indigenous bacteria in arsenic contaminated groundwater of West Bengal, India. *PLoS One* 10. doi:10.1371/journal.pone.0118735
- Pavelic, P., Dillon, P.J., Mucha, M., Nakai, T., Barry, K.E., Bestland, E., 2011. Laboratory assessment of factors affecting soil clogging of soil aquifer treatment systems. *Water Res.* 45, 3153–3163. doi:10.1016/j.watres.2011.03.027
- Purswani, J., Martín-Platero, A.M., Reboleiro-Rivas, P., González-López, J., Pozo, C., 2011. Comparative analysis of microbial DNA extraction protocols for groundwater samples. *Anal. Biochem.* 416, 240–242. doi:10.1016/j.ab.2011.05.024
- Quaiser, A., Bodi, X., Dufresne, A., Naquin, D., Francez, A.J., Dheilly, A., Coudouel, S., Pedrot, M., Vandenkoornhuyse, P., 2014. Unraveling the stratification of an iron-oxidizing microbial mat by metatranscriptomics. *PLoS One* 9, 1–9. doi:10.1371/journal.pone.0102561
- Ranjard, L., Lejon, D.P.H., Mougél, C., Schehrer, L., Merdinoglu, D., Chaussod, R., 2003. Sampling strategy in molecular microbial ecology: Influence of soil sample size on DNA fingerprinting analysis of fungal and bacterial communities. *Environ. Microbiol.* 5, 1111–1120. doi:10.1046/j.1462-2920.2003.00521.x

- Rentz, J.A., Kraiya, C., Luther, G.W., Emerson, D., 2007. Control of ferrous iron oxidation within circumneutral microbial iron mats by cellular activity and autocatalysis. *Environ. Sci. Technol.* 41, 6084–6089. doi:10.1021/es062203e
- Rinck-Pfeiffer, S., Ragusa, S., Sztajn bok, P., Vandev elde, T., 2000. Interrelationships Between Biological, Chemical, and Physical Processes As an Analog To Clogging in Aquifer Storage and Recovery. *Water Res.* 34, 2110–2118.
- Roh, S.W., Kim, K.-H., Nam, Y.-D., Chang, H.-W., Park, E.-J., Bae, J.-W., 2010. Investigation of archaeal and bacterial diversity in fermented seafood using barcoded pyrosequencing. *ISME J.* 4, 1–16. doi:10.1038/ismej.2009.83
- Romaní, A.M., Amalfitano, S., Artigas, J., Fazi, S., Sabater, S., Timoner, X., Ylla, I., Zoppini, A., 2013. Microbial biofilm structure and organic matter use in mediterranean streams. *Hydrobiologia* 719, 43–58. doi:10.1007/s10750-012-1302-y
- Romaní, A.M., Borrego, C.M., Díaz-Villanueva, V., Freixa, A., Gich, F., Ylla, I., 2014. Shifts in microbial community structure and function in light- and dark-grown biofilms driven by warming. *Environ. Microbiol.* 16, 2550–2567. doi:10.1111/1462-2920.12428
- Röske, I., Uhlmann, D., 2005. *Biologie der Wasser- und Abwasserbehandlung*. Ulmer.
- Salter, S.J., Cox, M.J., Turek, E.M., Calus, S.T., Cookson, W.O., Moffatt, M.F., Turner, P., Parkhill, J., Loman, N.J., Walker, A.W., 2014. Reagent and laboratory contamination can critically impact sequence-based microbiome analyses. *BMC Biol.* 12, 87. doi:10.1186/s12915-014-0087-z
- Schmidt, B., Sánchez, L. a, Fretschner, T., Kreps, G., Ferrero, M. a, Siñeriz, F., Szewzyk, U., 2014. Isolation of *Sphaerotilus*-*Leptothrix* strains from iron bacteria communities in Tierra del Fuego wetlands. *FEMS Microbiol. Ecol.* 90, 454–66. doi:10.1111/1574-6941.12406

- Schröder, J., Braun, B., Liere, K., Szewzyk, U., 2016. Draft Genome Sequence of *Rheinheimera* sp. Strain SA_1 Isolated from Iron Backwash Sludge in Germany. *Genome Announc.* 4, e00853-16. doi:10.1128/genomeA.00853-16
- Smith, C.J., Nedwell, D.B., Dong, L.F., Osborn, a M., 2006. Evaluation of quantitative polymerase chain reaction-based approaches for determining gene copy and gene transcript numbers in environmental samples. *Environ. Microbiol.* 8, 804–15. doi:10.1111/j.1462-2920.2005.00963.x
- Sobolev, D., Roden, E.E., 2002. Evidence for rapid microscale bacterial redox cycling of iron in circumneutral environments. *Antonie van Leeuwenhoek, Int. J. Gen. Mol. Microbiol.* 81, 587–597. doi:10.1023/A:1020569908536
- Stackebrandt E, E.J., 2006. Taxonomic parameters revisited: taenished gold standards. *Microbiol Today* 33:152-5, 152–155.
- Stewart, C.R., Muthye, V., Cianciotto, N.P., 2012. *Legionella pneumophila* Persists within Biofilms Formed by *Klebsiella pneumoniae*, *Flavobacterium* sp., and *Pseudomonas fluorescens* under Dynamic Flow Conditions. *PLoS One* 7, 1–8. doi:10.1371/journal.pone.0050560
- Stoecker, K., Bendinger, B., Schöning, B., Nielsen, P.H., Nielsen, J.L., Baranyi, C., Toenshoff, E.R., Daims, H., Wagner, M., 2006. Cohn's *Crenothrix* is a filamentous methane oxidizer with an unusual methane monooxygenase. *Proc. Natl. Acad. Sci. U. S. A.* 103, 2363–7. doi:10.1073/pnas.0506361103
- Stratil, S.B., Neulinger, S.C., Knecht, H., Friedrichs, A.K., Wahl, M., 2013. Temperature-driven shifts in the epibiotic bacterial community composition of the brown macroalga *Fucus vesiculosus*. *Microbiologyopen* 2, 338–49. doi:10.1002/mbo3.79
- Straub, K.L., Benz, M., Schink, B., Widdel, F., 1996. Anaerobic, nitrate-dependent microbial oxidation of ferrous iron. *Appl. Environ. Microbiol.* 62, 1458.

- Straub, K.L., Schönhuber, W.A., Buchholz-Cleven, B.E.E., Schink, B., 2004. Diversity of Ferrous Iron-Oxidizing, Nitrate-Reducing Bacteria and their Involvement in Oxygen-Independent Iron Cycling. *Geomicrobiol. J.* 21, 371–378. doi:10.1080/01490450490485854
- Szewzyk, U., Szewzyk, R., Manz, W., Schleifer, K., 2000. Microbiological safety of drinking water. *Annu. Rev. Microbiol.* 54.1, 81–127.
- Szewzyk, U., Szewzyk, R., Schmidt, B., Braun, B., 2011. Neutrophilic iron-depositing microorganisms, in: *Biofilm Highlights*. pp. 63–79.
- Táncsics, A., Farkas, M., Szoboszlai, S., Szabó, I., Kukolya, J., Vajna, B., Kovács, B., Benedek, T., Kriszt, B., 2013. One-year monitoring of meta-cleavage dioxygenase gene expression and microbial community dynamics reveals the relevance of subfamily I.2.C extradiol dioxygenases in hypoxic, BTEX-contaminated groundwater. *Syst. Appl. Microbiol.* 36, 339–350. doi:10.1016/j.syapm.2013.03.008
- Taylor, S.W., Lange, C.R., Lesold, E.A., 1997. Biofouling of Contaminated Ground-Water Recovery Wells: Characterization of Microorganisms. *Groundwater* 35, 973–980. doi:10.1111/j.1745-6584.1997.tb00169.x
- Terlizzi, A., Faimali, M., 2010. Fouling on Artificial Substrata, in: *Biofouling*. Dürr S., pp. 170–184. doi:10.1002/9781444315462.ch12
- Tschech, A., Pfennig, N., 1984. Growth yield increase linked to caffeate reduction in *Acetobacterium woodii*. *Arch. Microbiol.* 137, 163–167. doi:10.1007/BF00414460
- Tuhela, L., Carlson, L., Tuovinen, O.H., 1997. Biogeochemical transformations of Fe and Mn in oxic groundwater and well water environments. *J. Environ. Sci. Heal. . Part A Environ. Sci. Eng. Toxicol.* 32, 407–426. doi:10.1080/10934529709376551
- van Beek, C.G.E.M., 1989. Rehabilitation of clogged discharge wells in the Netherlands. *Q. J. Eng. Geol. Hydrogeol.* 22, 75–80. doi:10.1144/GSL.QJEG.1989.022.01.06

- Van Der Kooij, D., 2000. Biological Stability: a multidimensional quality aspect of treated water. *Water. Air. Soil Pollut.* 25–34. doi:10.1023/A:1005288720291
- van der Wielen, P.W.J.J., van der Kooij, D., 2013. Nontuberculous mycobacteria, fungi, and opportunistic pathogens in unchlorinated drinking water in the Netherlands. *Appl. Environ. Microbiol.* 79, 825–834. doi:10.1128/AEM.02748-12
- van Halem, D., de Vet, W., Verberk, J., Amy, G., van Dijk, H., 2011. Characterization of accumulated precipitates during subsurface iron removal. *Appl. Geochemistry* 26, 116–124. doi:10.1016/j.apgeochem.2010.11.008
- Van Leewenhoeck, A., 1676. Observations, Communicated to the Publisher by Mr. Antony van Leewenhoeck, in a Dutch Letter of the 9th of Octob. 1676. Here English'd: concerning Little Animals by Him Observed in Rain-Well-Sea. and Snow Water; as Also in Water Wherein Pepper Had Lain In. *Philos. Trans. R. Soc. London* 12, 821–831. doi:10.1098/rstl.1677.0003
- Videla, H.A., Herrera, L.K., 2005. Microbiologically influenced corrosion: looking to the future. *Int. Microbiol.* 8, 169–180.
- Vishnivetskaya, T.A., Layton, A.C., Lau, M.C.Y., Chauhan, A., Cheng, K.R., Meyers, A.J., Murphy, J.R., Rogers, A.W., Saarunya, G.S., Williams, D.E., Pfiffner, S.M., Biggerstaff, J.P., Stackhouse, B.T., Phelps, T.J., Whyte, L., Sayler, G.S., Onstott, T.C., 2014. Commercial DNA extraction kits impact observed microbial community composition in permafrost samples. *FEMS Microbiol. Ecol.* 87, 217–230. doi:10.1111/1574-6941.12219
- Wang, J., Muyzer, G., Bodelier, P.L.E., Laanbroek, H.J., 2009. Diversity of iron oxidizers in wetland soils revealed by novel 16S rRNA primers targeting *Gallionella*-related bacteria. *ISME J.* 3, 715–25. doi:10.1038/ismej.2009.7

- Wang, J., Sickinger, M., Ciobota, V., Herrmann, M., Rasch, H., Rösch, P., Popp, J., Küsel, K., 2014. Revealing the microbial community structure of clogging materials in dewatering wells differing in physico-chemical parameters in an open-cast mining area. *Water Res.* 63, 222–33. doi:10.1016/j.watres.2014.06.021
- Wang, J., Vollrath, S., Behrends, T., Bodelier, P.L.E., Muyzer, G., Meima-Franke, M., Den Oudsten, F., Van Cappellen, P., Laanbroek, H.J., 2011. Distribution and diversity of Gallionella-like neutrophilic iron oxidizers in a tidal freshwater marsh. *Appl. Environ. Microbiol.* 77, 2337–44. doi:10.1128/AEM.02448-10
- Wang, Q., Garrity, G.M., Tiedje, J.M., Cole, J.R., 2007. Naive Bayesian classifier for rapid assignment of rRNA sequences into the new bacterial taxonomy. *Appl. Environ. Microbiol.* 73, 5261–5267. doi:10.1128/AEM.00062-07
- Weber, K.A., Picardal, F.W., Roden, E.E., 2001. Microbially catalyzed nitrate-dependent oxidation of biogenic solid-phase Fe(II) compounds. *Environ. Sci. Technol.* 35, 1644–1650. doi:10.1021/es0016598
- Weber, K.A., Urrutia, M.M., Churchill, P.F., Kukkadapu, R.K., Roden, E.E., 2006. Anaerobic redox cycling of iron by freshwater sediment microorganisms. *Environ. Microbiol.* 8, 100–113. doi:10.1111/j.1462-2920.2005.00873.x
- Wingender, J., Flemming, H.C., 2011. Biofilms in drinking water and their role as reservoir for pathogens. *Int. J. Hyg. Environ. Health* 214, 417–423. doi:10.1016/j.ijheh.2011.05.009
- Wittebolle, L., Marzorati, M., Clement, L., Balloi, A., Daffonchio, D., Heylen, K., De Vos, P., Verstraete, W., Boon, N., 2009. Initial community evenness favours functionality under selective stress. *Nature* 458, 623–626. doi:10.1038/nature07840
- Wommack, K.E., Bhavsar, J., Ravel, J., 2008. Metagenomics: Read length matters. *Appl. Environ. Microbiol.* 74, 1453–1463. doi:10.1128/AEM.02181-07

- Yachi, S., Loreau, M., 1999. Biodiversity and ecosystem productivity in a fluctuating environment: The insurance hypothesis. *Proc. Natl. Acad. Sci.* 96, 1463–1468. doi:10.1073/pnas.96.4.1463
- Yang, B., Wang, Y., Qian, P.-Y., 2016. Sensitivity and correlation of hypervariable regions in 16S rRNA genes in phylogenetic analysis. *BMC Bioinformatics* 17, 135. doi:10.1186/s12859-016-0992-y
- Yang, L., Li, X., Chu, Z., Ren, Y., Zhang, J., 2014. Distribution and genetic diversity of the microorganisms in the biofilter for the simultaneous removal of arsenic, iron and manganese from simulated groundwater. *Bioresour. Technol.* 156, 384–388. doi:10.1016/j.biortech.2014.01.067
- Yeung, C.W., Woo, M., Lee, K., Greer, C.W., 2011. Characterization of the bacterial community structure of Sydney Tar Ponds sediment. *Can. J. Microbiol.* 57, 493–503. doi:10.1139/w11-032
- Zaa, Y.L.C., Mclean, J.E., Dupont, R.R., Norton, J.M., Sorensen, D.L., 2010. Dechlorinating and Iron Reducing Bacteria Distribution in a TCE-Contaminated Aquifer 44–55. doi:10.1111/j1745
- Zhang, Z., Schwartz, S., Wagner, L., Miller, W., 2000. A Greedy Algorithm for Aligning DNA Sequences. *J. Comput. Biol.* 7, 203–214. doi:10.1089/10665270050081478
- Zhou, J., 2008. The development of molecular tools for the evaluation of the bioremediation of chlorinated solvents. Utah State University.
- Zhou, Y., Kellermann, C., Griebler, C., 2012. Spatio-temporal patterns of microbial communities in a hydrologically dynamic pristine aquifer. *FEMS Microbiol. Ecol.* 81, 230–242. doi:10.1111/j.1574-6941.2012.01371.x